RECLAMATION
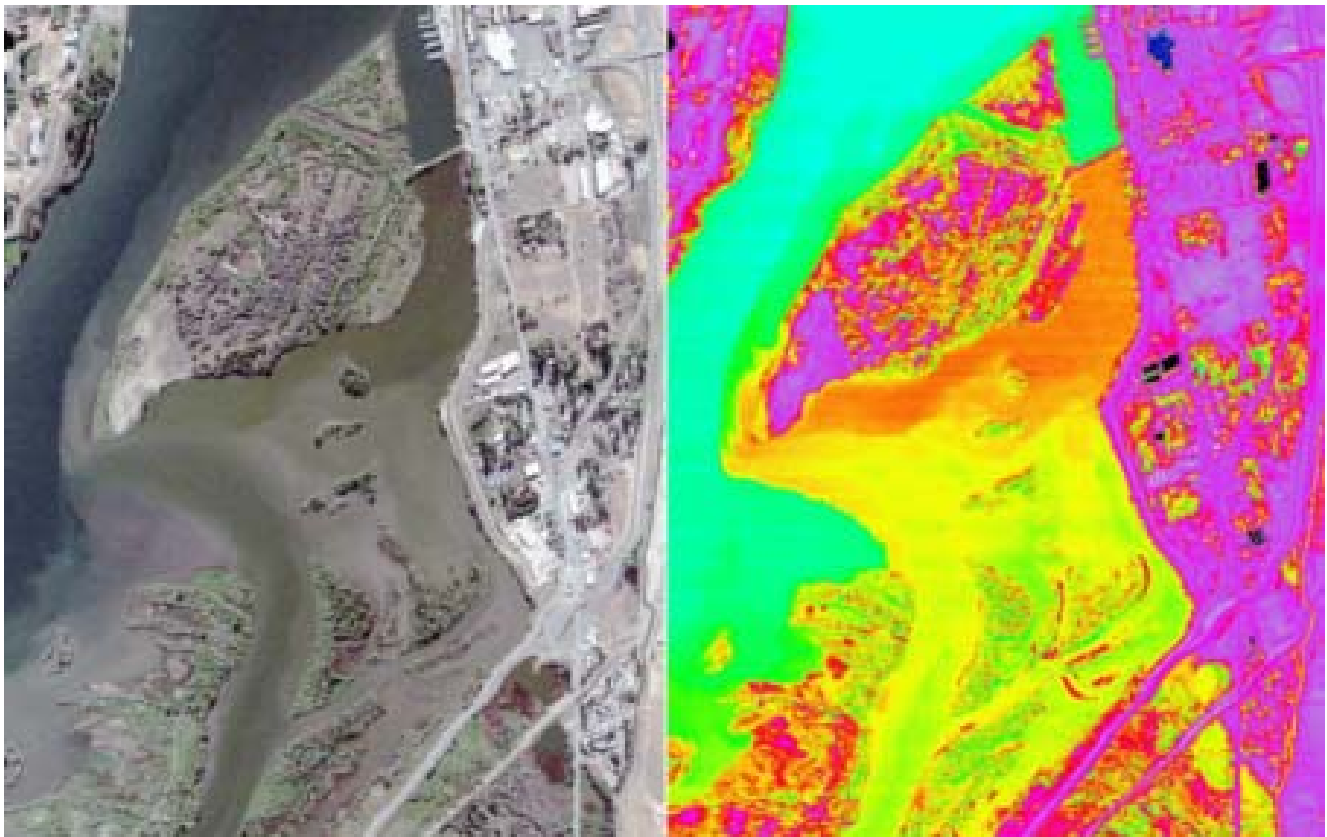*Managing Water in the West*

Remote Sensing Technology: Guidelines and Applications within the Bureau of Reclamation

U.S. Department of the Interior
Bureau of Reclamation

September 2005

Mission Statements

The mission of the Department of the Interior is to protect and provide access to our Nation's natural and cultural heritage and honor our trust responsibilities to Indian Tribes and our commitments to island communities.

The mission of the Bureau of Reclamation is to manage, develop, and protect water and related resources in an environmentally and economically sound manner in the interest of the American public.

BUREAU OF RECLAMATION
Technical Service Center, Denver, Colorado
Remote Sensing & Geographic Information Group, D882600

Technical Memorandum No. D-8260-05-05

Remote Sensing Technology: Guidelines and Applications with the Bureau of
Reclamation

_____

Prepared: Edmond W. Holroyd, III, Ph.D.
Retired, Remote Sensing & Geographic Information Group, D882600

_____

Technical Approval: Mike Pucherelli
Group Manager, Remote Sensing & Geographic Information Group, D882600

_____   _____

Peer Review: Douglas Clark   Date
Physical Scientist, Remote Sensing & Geographic Information Group, D882600

Table of Contents

List of Figures

iii

List of Tables

Abstract

Remote sensing might be defined as looking at something without touching it. Such a broad definition could also include weather radar views of precipitation and deriving earth interior structures from earthquake waves. Traditionally remote sensing includes looking at the Earth from aerial and satellite perspectives and interpreting the imagery, the perspective followed in this document. Topics include the physics of remote sensing, data sources, image processing, and preparation of data for inclusion in a geographic information system (GIS) for further analyses. A summary of former and current Denver Office remote sensing studies is appended to show the variety of possible topics.

Part I. Overview of Technology

1. Glossary and Abbreviations

The field of remote sensing and geographic information systems has accumulated a great number of technical words and phrases and acronyms. These are listed at the start of this report for reference and to help in understanding the later discussion.

> **Absorption**: the removal of energy from the radiation spectrum.
> **Albedo**: the percentage of incident light reflected from a surface. Equivalent to Reflectance.
> **Anti-solar point**: the location from the viewer directly opposite the sun; the potential shadow location. The point on the sphere 180 degrees from the sun.
> **Aspect**: the azimuth towards which a sloping surface is facing.
> **Attitude**: the orientation of a viewing platform, such as an aircraft.
> **Azimuth**: the horizontal orientation angle, 0 degrees = North, 90 degrees = East, etc.
> **Backscatter**: the reverse deflection of radiation roughly towards the source.
> **Band**: pertaining to a particular range of wavelengths.
> **Band combination**: a set of bands used for visualization or computation.
> **Band ratioing**: the division of an imagery band by another to reduce shadowing effects and enhance differences.
> **BGR**: blue-green-red; an order of displaying color bands; opposite of RGB order.
> **Blackbody**: a totally absorbing body that does not reflect radiation. Note: In thermal equilibrium, a blackbody absorbs and radiates at the same rate; the radiation will just equal the absorption when thermal equilibrium is maintained. This hypothetical body consists of a sufficient number of molecules emitting and absorbing electromagnetic radiation in all parts of the electromagnetic spectrum so that all incident radiation is completely absorbed and in all wavelengths bands and in all directions, maximum possible emission is effected.
> **CAD**: computer aided design; a set of points, lines, polygons, shapes, text often without the rigorous topological rules of vectors.
> **Calibration**: the adjustment of numerical values to a standard reference.

CIR: color-infrared, or false-color infrared A visualization that views the green, red, and near-infrared bands as blue, green, and red, often used in vegetation studies, where healthy green vegetation appears as bright red in the display or print.

Charge coupled device: (CCD) the type of light sensing device in digital cameras.

Clustering techniques: One pass, Fuzzy C Means, Minimum Distribution Angle, Adaptive resonance, K means, ISODATA, self-organization, etc.

Color style: the digital representation of colors, as 4-, 8-, 16-, 24-, and 32-bit numbers.

Cross-track scanning: the use of an imaging instrument whose view sweeps in a direction perpendicular to the forward motion of an aircraft or satellite viewing platform.

Data Base (DB): A computer-based management system for organizing data and descriptions.

DEM: digital elevation model, sometimes DTM, digital terrain model.

Differential Global Positioning System (DGPS): a GPS system that uses a base station for correcting and refining geographic positions.

DLG: digital line graph. Standard line vector product from the USGS.

DOQ, DOQQ: digital orthophoto (quarter)quad, a quadrangle version of an orthophoto.

DRG: digital raster graphic: an image of a scanned USGS topographic map including the collar information, georeferenced to the UTM grid.

Easting: a geographic coordinate east of some reference longitude.

Electromagnetic radiation: radiation made up of oscillating electric and magnetic fields and propagated at the speed of light. Includes gamma radiation, X-rays, ultraviolet, visible, and infrared radiation and radar and radio waves.

Elevation: (1) the height, usually above sea level. (2) the vertical orientation angle, 0 degrees = horizontal and 90 degrees = vertical.

Forward Fast Fourier Transform: the mathematical transformation of imagery into sinusoidal values of varying amplitude, frequency, and phase. Often used to start the removal of periodic noise in an image.

FLIR: Forward Looking Infra-Red. A sensor system for converting thermal imagery into television imagery.

Geographic Information System (GIS): a computer-based system for collecting, storing, retrieving, transforming, displaying, and analyzing spatial data.

Geostationary satellite: a satellite placed in an orbit about 22 thousand miles above the earth's equator such that its forward motion matches the rotation of the earth and it remains at a fixed longitude.

Global Positioning System (GPS): a system by which receiver equipment electronically monitors signals from a constellation of a couple dozen satellites to accurately determine the geographic position of the receiver in terms of latitude, longitude, and altitude.

Hyperspectral: imagery having dozens to hundreds of spectral bands at fine resolution.

IFSAR: interference synthetic aperture radar; a technique for analyzing radar imagery for fine detail.

Interference mode: a technique of analyzing radar imagery to reveal slight changes in elevation over time, such as those caused by tectonic and earthquake movements.

IR: infrared.

L1A and L1B: satellite imagery processing levels. L1A is essentially raw data. L1B is calibrated.

Lambertian reflector: a theoretical surface that reflects energy equally at all angles.

LIDAR: an instrument that determines distances by timing the return reflection of a laser beam.

Linear photodiode array: an imaging device whereby a scene is focused upon a line of photodiodes on an electronic microcircuit chip.

Mask: an image overlay whose numerical values specify the region of interest in other images.

Maximum likelihood classifier: an automated scheme of classifying pixels in an image based upon color resemblance to specified reference values.

Median filter: a numerical technique whereby a cluster, of specified extent, of adjacent pixels is examined for a median numerical value which is then placed in an output image at the cluster center. This removes the effects of extreme (noise) values.

Minimum distance to means classifier: an automated scheme of classifying pixels in an image by choosing the closest color match to specified reference values.

Mixed pixel: a color blending of numerous substances within the view of a single pixel.

Monochrome: sensed and displayed as intensity in only one spectral band; black & white.

Multispectral: having at least three spectral bands but usually less than ten.

Nadir: the location straight down from the viewpoint.

NIR: near infrared. The shortest wavelengths of the infrared region, nominally 0.75 to 3 μm.

Northing: a geographic position north of some reference latitude.

NTSC: a video format used in the USA and some other countries (PAL elsewhere). The code used to describe the United States system of color telecasting.

Othophoto: an image in which positional differences caused by the camera-landscape geometry, particularly by elevation, are removed by resampling. An orthophoto is a planimetrically correct image whereby features are in their true orthographic positions

PAL: "Phase Altering Line": a video format used in Europe and elsewhere, not in USA. Gathers data at a rate of 25 rather than 30 frames per second.

Panchromatic: same as monochrome, B&W, a single-band image.

Parallelepiped classifier: an automated scheme of classifying pixels in an image by partitioning band brightnesses at particular numerical ranges.

Pixel: smallest element of an image. Stands for "picture element".

Planck's Constant: the constant of proportionality (h) that relates the energy of a photon (E) with the frequency of the associated wave (η). where h = 6.626 × 10^{-34} joule•second.

Polarization: the forced orientation of the electric vector of electromagnetic energy.

Principal components analysis: a mathematical transformation of imagery data from a set of bands into the same number of bands but which are mathematically independent (orthogonal) of each other. The dominant variability appears in the first band (usually scene brightness) and the least in the last band (which appears as almost entirely noise). The transformation does not indicate the spectral causes of the resultant features, just that there is a significant difference.

Projection: any mathematical transformation of the globe onto some other usually flat surface.

Radiance: the spectral energy received by a sensor.

Raster: xy matrices of adjacent picture element values.

Rayleigh scatter: the scattering of radiation by very tiny aerosols and molecules in the atmosphere.

Remote Sensing (RS): the science the gathering of information about an object, area, or phenomenon through the analysis of data acquired by a device not in contact with them.

RGB: red-green-blue; also BGR for reverse order and R, G, B separately.

Reflectance: ratio of outgoing to incoming spectral energy. Also Albedo.

Resolution: the smallest distance represented by a single pixel.. It is minimum distance between two objects that a sensor can record distinctly.

SAR: synthetic aperture radar.

Scale: the ratio of a distance on a map or image to the real distance on the ground. Usually expressed in the form 1:5000, which is interpreted as 1 cm on the image represents 5000 cm on the ground, or in whatever units are preferred.

Signal to noise ratio: the strength of real data compared to noise values.

Spectrometer: a device that measures the intensity of radiation at different wavelengths.

Specular reflector: a mirror.

Stretching: the adjustment of a brightness distribution to a different range of values.

Supervised classification: a classification system by which a human analyst determines the classification of pixels.

SWIR: short-wave infrared. (1-3 μm).

Tasseled Cap: referring to the shape of a 2-dimensional distribution of pixel values (red and near-IR) of a scene containing vegetation.

TIN: triangular irregular network, a series of triangles often used to represent a continuous surface.

TIR: thermal infrared. Electromagnetic radiation emitted from the Earth's surface by all objects having a temperature warmer than absolute zero. Wavelengths in this range of the spectrum are within the infrared region, longer than 3 nanometers.

Training: the development of an automated classification system based upon known features and objects.

Transmissivity: the ratio of transmitted energy to the incoming energy.

Triangulation: the determination of positions by means of angles to other known positions.

Unsupervised classification: various automated classification systems.

UTM: Universal Transverse Mercator, a cylindrical, conformal projection system for generating maps of the curved Earth.

UV: ultraviolet. It is part of the electromagnetic spectrum that lies at wavelengths shorter than the violet range of the visible spectrum. The ultraviolet spectrum has wavelengths between 100 and 400 nanometers (nm).

Vector: a set of points, lines, polygons, and nodes used to describe feature locations, but with rigorous topological rules.

VNIR: visible and near infrared.

Wien's Displacement Law: For a blackbody, the product of the wavelength corresponding to the maximum radiancy and the thermodynamic temperature is a constant. As a result, as the temperature rises, the maximum of the radiant energy shifts toward the shorter wavelength (greater frequency and energy) end of the spectrum. $\lambda_m = A/T$ where λ_m is the wavelength of maximum spectral emittance, $A = 2898 \ \mu m°K$, and T = temperature, °K. Thus, the wavelength of maximum emitted radiation is inversely proportional to the absolute (°K) temperature.

Zenith: the location straight up from the viewpoint.

2. Physics of Remote Sensing

Remote sensing (RS) can be considered to have its origins in the 1800s with photography, though it was originally confined to views from the Earth's surface towards objects in the distance. The growing availability of aerial platforms in the 1900s provided vertical views of the Earth. Such were used primarily for general mapping and for military purposes. Altitudes for RS cameras can range from hand-held close-ups to balloons and aircraft as high as in the stratosphere. The second half of the 1900s introduced space-borne platforms for viewing the Earth. Weather satellites led the way, showing the organized cloud patterns around the globe. That was followed by satellites viewing the Earth surface at increasingly fine resolutions, though coarse resolutions are still appropriate for some global mappings.

RS generally examines objects, areas, and phenomena using the electromagnetic spectrum (Fig. 1; gamma, X-rays, ultraviolet, visible, infrared, thermal IR, microwave, radio), with wavelengths ranging by many orders of magnitude.
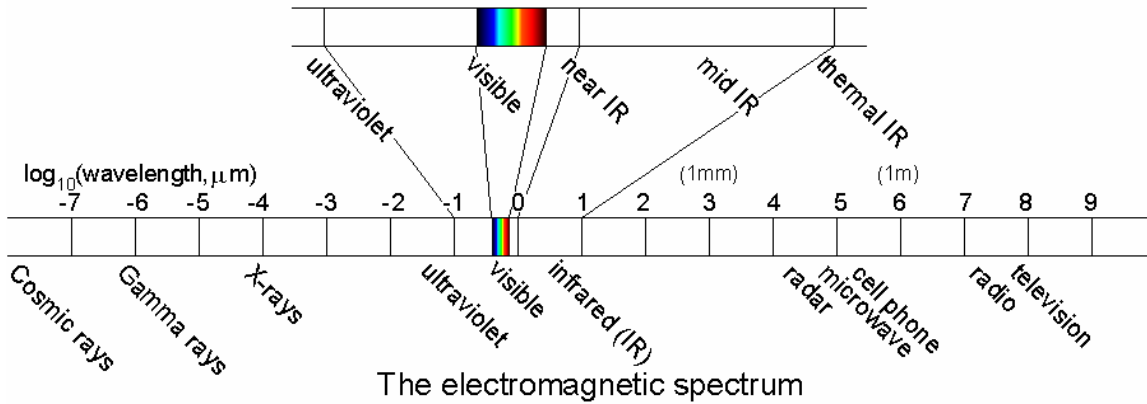
Fig. 1. The electromagnetic spectrum wavelengths cover many orders of magnitude.

The visible part of the spectrum is relatively narrow. The energy emitted by a theoretical black body has a distribution described by Plank's Law (Fig. 2), and the location of the peak energy is described by Wien's Law. As a substance becomes hotter, it emits more energy at all wavelengths, but the increase is greater at shorter wavelengths. The integral of Plank's Law curves gives the total energy as proportional to the fourth power of the absolute (Kelvin) temperature. The energy from the sun gets diluted by the distance to the Earth.
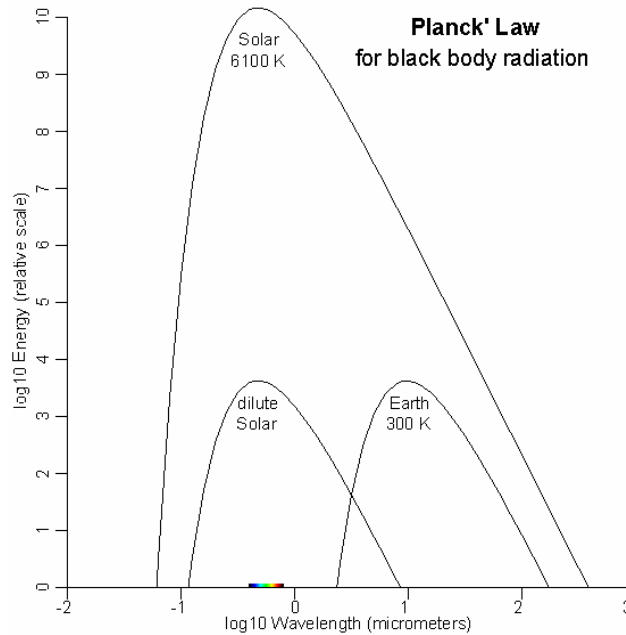
Fig. 2. Theoretical black body radiation from the Sun surface, diluted by distance to the Earth, and approximate radiation produced at Earth temperatures.

The total solar energy intercepted by some unit area is comparable to that emitted by a black body at a temperature of roughly 300° K and seen at close range. It is the balance of the incoming solar radiation and the outgoing Earth reflection and radiation that maintains a generally constant global temperature for the Earth.

6

The atmospheric gases absorb electromagnetic energy at chemically specific wavelengths, some of which are labeled in the darkened regions of Fig. 3 (adapted from http://orbit-net.nesdis.noaa.gov/arad/fpdt/tutorial/absorb.html). There are atmospheric "windows" (light regions of graph) which permit energy passage. The absorptions by these and other greenhouse gases keep the Earth significantly warmer than it would be without an atmosphere.
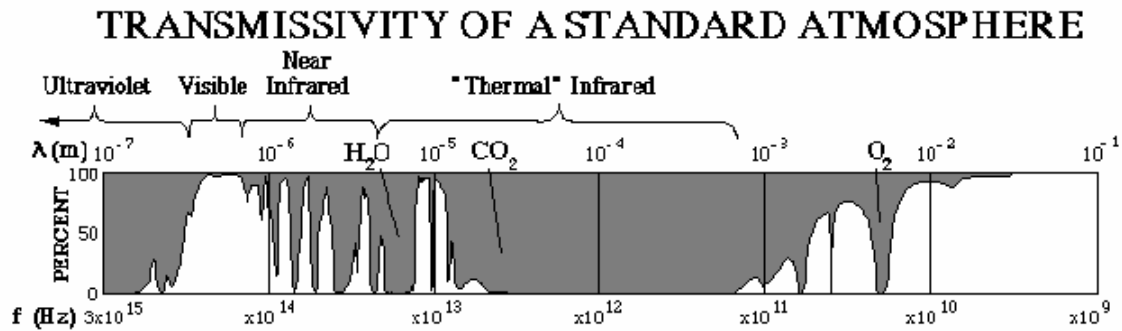
Fig. 3. Atmospheric absorptions of radiation.

RS need not be restricted to the electromagnetic spectrum. Other RS measurement styles use gravity and/or magnetic fields to probe into the Earth's surface in search of anomalies. RS can use acoustic waves, such as sonar, earthquakes, and man-made sound pulses, to reveal objects and surfaces that are inaccessible by electromagnetic devices. However, this document will focus on electromagnetic-based of RS rather than these others.

Remote sensing detectors have greatly multiplied in types and spectral abilities, initially led by the field of astronomy and astrophysics. Photographic response to light intensity is logarithmic and even non-linear on the logarithmic scale. Photographic response starts in the near-infrared (NIR) and extends through the visible wavelengths to ultraviolet (UV) and x-rays. Electronic substitutes for photography provided linearities in signals, better sensitivities, and especially data in both longer and shorter wavelengths that are not accessible to photography. Detectors increased from single elements (photocell and photodiode scanners) to linear arrays ("pushbroom" scanners) to 2D arrays (digital cameras). The electronic data are most convenient for computer processing.

RS can be passive or active. Passive RS means that the electromagnetic radiation emitted or reflected from a surface is recorded. Examples are photography, videography, electronic cameras and some microwave devices. The sun is the usual illuminator for visible and near infrared (VNIR) bands. Thermal emission provides the signal at typical earth temperatures, mostly at thermal infrared (TIR) wavelengths of roughly 10 micrometers. Fires are easily detected at the short wave infrared (SWIR) wavelengths (roughly 3 to 5 micrometers).

Active means that the RS system illuminates its target and records the returning radiation. Examples are radar, LIDAR, and fluorescence. The latter anticipates that a surface will emit radiation in a longer wavelength (lesser energy) than that of the illumination.

Technologies have allowed an increase in spectral resolution. Monochrome (panchromatic) provides imagery in shades of gray, such as black-and-white photography. Traditional color imagery is produced by three bands, usually Red, Green, Blue (RGB). Infrared color imagery is usually presented as CIR, where the sensor band sequence of NIR, red, green are displayed as RGB. Multispectral systems have 3 to several spectral bands of data. Hyperspectral systems usually have dozens to hundreds of spectral bands of fine resolution. The transition from multispectral to hyperspectral is not precisely defined.

Color

Color to our eyes is the reception of red, green, and blue bands of light energy. Our brain then interprets intermediate colors based upon the proportion of those three. Colors are not linearly related to wavelength; red (R), yellow (Y), green (G), cyan (C), and blue (B) are not equally spaced in the spectrum. Magenta (M) is not even the color of a particular wavelength. Tans and browns do not exist as particular wavelengths but are composites of the primary colors, forming a diagonal line in the spectrum, increasing from blue to red.

The composition of color varies, depending upon whether the color is created by light sources or by light-absorbing substances or surfaces (Fig. 4).

Light is additive
Red + Green + Blue = White
Red + Green = Yellow
Green + Blue = Cyan
Blue + Red = Magenta
none = Black

Dyes are subtractive
Cyan + Yellow + Magenta = Black
Cyan + Yellow = Green
Yellow + Magenta = Red
Magenta + Cyan = Blue
none = White

Cyan : no Red
Yellow : no Blue
Magenta : no Green
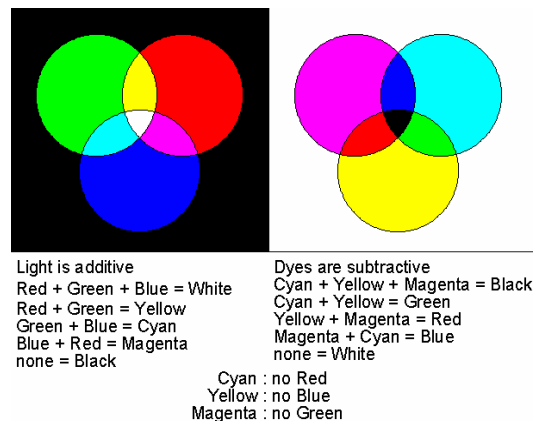
Fig. 4. Color combinations from light emitting and absorbing sources.

There are three primary colors for light sources, as provided by luminous bodies like the sun, lamps, and TV and computer screens: red, green, and blue. These combine in pairs to form yellow, cyan, and magenta. All three, of equal intensity, form white. The absence of all form black.

Dyes are examples of light absorbing substances. The three primary dye colors are yellow, cyan, and magenta. They may also be thought of as "not-blue", "not-red", and "not-green", respectively. They add in pairs to form red, green, and blue. All together make black. The absence of all makes white.

Color can also be defined as a combination (Fig. 5) of hue, intensity, and saturation (HIS). Hue defines a color on a circular scale of 0 to 360 degrees (or 0 to 255 to stay in the byte range). The six pure colors (B, M, R, Y, G, C, back to B) are at multiples of 60 degrees. Intensity indicates the brightness of the image pixel, ranging from black (0) to white (255). Saturation shows the richness of the color. A saturation of 0 produces a colorless grayscale according to the intensity value. A saturation of 255 produces a maximum of a pure color, shown in this illustration as green. The color fusion (pan sharpening) process, to be discussed elsewhere, allows a fine resolution panchromatic image to be colorized by a coarser 3-band color image. The color image is converted to HIS. The panchromatic image is substituted for the intensity. A revised color image is then calculated from the H, new I, and S.
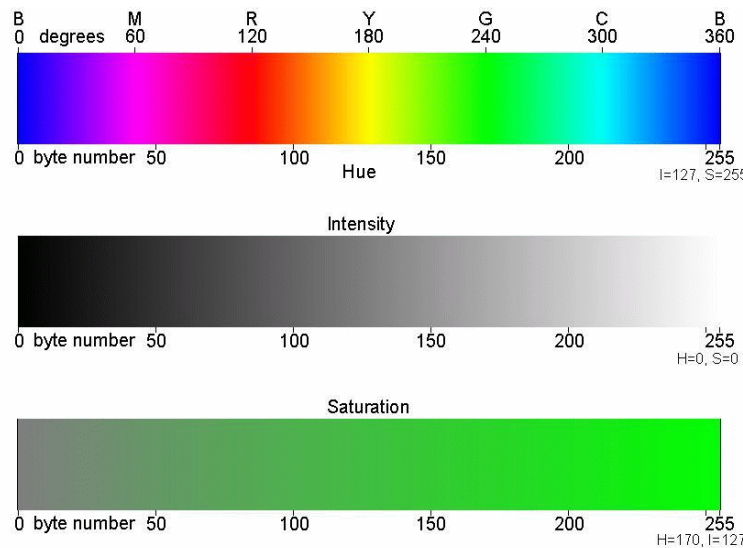
Fig. 5. The effects of color definition by hue, intensity, and saturation.

Sample Spectra

Photographic and eventually electronic recordings of the absorption spectra of thousands of substances, chemicals, and minerals were made over the past century for industrial and research purposes. Such spectra helped identify the presence of those specific substances in unknown materials. However, most plants have similar spectra; the differences are usually in the visible colors and caused by features such as flowers and autumn leaf colors that we can also see by our own eyes. Some common minerals have generally featureless spectra in the VNIR to SWIR range. Other minerals have spectra so unique that their presence in a mixture of substances can be readily detected. Fluorescence spectra are usually unique and can be excited by gamma, x-ray, and ultraviolet

illuminations. However, atmospheric absorptions of such illuminations restrict RS to very short observational distances. The following graphs were made using measurements from an ASDI Field Spectrometer - Full Range or gathered from similar spectra published by the USGS Spectral Laboratory. Those made using sunlight usually have noise bands from water vapor near 1.4 and 1.9 micrometers.

The following graphs show the spectra (horizontal axis: wavelength, 0.35 to 2.50 micrometers; vertical axis: reflectance) of several inorganic materials. Rocks and soils usually contain significant quantities of the quartz (Fig. 6) and feldspar (Fig. 7) minerals. Most have featureless spectra. However, some narrow bands, caused by water, can be seen in special minerals like opal. The bright carbonates Fig. 8) have some distinctive narrow bands deep into the infrared. The copper carbonates show peaks in the blue and green. Various types of oxidized iron (Fig. 9) have a distinctive wide band in the very near infrared.
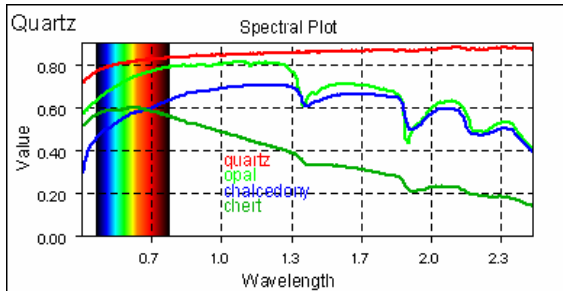
Fig. 6. Reflectance spectra of varieties of quartz minerals.
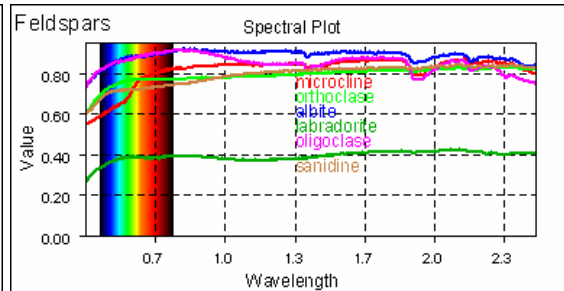
Fig. 7. Reflectance spectra of varieties of feldspar minerals.
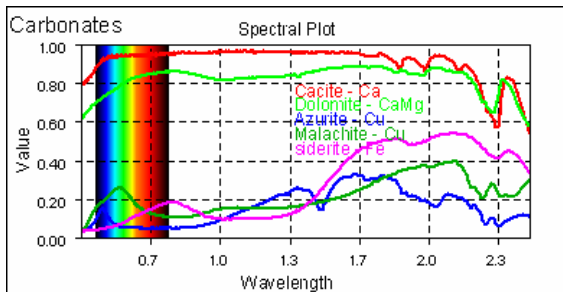
Fig. 8. Reflectance spectra of carbonate minerals.
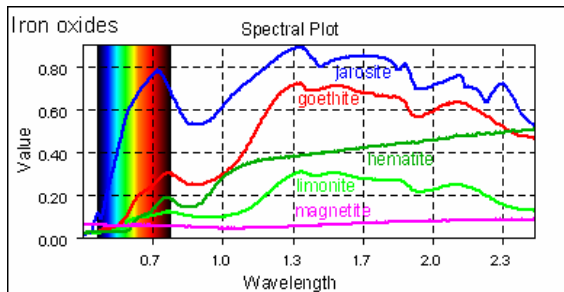
Fig. 9. Reflectance spectra of varieties of iron oxide minerals.

Some of the micas (Fig. 10) have a very narrow band in the middle of the spectrum. Feldspars and volcanic ash weather into the clays (Fig. 11), some of which are distinctive in their band shapes and placement.
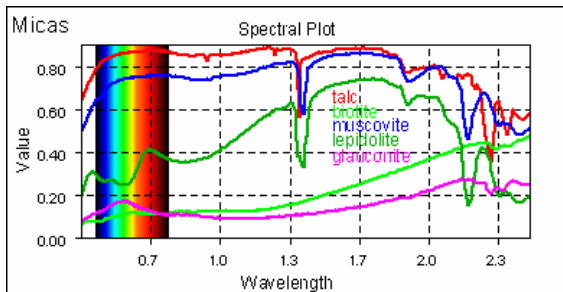
Fig. 10. Reflectance spectra of varieties of mica minerals.
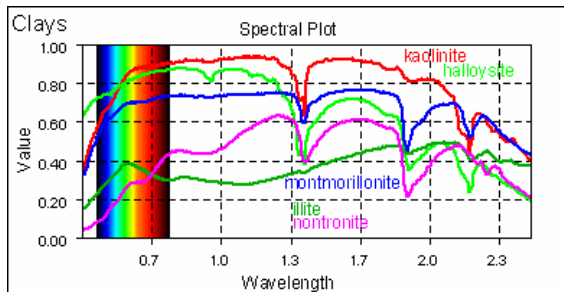
Fig. 11. Reflectance spectra of varieties of clay minerals.

10

Weather phenomena (Fig. 12) provide some special patterns. Blue sky becomes exponential in the blue to ultraviolet as a result of molecular scattering (the sky is pink on Mars because of scattering in the carbon dioxide atmosphere; Titan with a nitrogen and methane atmosphere has a different color). Such blue scattering and particle scattering from haze greatly degrade the remote sensing signal in the blue band. It is even worse in the near ultraviolet. In photography, a haze (meaning ultraviolet) filter is used to reduce the exposure of the blue band by ultraviolet scattering. Clouds, whether of water droplets or ice crystals, have multiple banding. Freshly fallen snow has deep black bands in the infrared.
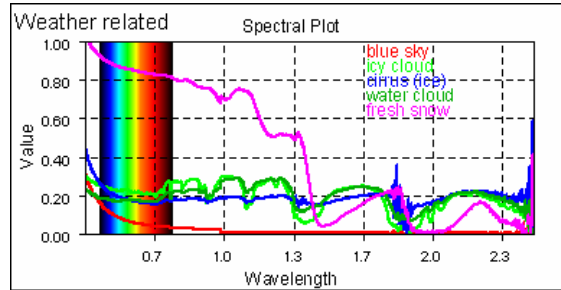
Fig.12. Reflectance spectra of weather related features.

Water (Fig. 13; note the vertical scale) strongly absorbs energy, especially in the infrared. (There is strong noise in the infrared caused by water bands in the atmosphere.) The colors in the visible and near infrared vary according to what is in or under the water.
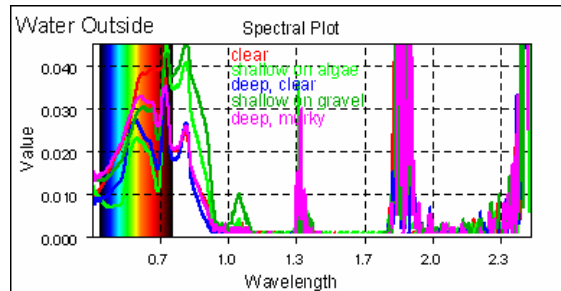
Fig 13. Reflectance spectra of water bodies.

Computer screens are light emission devices. Phosphorescent materials (Fig. 14) and light emitting diodes are made to glow. Liquid Crystal Displays (Fig. 15) shutter the light, while electrons control intensity of a CRT display. In both cases the ultraviolet light is much stronger than the green and red in order to get a similar intensity in the blue. Notice that the two different displays have different spectra. Both are dark in the infrared.
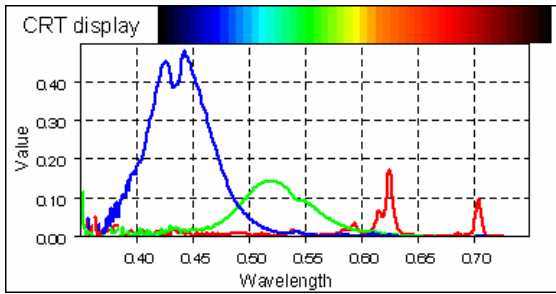
Fig. 14. Emission spectra of CRT computer display.
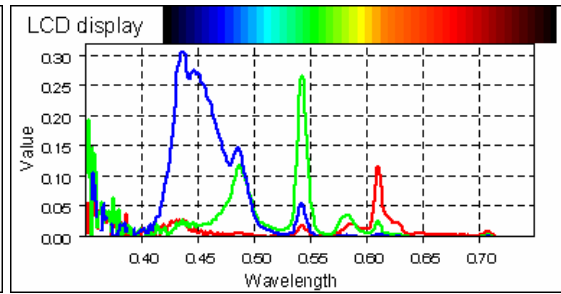
Fig. 15. Emission spectra of liquid crystal computer displays.

Green plants (Fig. 16) have a minor peak in the green wavelengths because chlorophyll strongly absorbs in the red. However, healthy green plants are very bright in the infrared. That enables their detection by false color infrared imagery. The main difference for plants is in the amplitude of the spectrum. Conifers are darker than deciduous trees. Grass is brightest.
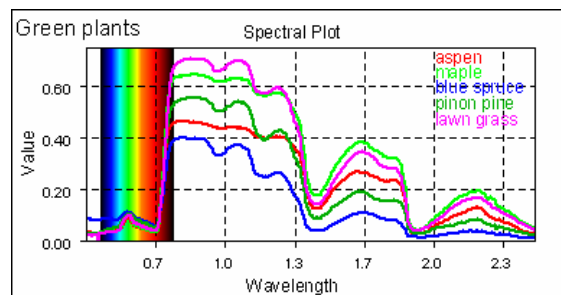
Fig. 16. Reflectance spectra of green plants.

Flower color variations (Fig. 17) are mostly in the visible wavelengths. Lichens (a combination of algae and fungus; (Fig. 18), however, do not resemble green plants. Notice the wavy spectra in the infrared. The noxious wetland weed, purple loosestrife, can illustrate seasonal changes (Fig. 19). The green leaves look like most other green plants. The purple flowers have a special peak in the blue and ultraviolet, which makes them attractive to bees. Autumn makes the leaves dark red. Winter kills the foliage and makes it tan. Biocontrol insects seriously harm the health of purple loosestrife. As they chew greater percentages of the leaves there is a strong drop in brightness in the very near infrared (Fig. 20). Eventually the leaves turn a chocolate brown.
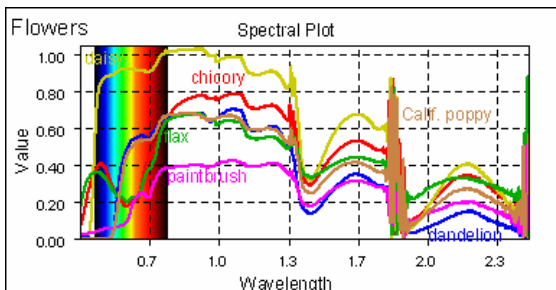
Fig. 17. Reflectance spectra of some flowers.
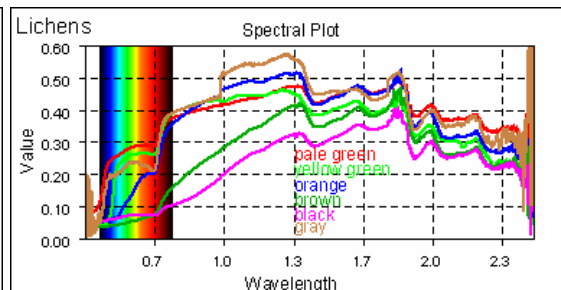
Fig. 18. Reflectance spectra of lichens.

12
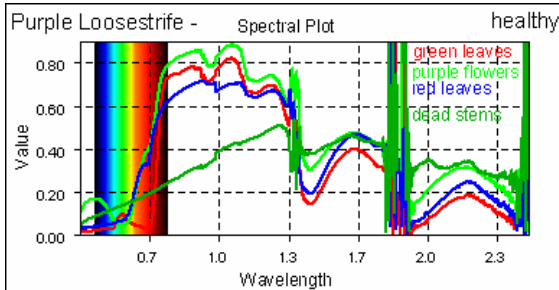
Fig. 19. Reflectance spectra of Purple loosestrife parts.   Fig. 20. Reflectance spectra of damaged purple loosestrife.
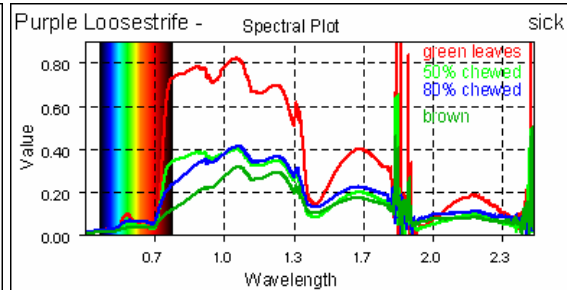
The spectra illustrated above were collected at about 2000 narrow wavelength intervals. Color photography collects in three broad bands: blue-green-red for natural color and green-red-NIR for false color infrared. Most Earth-observing satellites have similar broad-band sensors which must miss the very fine detail shown in these spectra. Special instruments aboard satellites, such as MODIS and ASTER, record 36 and 14 bands with some bands being broad and others narrow. Hyperspectral instruments are mostly mounted on aircraft. Apart from the limited view of the Hyperion hyperspectral instrument, satellite attempts have failed to become operational. Such instruments may have up to about 220 bands to record the spectral range illustrated in these graphs. The AVIRIS instrument is considered the best for hyperspectral work. Hyperspectral data need special techniques to remove atmospheric absorption effects from the spectra received at the sensor. A critical look at the graphs should show that hyperspectral data are excellent for a limited number of subjects but of no special additional value for others. Hyperspectral instruments produce such large volumes of data that computational time and storage considerations become huge and expensive.

Very fine spectral resolution also allows the determination of properties at increasing optical depths within a substance. The core of a spectral absorption band shows the top surface, while the "wings" of the band penetrate to greater depths. The weather satellites can use this technology for atmospheric properties, but it probably applies to water penetration as well.

All electronic media have a "mixed pixel" problem. That is a term that indicates that within the view of a single pixel there are many different objects with different spectral signatures. For example, a 30 meter pixel where a road is at a shoreline will have the road, water, bare soil, and vegetation all contributing to the signal of that pixel. This produces interpretation challenges, especially for automatic processing of scenes by computers. Some special techniques exist in several software packages to "unmix" the spectral signatures within hyperspectral pixels if a set of "end member" reference spectra are supplied to show the program what the pure target spectra look like.

13

Reflections and scattering

The incoming energy has many interactions on its way to the remote sensor. Though usually from the sun, this energy can come from the moon, lasers, and radars. The incident energy striking a surface divides into three components: absorbed, transmitted, and reflected. It is normally the reflected energy that is used in remote sensing.

All remote sensors record spectral energy, radiance, that actually gets to the sensor. This is usually different from the illumination of a scene and its reflectance (Fig. 21). The illumination may be scattered into direct and indirect, such as direct sunlight and diffuse light from the blue sky or from clouds. The surface can reflect, absorb, or transmit part of the illumination energy, usually with a spectral change. Energy coming from the surface can be absorbed or supplemented by atmospheric effects, such as haze and water vapor, or fully blocked, such as by clouds. Such processes often have a wavelength dependence. Precision remote sensing needs to account for all such processes that affect what actually is seen by the sensors.
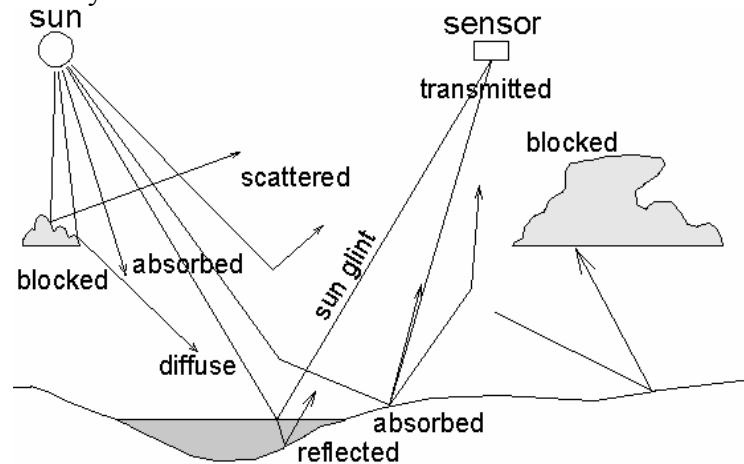
Fig. 21. Light can follow many paths on its way to the sensor.

The reflected energy may not follow traditional optical angles. An ideal specular reflector, such as a mirror, sends the energy at an angle of reflection equal to the angle of incidence. A near-perfect specular reflector, such as a wavy water surface, sends its energy at a variety of angles close to that of an ideal reflector. When a surface is mirror-like and positioned to reflect illumination into the sensor, sunglint often results, creating a bright spot (Fig. 22). Such sun glint can become a major problem in both aerial and satellite images.

The anti-solar point (at the potential shadow of the sensor on the imaged surface) and surrounding area is usually bright because of strong backscatter from most objects. Glass beads in paint provide the same effect for highway markers and signs. The illustration from the Winchester Wasteway, Washington, shows sunglint off calm water in the lower right and, opposite the nadir, a bright anti-solar spot in the upper left, where the sunshine is on sand dunes coated with volcanic ash from Mount St. Helens. Notice that the general ground is darker at the bottom of the image than at the top, creating challenges when

anti-solar spot

dunes

nadir +

water
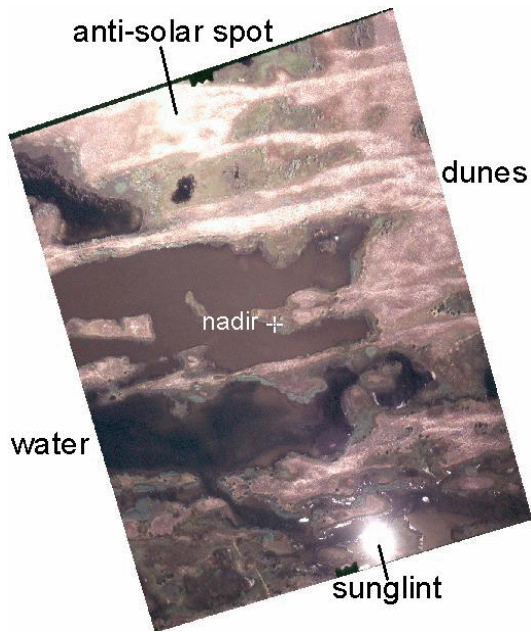
sunglint

Fig. 22. Sunglint and anti-solar spot can appear bright.

mosaicking adjacent views and trying to match brightnesses. The solar illumination was uniform over the entire area, but the directional scattering was not uniform.

The anti-solar point is usually the brightest location in an image. Most substances preferentially reflect light back towards where it came from. Sometimes the shadow of the aerial platform (aircraft) can be seen at that location. The location at the opposite side of the image, through the image center, is sometimes the darkest location in the image. If trees are there, the camera sees not only the shaded side of the tree, but also its shadow. That same location is also the mirror position of the sun, producing a bright solar image on flat water surfaces. If the water has waves, a general sun glint is produced about the mirror position of the sun. The greater the amplitude of the waves, the greater the lateral extent of the sun glint. Satellite views of the sun glint on ocean surfaces can estimate the amplitude of the waves for describing the state of the sea.

The ideal diffuse reflector (Lambertian) scatters the energy equally in all directions (Fig. 23). Most natural surfaces are not ideal. Instead there are energy peaks in the specular reflection direction and more so in the reverse direction to the incident energy. The latter causes brightening in a spot about the anti-solar point. In low altitude aerial photography there can be such brightening about the shadow of the aircraft. The effects of non-Lambertian surfaces appear as apparent non-uniform illumination when mosaics are made of aerial photographs.

Energy Distributions

Ideal specular reflector

equal angles of incidence, reflection

all energy

mirror

Ideal diffuse reflector (Lambertian)

uniform energy

flat white

Near-perfect specular reflector

sun glint

concentrated energy

water ripples

Non-ideal reflector

anti-solar reflection

micro-shadowing

natural
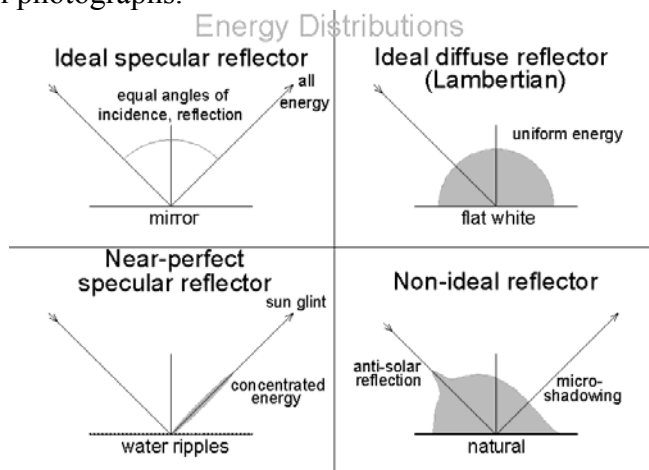
Fig. 23. Theoretical reflections seldom occur in nature.

In general, it is good to keep an open mind about what RS can do for a project. Technologies keep improving, allowing us to sense more and more phenomena at

15

increasing sensitivities and spectral resolutions. The traditional types of remote sensing, aerial photography and simple satellite imagery, are now being supplemented by many other types. The challenge is to determine the most appropriate technology for the task at hand. It may be "old" technology or something exotic.

Data Types

Image data are of two basic types, analog and digital. Analog data (Fig. 24) are continuously varying, such as the voltages in a photocell or optical density in photographic film. Analog data can be in either of three dimensions: point, line, or area. A prism or diffraction grating can split light into a spectrum for analog recording.
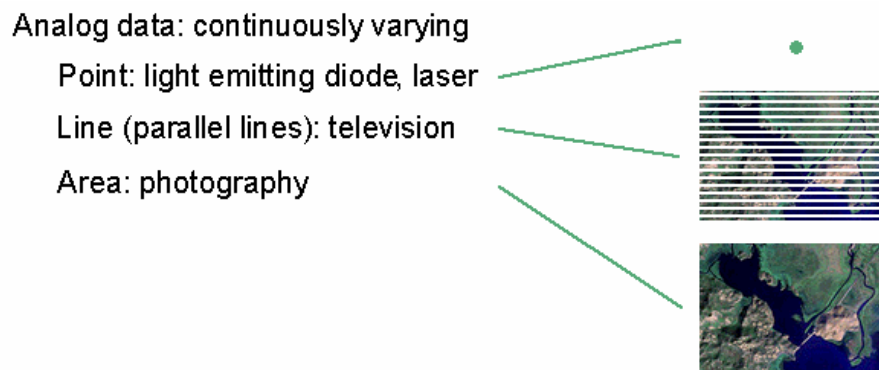
Fig. 24. Analog image data are continuously varying.

Digital data (Fig. 25) is quantized into integers for computer processing. The smallest image unit is known as a "pixel" or point picture element. It has a brightness value associated with it. Data can be recorded as monochrome (one color), multispectral (3 to a few colors), and hyperspectral (many colors). Data can be imaged as points, lines, and areas. Two-dimensional images can be made from single point sensors by cross-track scanning with forward motion. They can be made from line data (linear photodiode array) by forward motion perpendicular to the line. Digital cameras directly make two-dimensional images by use of two-dimensional array CCD (charge coupled device) sensors.
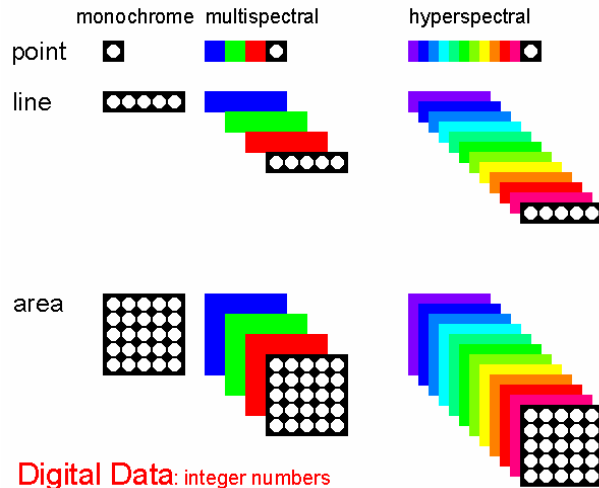
Fig. 25. Digital image data have specific numbers for each pixel.

Digital data can be quantized into any number of bits, or binary digits. Binary images have values of 0 and 1, black and white. Four-bit images have 16 levels of gray from black to white. Eight-bit (byte) images have 256 gray levels. 16-bit images have 65,536 gray levels.

Color images come in several types. Four-bit and eight-bit images have lookup tables assigning particular colors to the various integer numbers. 16-bit images usually have 5-bit (32 gray levels) shading for each of 3 colors (R=red, G=green, B=blue). 24-bit images have 8-bit (256 gray levels) shading for the 3 colors.

Resolution and scale

Resolution can be expressed, for digital images, as the pixel size. Weather satellite images can be as coarse as several kilometers per pixel. Aerial images and the newest generation of satellite images can achieve 1 meter pixels. Close-up photography can achieve sub-millimeter resolution if necessary.

Resolution is determined by a combination of three factors. First is the sensor system itself, such as the film grain size or the size of the CCD elements in a digital camera. Second is the optical system, expressed by the focal length of the lens.

Third is the altitude of the sensor above the subject. The resolution can be estimated in advance by simple trigonometry using similar triangles (Fig. 26). For detecting element size, d; focal length, f; and height, h; the pixel size, p is given by $p = h * d / f$. Similar triangles can also be used to determine the total field of view of the image.
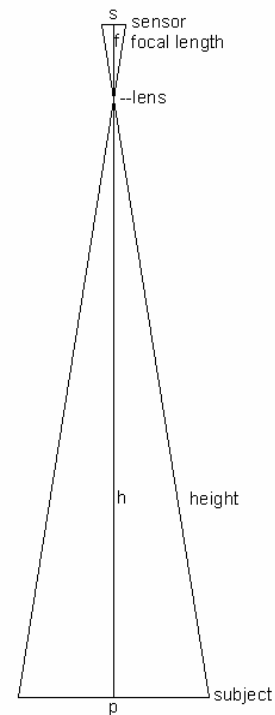
Fig. 26. Simple triangle for determining pixel size and view width.

17

A variety of surface resolutions are available from today's fleet of earth-observing satellites. Fig. 27 shows actual or simulated views, progressively zooming in on Henry Lake on the southwest side of Denver. In the upper left is a view of Colorado from a geostationary weather satellite (GOES) image, shown at 5 km resolution. It has the ability to do close-ups at 1 km. Next is a view from a polar orbiting weather satellite (NOAA-AVHRR) at 1 km resolution. An Indian satellite has a 2-band wide angle view at 180 meter resolution, useful for general vegetation mapping. The red band is simulated as the third image.
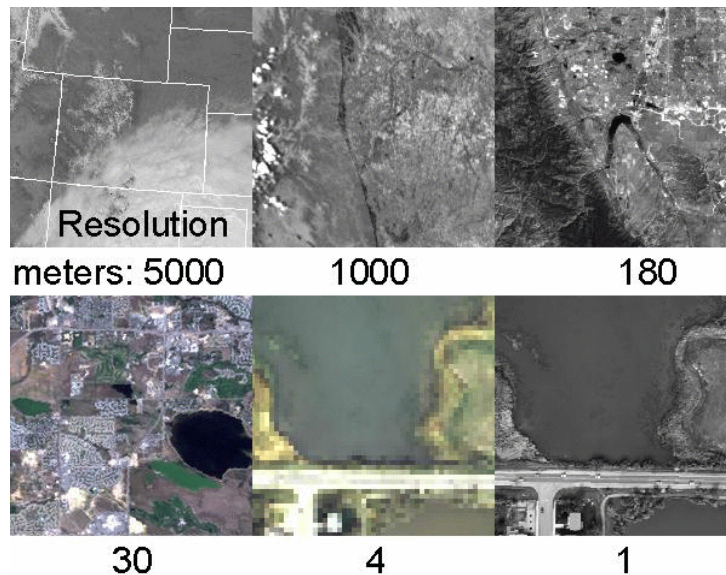
Fig. 27. A series of satellite views, at different resolutions, of Henry Lake, Southwest of Denver.

The Landsat TM series has 30 meter resolution in 6 bands (B,G,R, 2 NIR, and mid-IR) and a thermal-IR band of lesser resolution. The visible bands are displayed here in natural color.

The new high resolution satellites, IKONOS and Orbview-3, have 4 meter color in 4 bands: B,G,R, NIR. QuickBird has a similar camera, but a lower orbit gives it 2.4 meter color and 0.6 meter panchromatic resolution. The two lower rightmost views of the illustration show the same view of the south end of Henry Lake as simulated 4 meter color and 1 meter panchromatic.

The target in the Henry Lake study was an infestation of the invasive noxious weed purple loosestrife. The individual plants cannot be seen with even the finest satellite resolution. There is a "mixed-pixel" problem in addition to resolution; each pixel contains contributions of many items within the view - ground, grass, water, and other plants. Aerial photography might resolve the weeds but only if an appropriate resolution is selected.

Fig. 28 shows the same scene of a vertical view of flowering purple loosestrife at a series of simulated resolutions, differing by a factor of 2. The two lower rightmost views are enlargements of the upper left portion of the main view. The last view, at 0.5 mm resolution, shows a flower cluster, leaves, a dry seed stalk from the previous year (top) and a cattail seed head (lower left), in addition to dark views of the undergrowth. An analyst needs to select a resolution at which the presence of flowering purple loosestrife can be distinguished from other things in the view. A resolution of about 10 mm/pixel seems appropriate for presence identification but does not clearly resolve what else is in view.

Satellite resolution is fixed at specified values, such as 1 meter/pixel for panchromatic imagery from IKONOS and Orbview-3. Aerial resolution can be adjusted by the height
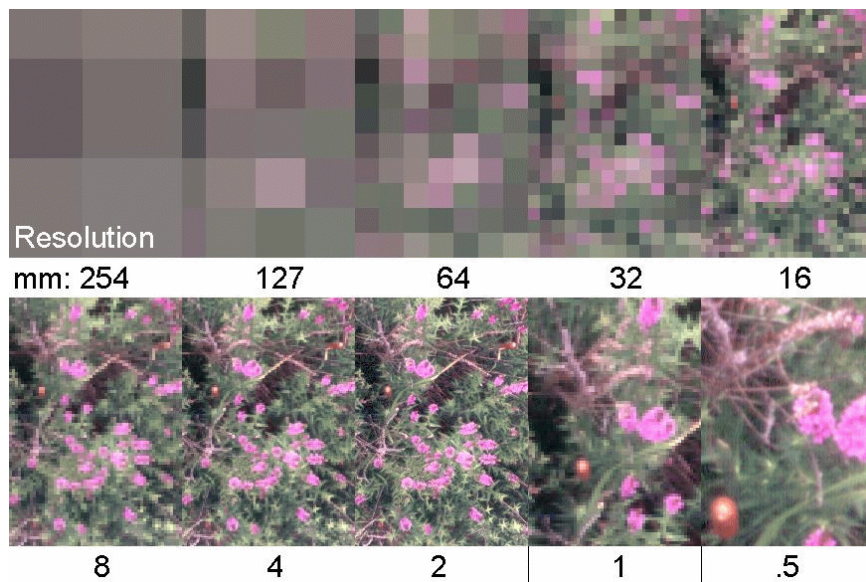
Fig. 28. A series of views of purple loosestrife flowers at different resolutions.

(altitude) of the camera above the surface, using a variation of the equation $p = h * d / f$ associated with the triangle of Fig. 26. For digital cameras the sensor resolution, d, is fixed and usually difficult to identify in the specifications. It may have to be calculated from the size of the CCD array and the number of pixels across its view. For photographic film that is scanned, the scanning resolution (usually in dpi - dots per inch = pixels per inch) is the inverse of d. Inserting the numbers into the equation then produces a need to carefully deal with the mixture of English and metric units! (dpi) * (pixel resolution) * (focal length) = (altitude) becomes (pixels/inch) * (meters/pixel) * (millimeters) = (feet) with the obvious need for conversion factors. In review, satellite resolution is fixed, aerial resolution can be adjusted by aircraft altitude, camera (digital or photographic) resolution can be adjusted by zooming or lens switch before picture acquisition, and scanned photographic film resolution can be adjusted by the scanner resolution up to the limit of film grain size. The resulting resolution is a solution of the available adjustments.

3. Data sources

Photography

Aerial imagery usually comes from photography, videography, and scanners. Traditional aerial mapping cameras use film as 9x9 inch frames and a 6 inch lens. The flight altitude in feet is then half of the scale number; 1:5000 scale imagery is flown at 2500 feet. Sometimes 35 mm photography is appropriate. Film types can be panchromatic (B&W), natural color, and CIR (false color). Photographic style can be negative (for positive prints) or positive (for transparencies). The transparencies usually have the greater resolution and color brilliance.

Film speed is important and interacts with shutter speed and diaphragm aperture for proper exposure and depth of view. Slow speed films have fine resolution while fast speed films are coarse grained. This is true for both panchromatic and color films. Therefore, using films which promote capabilities in situations with dim illumination results in a serious drawback of poorer resolution. Diaphragm apertures have settings, known as "f-stops", that are on a logarithmic scale of powers of the square root of 2: 1, 1.4, 2, 2.8, 4, 5.6, 8, 11, 16, 22, 32. The smaller numbers indicate wide open apertures and the larger numbers very narrow apertures. For a constant illumination, shutter speed increases by a factor of 2 must be compensated by f-stop changes to the next smaller number. The depth of field is the range of distances at which objects are in reasonable focus. As the f-stop number gets smaller, the depth of field gets narrower. Therefore, as illumination decreases and an f-stop is adjusted to compensate, the need for precise focusing becomes greater. Popular hand-held cameras rarely have such independent controls of shutter speed and f-stops. Full control of these features allow a photographer the options of having everything in focus, from nearby objects to infinity, or only a particular object in focus while things in the foreground and background are out of focus.

For aerial photography from great heights, aircraft motion has little effect. When flights are close to the ground (1:5000 or finer scales, for example) fast shutter speed or fast film speed become important. A camera with "forward motion compensation" is needed for such close-up work. Such cameras move the film during exposure at a speed that compensates for the aircraft speed. Though the image is moving within the camera, it stays at a fixed location on the moving film itself.

The new technology of digital cameras has recently become available. Imagery is recorded electronically instead of on physical film. Data are then already compatible with computer analysis. Imagery can be viewed and downloaded soon after acquisition. Resolution is not as good as film photography, but some cameras (such as about 4000 x 4000 pixels) are reasonable substitutes. Some expensive mapping cameras are becoming available which have a much greater number of pixels across the scene. The time between subsequent exposures is limited by the time to download an image to the storage device; it increases with image size. Various image compression techniques are offered with the better cameras to speed storage times and save storage space. Some digital

cameras are configured for CIR imagery. Numerous aerial imagery vendors are now offering digital imagery.

Videography

For some projects, videography offers an inexpensive RS system. Videotape is much cheaper than photographic film and can be viewed soon after acquisition. Home video cameras used to be of a quality that was inadequate for RS work. That was easily demonstrated by grabbing and viewing a single video frame. Imagery was grainy. A broadcast quality (expensive) camera is needed for most RS work. However, both cameras produce imagery of limited resolution. Though the computer might render an image as 480 x 640 pixels, the vertical part of the image is really made of roughly 350 lines. Furthermore, each frame is captured in a total of 1/30 sec, but in two halves. First, every other line is sampled in 1/60 sec. Then the camera captures the intervening lines in the next 1/60 sec. If there is forward motion of the scene, as from a camera pointing directly downward (at nadir) from a helicopter or aircraft, the movement will create offset duplication of scene features, as in a double exposure. The video capture system then needs to be instructed to capture only the first or second half (field) of the scan and duplicate it as the missing lines of the other 1/60 sec. That reduces the effective resolution even further.

Video systems in use in the USA and some other countries are in the NTSC format. Systems in Europe and many other countries use the PAL format. Though cassette tapes are physically identical, the data are so different that a PAL tape played on an NTSC machine does not produce anything visible on the display. This becomes a problem only if foreign projects are under consideration. Special equipment is required to convert between the video formats.

The half-inch video tapes common for home use are inferior to broadcast (3/4 inch) tapes in terms of image quality. The latter require special players to view. The use of the better tapes reduces the graininess of the video imagery, making it more suitable for remote sensing investigations. Recording media are rapidly improving and storage devices are becoming tiny. The image resolution and quality for the new systems have not yet been evaluated by our office.

A new technology of digital video is becoming available, promising greater quality of imagery and greater resolution, with recording onto much smaller tapes and devices. This may be the preferred system in the future. We are beginning to test the modern digital video cameras.

Scanners

A scanner views the Earth (or other scene) one to several lines at a time at an orientation perpendicular to the flight direction of the aircraft or satellite. One style of operation has

the view of the sensors mechanically moved along the line of examination, recording the variation of radiance reaching the instrument in various spectral bands. Another style is to have a linear array of detectors ("pushbroom") that views the scene (a slit view) simultaneously. The array of detectors is interrogated sequentially for the radiance values at each location along the viewing line. Either style produces a stream of data, line by line, for recording. The forward movement of the platform provides the displacement for the perpendicular dimension in order to create 2-dimensional imagery. Scanners have been designed with variable numbers of spectral bands, from monochrome to multispectral to hyperspectral.

Satellites

Earth-observing satellites began with weather satellites in the 1960s. The AVHRR instrument on the modern NOAA weather satellites is additionally used for coarse (1 km) vegetation health mappings. The satellites were soon adapted to the Landsat series of polar orbiters in sun-synchronous, low-earth (LEO) orbits, gathering their images at about 10:30 a.m. each day at about 30 m resolution. Imaging technology grew from videography to multispectral scanners (MSS) to thematic mapper (TM, a better scanner), and subsequent enhancements. The French put up a series of SPOT satellites for land cover imagery. India then had a series, IRS, with a wide range of resolutions. Some other systems specialized in oceanic views (Orbview-2). The new trend is towards much finer resolution (4 m 4-band color, 1 m panchromatic or better) from IKONOS, QuickBird, and Orbview-3. The Terra satellite (10:30 a.m.) carries the MODIS (wide angle, coarse resolution, three dozen bands) and ASTER (14 bands, VNIR, SWIR, TIR, comparable to Landsat resolutions) instruments; the Aqua satellite (1:30 p.m.) carries another MODIS instrument.

The navigational satellites, GPS and the Russian and European equivalents, are in a middle altitude above the earth, with orbital periods of about a half day. They are not used for imagery. The geostationary imaging satellites, such as the GOES series are mainly used for weather surveillance, always viewing from the same position over the equator. Most geostationary satellites are used for communications of various types.

An important consideration is repeat coverage. The modern Landsat series images the same location every 16 days. Other satellites can be aimed off-nadir for more frequent views, such as every couple of days. Off-nadir viewing allows the creation of stereo pair imagery from which elevations can be derived. The several decades of Landsat coverage allow for change detection studies. However, that coverage will become reduced because of a component failure in Landsat-7 at the end of May 2003. Landsat-5 (launched March 1985), which still takes images well after its designed lifetime, can substitute for a limited time. There are several satellites using microwave energy. Those like Radarsat (and comparable European and Japanese satellites) and a few Shuttle flights operate(d) radar to measure surface topography and texture. They could view through clouds and operate at night. The latest Shuttle series has acquired topographic data for most of the earth. Radar is good at mapping flooded ground and oil slicks on water. Other satellites

passively measure falling rain or the water content of snow packs, though at coarse resolution.

The Civil Applications Committee is promoting use of Department of Defense satellites for government projects and studies. However, viewing of such products must be done in secure facilities and the analysts must have security clearance. More recent directives have suggested that commercial satellites be used whenever possible.

There are now dozens of past and present satellites with available data in the visible and infrared bands. Fig. 29 shows the spectral ranges and pixel resolutions of most of them. Our satellite remote sensing has traditionally used the Landsat series. The old satellites provided MSS data in 4 bands (green, red, two near-IR) with coarse pixels that were not square. The Thematic Mapper (TM) then provided 6 visible and infrared bands at 30 m resolution and a thermal band at 120 m resolution. Landsat-7 improved the thermal resolution to 60 m and provided a 15 m panchromatic band. However, Landsat
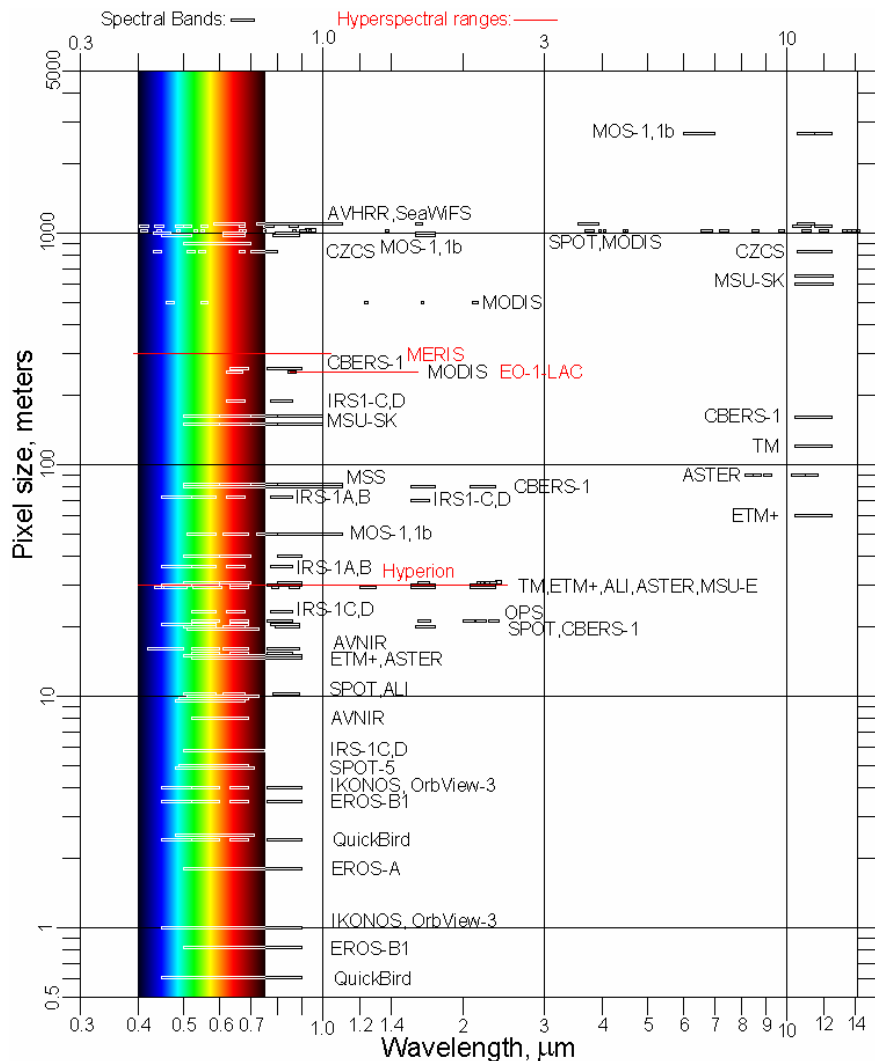
Fig. 29. A graph showing the spectral and pixel resolutions of various satellites.

23

data are becoming unreliable for future use. Landsat-5 is much older than design specifications. Landsat-7 has lost its scanning correction for getting its scan lines parallel with respect to the earth, creating gaps in coverage away from the orbital path. There is no good replacement when these satellites fail completely.

The EO-1 satellite, in orbit 1 minute behind Landsat-7, carries the ALI (Advanced Land Imager) camera which occupies only a quarter of the Landsat swath. It has more numerous bands in the visible to mid-IR, at much better signal-to-noise ratios than Landsat. However, there is no thermal band. The satellite also carries the Hyperion hyperspectral instrument with about 190 useful spectral channels (visible to short-wave-IR) but only a 7.5 km swath at 30 m pixel resolution.

We have made limited use of the French SPOT satellite system data. The latest SPOT-5 has a variety of resolutions from 1 km to 2.5 m in various wavelengths but no thermal imagery. The Indian IRS-1C and -1D and the new Resourcesat have resolutions near 180 m, 23 m, and 5.6 m, but without thermal imagery. Both satellites do not automatically take pictures but must be tasked for specific views.

The ASTER camera can be a good substitute for Landsat imagery, but it must be tasked
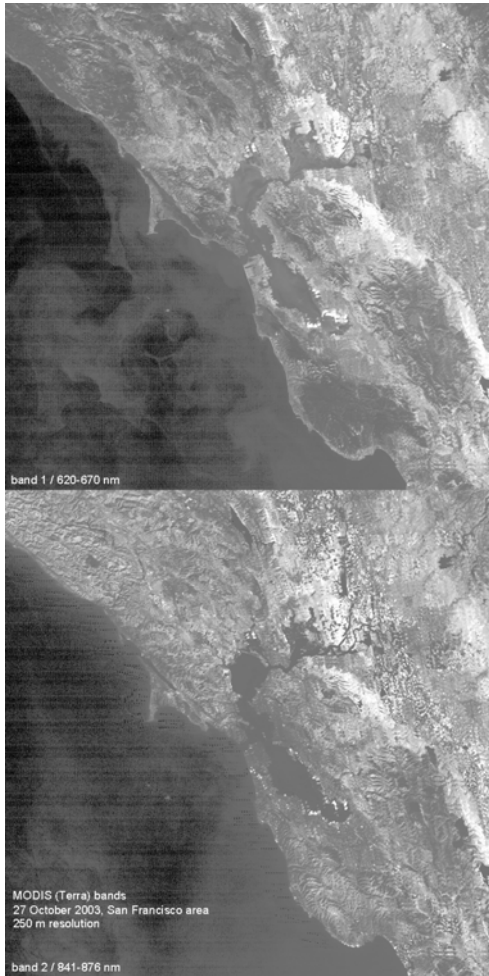
for its views; it does not routinely take pictures. The 3 VNIR bands are at 15 m resolution, good for vegetation and cultural mapping. 6 SWIR bands are at 30 m resolution, possibly good for mineral mapping. 5 thermal IR bands can not only give temperature data (useful for evapotranspiration calculations) but can be manipulated to yield basic rock types: carbonate, silicate sands and shale, and igneous/metamorphic.

The MODIS camera on the Terra and Aqua satellites provides only coarse resolution of limited use to Reclamation needs. Some of the bands are designed for water penetration and are saturated over land and clouds. Some of the bands have excessive noise.

Three figures for the different resolutions are provided for viewing. The scene is of the San Francisco area on 27 October 2003, a date with extensive fires farther south. Fig. 30 shows the two bands at 250 m resolution. Fig. 31 shows the five bands at 500 m resolution. Fig. 32 shows the 29 bands at 1 km resolution. Notice the horizontal striping in the images, indicating that the elements in the sensor arrays are not

Fig 30. Two MODIS 250m band views of San Francisco area.

24

balanced. This striping becomes strong in some of the 1 km bands. Some of the 500 m bands show artifacts of dark ocean signatures below threshold. The top half of Fig. 32 is for reflective bands. Bands 13 and 14 are given in low and high gain versions. Bands 15 and 16 saturate on land. The lower half of Fig. 32 are emissive bands, sensing only the energy emitted by the earth's surfaces. Bands 27 and 28 do not see the ground. Band 36 seems worthless. All of the bands have georeferencing challenges that increase from the nadir (orbital path) sidewards to the edge of the view.

Fig. 33 shows the Terra view of the Salton Sea, near the eastern edge of the view. The 250 m pixels are acquired in a swath of 40 pixels. The 500 m pixels are acquired in a swath of 20 pixels. The 1 km pixels are acquired in a swath of 10 pixels. When viewing near the nadir the swaths abut but do not overlap. Near the edge of the view, far from the satellite, the views expand greatly so that the swaths significantly overlap, as shown by the segmented view of the Salton Sea. This suggests that it may be better to get summarized and georeferenced data rather than the basic L1B data. In contrast, Fig. 34 shows the Aqua view of the Salton Sea 3 hours later, which was near-nadir. The Sea is larger in the figure because it is closer to the satellite. Image overlaps are difficult to detect in the Aqua view.
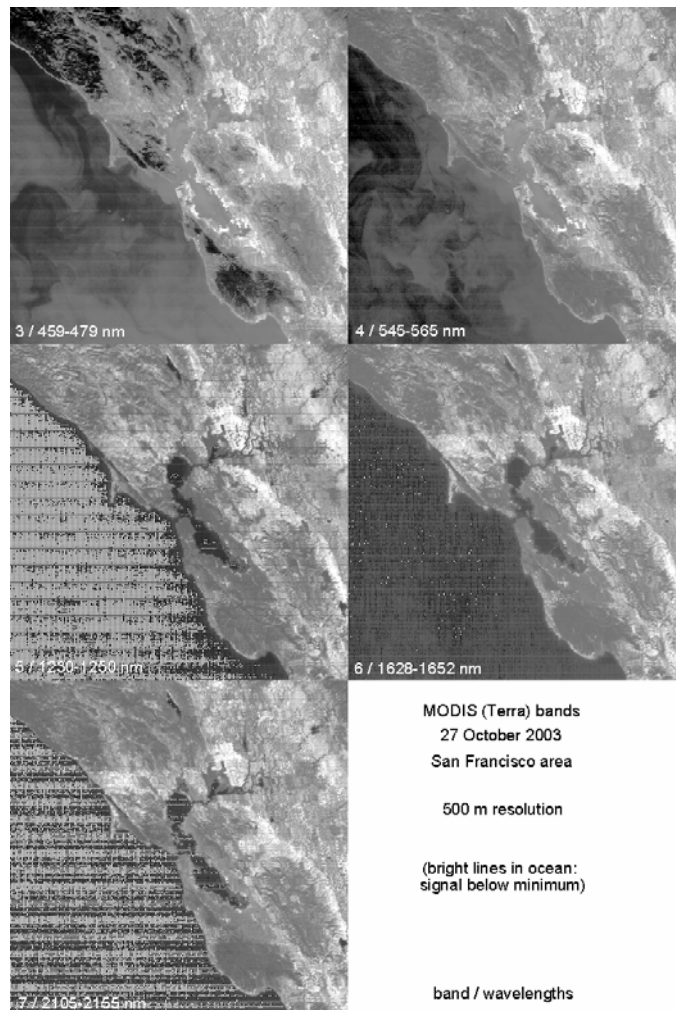
Fig. 31. The five MODIS 500m band views of the San Francisco area.
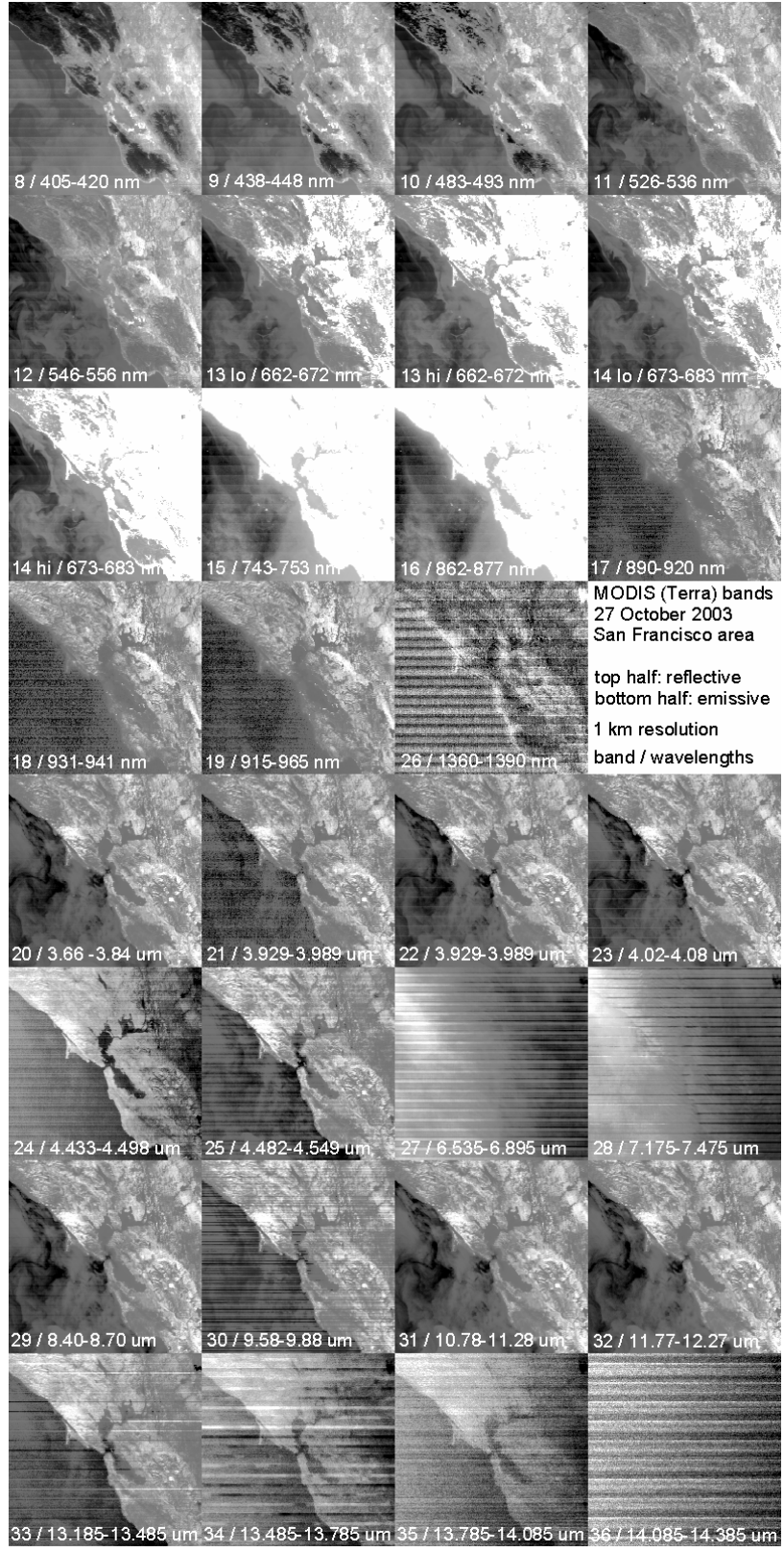
Fig. 32. The 29 MODIS KM band views of the San Francisco area.
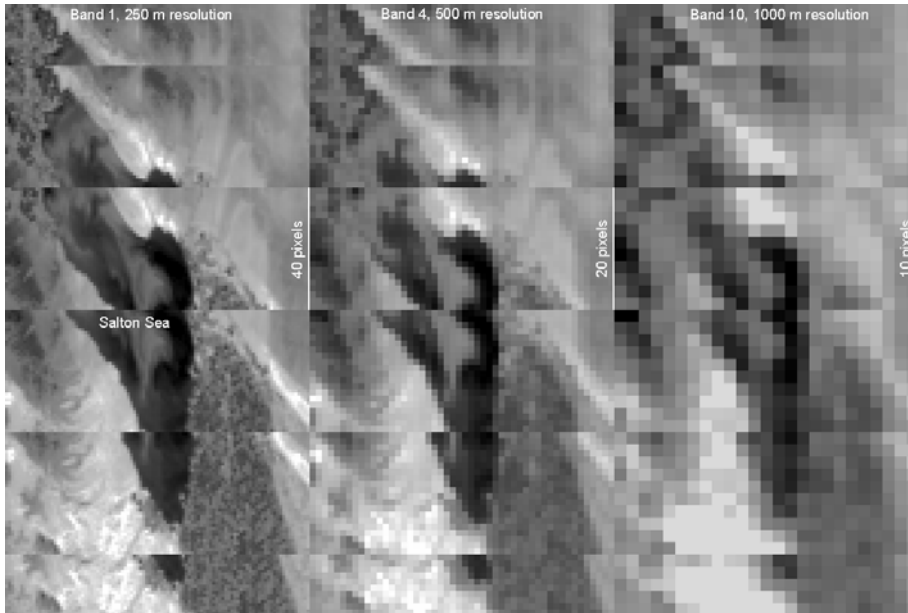
Fig. 33. The edges of the MODIS scans overlap.
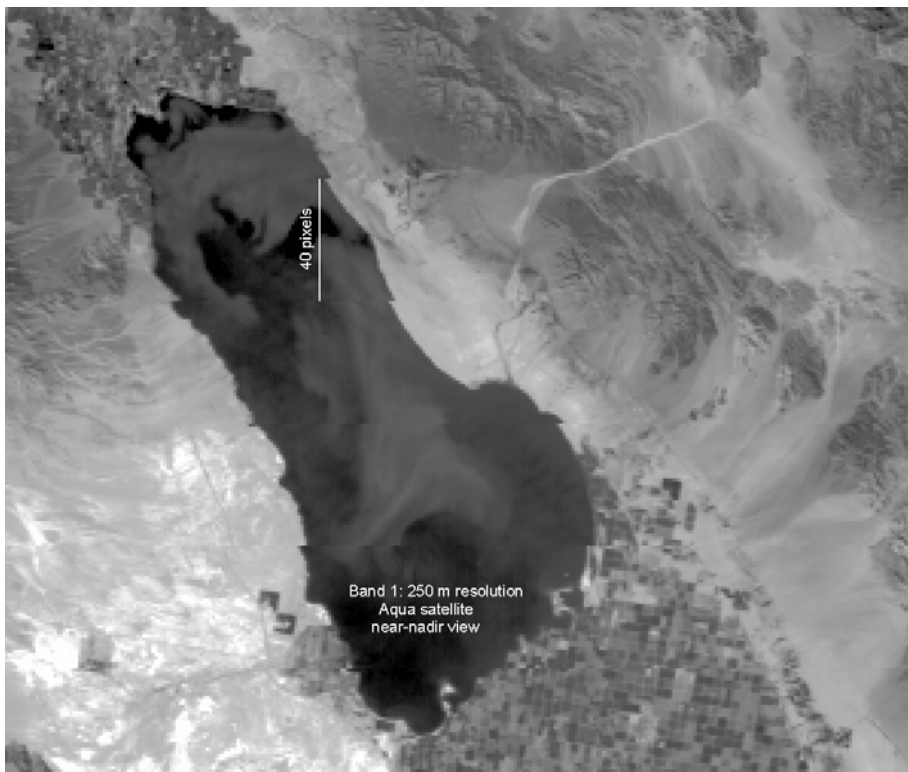
Fig 34. Objects are larger in the nadir view, with minimal scanning overlap

Radar

Radar involves illuminating a scene with pulses of radar energy. The timing of the reflection indicates the distance to objects in view. Radar beams are normally transmitted at a slant angle to the ground. Tall objects will appear closer to the radar unit than their

map position indicates. Terrain can block radar beams, causing shadows. The strength of the return signal indicates something of the nature of the surfaces. The orientations of the polarization of transmitted and returned energy give additional information about the surfaces. Mirror-like surfaces, like smooth water, return nothing. Geometric surfaces, like buildings, can act like corner reflectors, sending back a strong return pulse. Therefore there are interpretation challenges for raw radar data.

Radar has long wavelengths, compared to other parts of the electromagnetic spectrum. It therefore requires transmit and receive antennas comparable in size to the wavelengths. Larger antennas give greater focus to the radar beams, but large antennas may be too large to carry on aircraft and spacecraft. The solution is to continuously record radar data as the antenna is moved along to different locations. The technique is called Synthetic Aperture Radar (SAR), simulating a line with lots of antenna segments that, with computer processing, appear to be parts of one giant antenna. Most airborne and satellite radar systems are operated in such a mode. The Shuttle Radar Topographic Mission (SRTM) recorded elevation data for most of the earth. It has been processed to 1 arc-second (about 30 meter) resolution for continental USA and 3 arc-second resolution for the rest of the world except polar and ocean areas. Similarly, SAR data from different aerial flight lines can be used to produce digital elevation modes of the terrain.

For additional refinement, radar data can be analyzed in an interference mode. For example, data from different dates can be compared for minute differences, thereby indicating topographic changes from earthquakes and volcanoes and speeds of glacier flows.

Fig. 35 is from east of Yuma, Arizona, taken by the Radarsat-1 satellite. The brightness indicates the strength of the radar reflection. Hills in the lower right appear to lean eastward towards the satellite, as is typical for radar data. Agricultural patterns are visible near the Gila River.
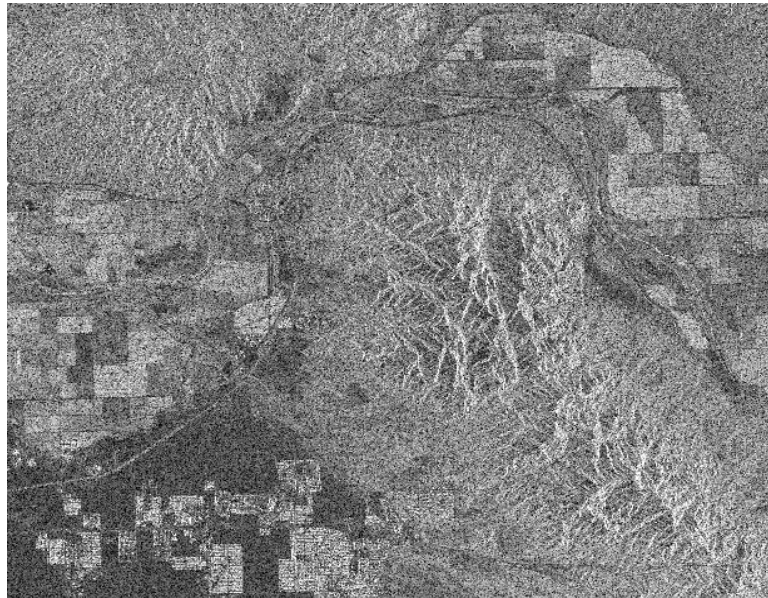
Fig. 35. A Radarsat view of the hills east of Yuma, AZ degraded to Landsat resolution.

The enlargement of the river area (Fig. 36) shows more detail of roads, a railroad, the river, and fields. The hills are brightest on the east side, being illuminated from the east by the satellite.
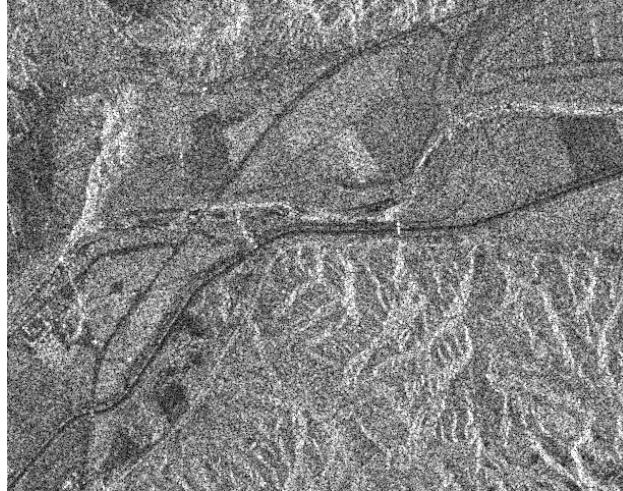
Fig. 36. A Radarsat view of the Gila River, full resolution.

The suburban area in Fig. 37 is strongly reflective, with the geometric buildings acting like corner reflectors. A limited access highway interchange is weakly visible in the center of the view. Street patterns contrast strongly with the buildings.

Fig. 37. A Radarsat view of housing east of Yuma.

Satellite radar imagery is valuable for mapping the extents of flooding. The area covered by water gives essentially no radar return, appearing black in intensity. This Fig. 38 scene is from the Red River flood, showing a region near the junction of Minnesota, North Dakota, and Manitoba. The scene is artificially colored with blue indicating the water areas. Using the section patterns of the fields indicates a flood roughly twenty miles across. Trees give a signal along the river corridor. Such evaluation of floods can be done day or night and through any kind of cloud cover. The satellite provides the illumination energy and clouds are transparent to the radar beam.
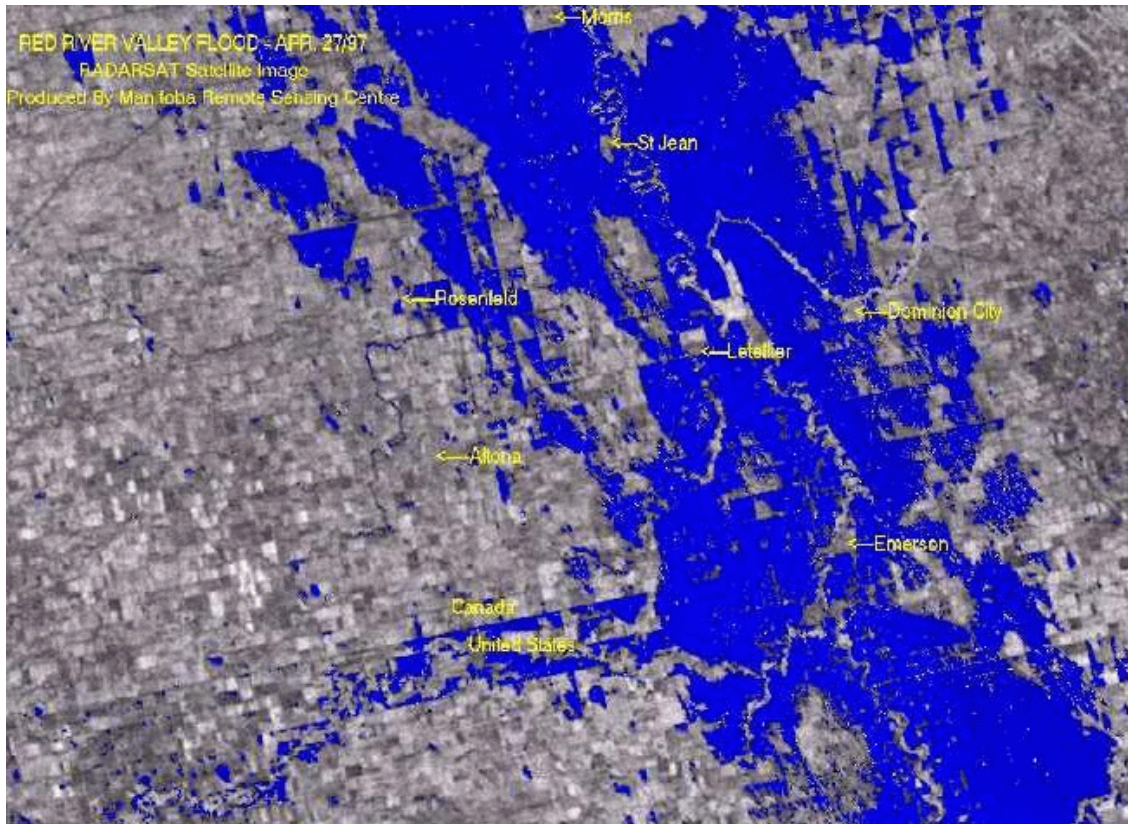
Fig. 38. A Radarsat view of the Red River floods, colorized blue.

LIDAR

Light Detection and Ranging (LIDAR) is another tool that many larger photogrammetric mapping companies have incorporated into their elevation data collection methods in recent years. LIDAR works in a similar way to radar: ranging based upon the speed of light. The beam can be focused to a more narrow point than radar. Both visible and infrared lasers are possible, but there is much atmospheric scatter for blue light. The sensors can receive back multiple reflections from a single pulse, indicating a succession of surfaces at increasing range or depth.

There are two basic types of LIDAR systems, one is used to collect topographic elevation data and the other is used for bathymetric data collection. There is even a hybrid LIDAR system that is supposed to be able to collect both topographic and bathymetric data simultaneously. Aerial use of LIDAR requires knowing precisely where the aircraft is located in 3-dimensions and its 3-axis orientation. An airborne LIDAR systems primary components are a focused infrared laser that emits laser energy pulses toward the ground by means of a scanning mirror, an interfaced inertial measurement unit (IMU), airborne GPS (global positioning system, likely differential), required hardware/software, and the expertise to make it all work properly. Quite often companies will pair a digital camera with the LIDAR system to capture digital imagery simultaneously.

LIDAR systems can capture tremendous amounts of point (x,y,z) coordinate data in a relatively short time frame. Currently many LIDAR systems can collect data at a 1-5 meter post spacing, with a horizontal point accuracy of 1-meter or less, and an expected vertical point accuracy in the range of 15-25 cm. LIDAR data can be collected in daytime or nighttime, and in overcast conditions (if the clouds are above the LIDAR system platform). However, good LIDAR data cannot be collected during adverse weather conditions such as snowstorms, rain, smoke, mist, and fog.

Laser altimetry operates with similar geometric considerations as across-track scanning. Objects away from nadir are seen increasingly from the side as the off-axis angle increases. Near nadir views can permit sometimes seeing the ground through a vegetative canopy, but that can become rare with off-nadir measurements. Bare-earth elevation data is what most Reclamation projects require. Most LIDAR contractors have developed algorithms to classify and remove vegetation, buildings, and other above ground features from the raw LIDAR data in order to produce the bare-earth elevation data. In some instances, such as vegetation/canopy height or infrastructure mapping the multiple-return LIDAR data is needed. However, keep in mind that LIDAR is not always a "silver bullet" solution to your elevation data needs. Contrary to what some contractors say LIDAR does not always penetrate vegetation cover and put the point on the ground, especially in dense vegetation conditions. In some cases the resulting bare-earth LIDAR data points may not have dense enough point spacing for applications such as hydraulic modeling. Just because you specify the LIDAR data be collected with a 2-meter post spacing, you'll likely find the bare-earth post spacing in some places will exceed several times 2-meters. You will still end up with more data points being collected, more quickly, than with about any other method. Don't be surprised if it falls short in some areas. Also remember that LIDAR systems collect "mass points" data, and not necessarily break line data. Your own application may require the collection of aerial photography or digital imagery, so that 3-D stereomodels can be setup on a stereoplotter or a photogrammetric workstation to collect breakline data for your elevation needs. Dense foliage adversely impacts photography and imagery; you can't map what you can't see.

Sample LIDAR data: All in feet, United States Plane 1983, Washington South.

Northing	Easting	Elevation(FT)
374333.5	5015936.6	1508.27
374324.3	5015935.8	1508.48
374321.9	5015934.9	1508.53
374383.3	5015860.4	1508.34
374384.0	5015856.7	1508.30
374378.8	5015852.6	1507.99
374372.2	5015855.4	1508.61
374296.8	5015864.0	1508.71
374276.2	5015879.3	1508.72
374295.3	5015862.5	1508.40
374295.3	5015861.6	1506.67
374272.5	5015879.9	1508.82

These successive records are of variable spacing, and a data set is likely to be many hundreds of megabytes in size. They can be imported as a 3-D vector set or as a surface.

The Fig. 39 orthophotograph is at Dry Falls, in central Washington state. LIDAR was used to accurately map the topography downstream for input to a model of water flows in case of dam failure . The LIDAR data in Fig. 40 were contoured at 1 foot intervals and are here overlaid on the orthophoto. Trees and buildings have been edited out of the data set.

Fig. 39. An orthophoto view of the Dam at Dry Falls.

Fig. 40. LIDAR generated elevation contours at 1' resolution.

LIDAR instruments are also available for use on a tripod mounted on the ground. They can generate a fine scale array of 3D data points which can be edited to remove unwanted artifacts such as trees and other non-surface features. They also record the brightness of whatever the laser beam hits so that a B&W image of the scene can be created for reference.

The Bureau of Reclamation has also used bathymetric LIDAR. It was arranged by Robert Hilldale who supplied these examples. The instrument was a Shoals 1000T manufactured by Optech. It was flown over the upper Yakima River in Washington State, where the water is very clear. Ground truth was provided by a physical probing of the river by poles, with GPS locations. In Fig. 41 the LIDAR provides many more data points (yellow) than the ground crew (blue points connected by a green line) and much more rapidly.
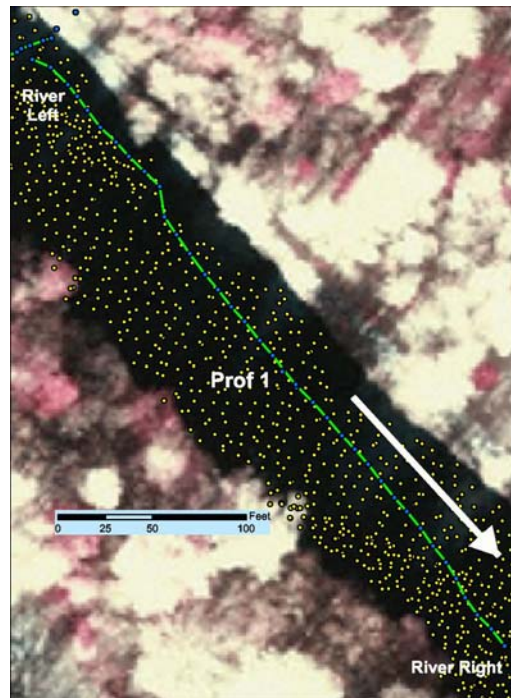
Fig. 41. The distribution of water depth measurements in Yakima River by wading survey and LIDAR.

A comparison (Fig. 42) of the two methods was made by selecting LIDAR points closest to the survey line and within a set distance. The LIDAR measurements are connected by the magenta line, the ground survey by the black line. Differences exist. An instrumental offset was discovered such that the LIDAR processing software needs some adjustments. Sometimes holes and submerged obstructions were discovered by the LIDAR but not the ground survey. It must also be remembered that the LIDAR works primarily in clear, not muddy water.
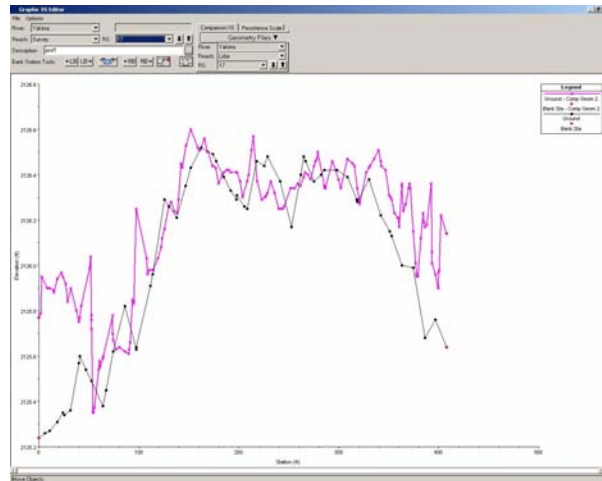
Fig. 42. The relation between hand measured water depths and
LIDAR values.

Thermal

Thermal imagery is available from some airborne scanners or FLIR (Forward Looking InfraRed), and from satellites. Airborne scanner units may be of the Daedalus brand; the thermal band being just one of several wavelengths observed. FLIR instruments were developed for the military and police surveillance and produce a television format output of the thermal data, sometimes with an additional natural color video image of the same scene. Thermal images are affected by the diurnal curve. Water bodies have relatively slow and minor temperature changes as the day progresses. Soil and rocks have little thermal inertia and heat and cool rapidly. Therefore, water can be warmer than land near sunrise but strongly the reverse in the afternoon.

The Fig. 43 FLIR image from the canyon of the Little Colorado River shows the video (visual) view on the left and the thermal view on the right in the hours after sunrise. The shores of the river are dark in the thermal because the damp soil cools to the "wet bulb" temperature in addition to being cooler from overnight radiation loss. Therefore thermal remote sensing can sometimes give an indication of soil moisture. Dry rocks and soils are not as cool. Rock ledges are often visible because of differing thermal inertia from the surrounding rocks. In addition there is a flow of warmer water entering the river from a warm spring on the side, contrasting with the cool shores.

FLIR video and temperature patterns
28 May 1994, 07:51:48 am

0   scale   100 m
LCR river mile 12.6

E 233,600
E 233,700 m
N 568,000 m
N

—wide plume

<--spring

flow->

N 567,800 m
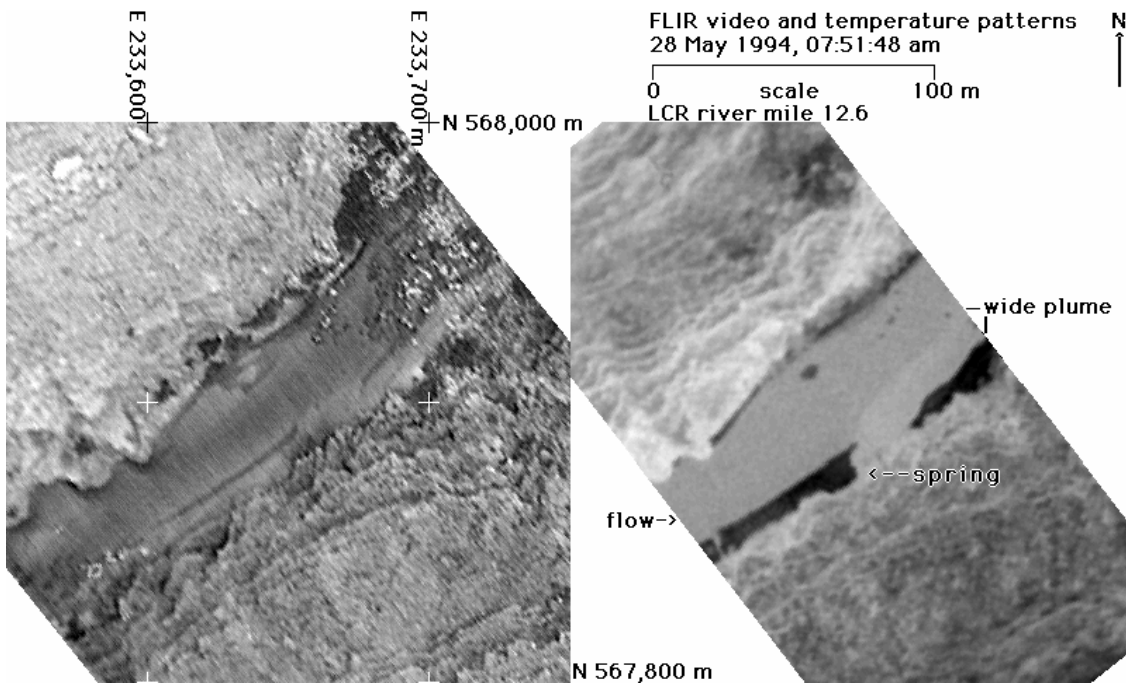
Fig. 43. An example of a hot spring in the Little Colorado River measured by FLIR in Visible and thermal wavelengths.

When properly calibrated, water temperatures can be measured to about 0.2 C precision. The Fig. 44 image is from the confluence of the Colorado River and the Little Colorado River. It was obtained with a FLIR instrument from a helicopter flight about 2500 feet above the river. The Colorado river (blues) is constantly cold, drawing its water from the bottom of Lake Powell behind the Glen Canyon Dam. The Little Colorado is about ten degrees C warmer (reds). It flows along the north edge of the sandbar, then starts to split its flow and rapidly merges into the turbulent and much colder Colorado River. The thermal pattern reveals the dynamics of the mixing waters.

6   8   10   12   14   16   18   20   22   24 °C
Temperatures from FLIR, 28 May 1994
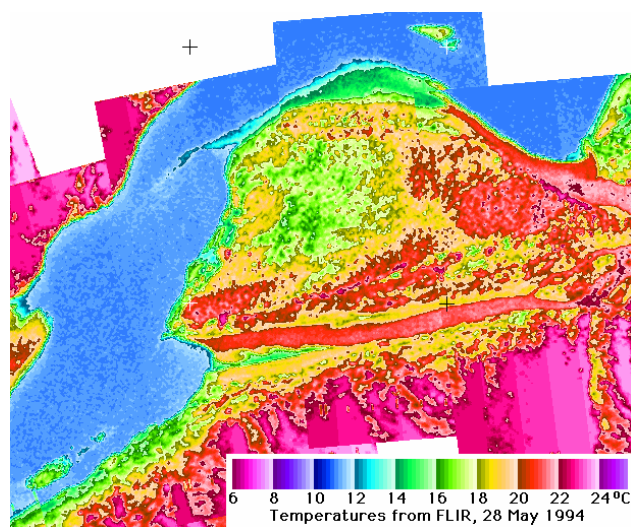
Fig. 44. FLIR thermal data colorized according to temperature.

A Daedalus scanner recorded 3 visible and 3 infrared (including thermal) bands at the confluence of the Columbia and Yakima Rivers in central Washington state. The visible scene is at the left of Fig. 45 and a colorized thermal scene is at the right. The river temperature patterns are strongly evident. The Columbia River (left) is cool (cyan) and mostly uniform. The Yakima river (bottom) is warm (green to orange), especially as it becomes shallow over mud flats near the large island. Thermal scanners can also determine the radiative temperatures of manmade objects, such as house roofs and power plants to see the thermal losses of energy or unusual emissivities. Many of the roofs in the right side of the view look unusually cool (dark blue) because emissivity.
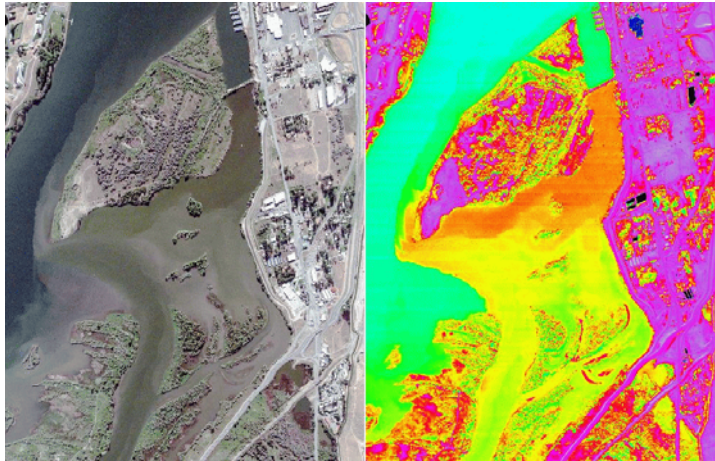
Fig. 45. The visible and thermal (colorized) views of the confluence.

Image geometry

The scale of a photograph is the ratio of the focal length of the lens to the height above ground. For example, a 6 inch lens flown at 2500 feet above ground gives a scale of 1:5000 on the film.

If the camera axis is not vertical, the center of the photograph will not be at the nadir and there will be distortions in the image, shown in Fig. 46, compared to a map view. If the off-nadir direction is parallel to one of the edges of the image, the camera will view flat terrain in the shape of a trapezoid. Otherwise the view will be a more complicated quadrilateral.
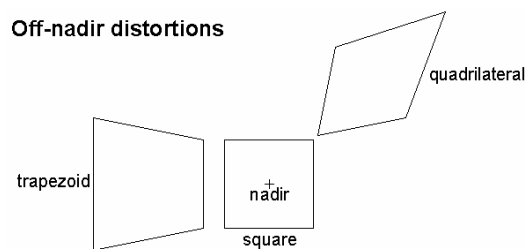
Fig. 46. Image distortions from off-nadir viewing.

Aerial photos are close to agreement with maps only if the subject is flat and the camera is pointed at the nadir. Where there are vertical displacements, the position of an object in the photograph will be displaced radially from its true position. Fig. 47 and the corner enlargements in Fig. 48 are from the Spring Creek development south of Buffalo Creek. Notice that the conifer trees are leaning back radially, with the greatest distortion at the edges. The scene also has vignetting: a darkening with distance from the center that is most severe in the corners.

Fig. 47. Radial leaning of conifer trees.
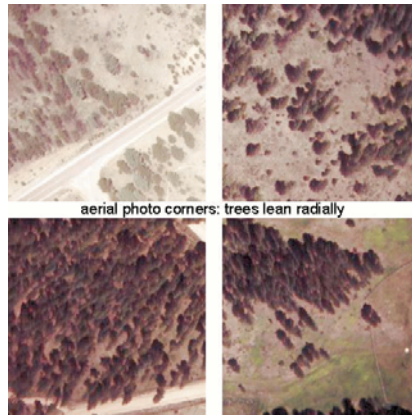
Fig. 48. Enlargements of the photo corners.

The apparent brightness of the scene varies across the view. The anti-solar point (upper left) is brightest. Some vegetation types reflect light back along the incoming path to a greater extent than in other directions. Furthermore there is a minimum of shallowing there. The maximum shadowing is seen in the opposite side (lower right, Figs. 47 and 48) of the photo; both the dark sides of the trees and their shadows contribute there.

Higher terrain causes the terrain to move radially outward on the aerial image. Lower terrain moves inward. In the Fig. 49 image of an entire section of land the roads do not form the perfect square shown in the topographic map, Fig. 50. The view is off-nadir. Furthermore, the road at the top of the image goes over a hill, making it bow outward in the photo. Outward bowing of straight lines is also a symptom of some lenses, particularly those with relatively short focal lengths which approach wide angle or fish-eye lenses.

Fig. 49. Distortion of photo caused by topography.
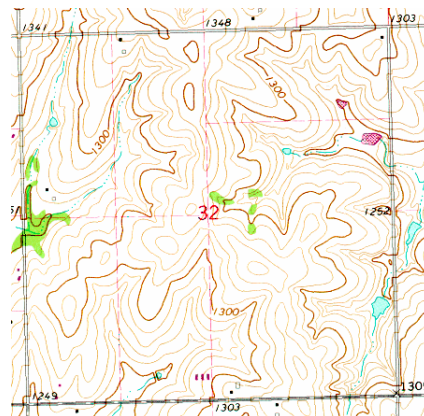
Fig. 50. Topographic map of the section.

36

Scanner geometry is different. As shown in Fig. 51, tall features lean back in a direction perpendicular to the flight path, away from the flight line.
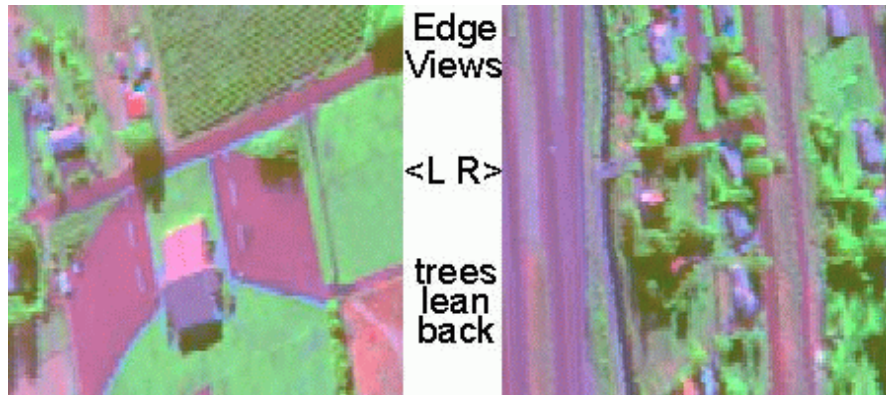
Fig. 51. High features lean away from and perpendicular to the flight track of scanners.

Platform attitude

Aerial images can be distorted by the orientation of the aerial platform. Off-nadir viewing has already been illustrated. Other effects are noticeable with scanner instruments, which put an image together by splicing successive lines of image data. The angular movement of the aerial platform, such as an aircraft, is known as "attitude".

A change in the pitch (angle of attack) of an aircraft results as the nose moves up or down with respect to the center of the aircraft. In Fig. 52, from just northwest of Golden, Colorado, the ER-2 (modified U-2) stratospheric aircraft encountered a wave in the atmosphere as the air bounced as it came over the continental divide and front range. The aircraft's pitch oscillated, causing alternate stretching and compression of the image along the flight direction. Notice that the blurring is parallel to the front range.

Fig. 52. Distortions in caused by pitch.

The roll angle of an aircraft is changed as the aircraft rotates around the flight direction, as in left or right banking. Some aerial instruments can adjust for a limited degree of roll changes by means of gyroscopic control, but the angular changes in Fig. 53 are excessive. This is scanner data. The margins are blackened where the image system could not compensate enough. Elsewhere the distortions can be seen by roads that are not straight.
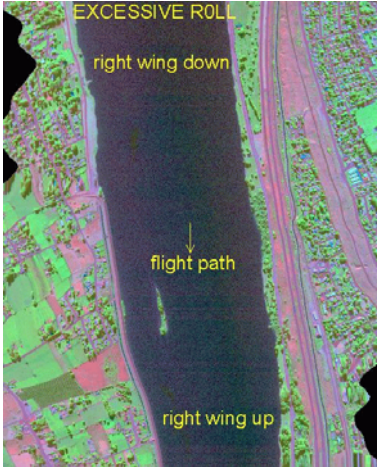
Fig. 53. Distortions caused by roll.　　Fig. 54. Distortions caused by yaw.
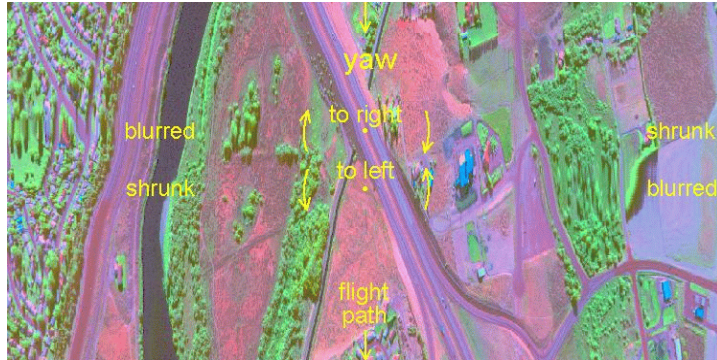
Yaw is a twisting movement as the forward orientation of the aircraft moves to the right or left. For scanner data, in Fig. 54, yaw will create compression on one side of the flight track and expansion on the other, with minimal distortion near the flight track. For aerial photography, in Fig. 55, yaw shows up in successive images that are not at the same orientation with respect to the flight track.
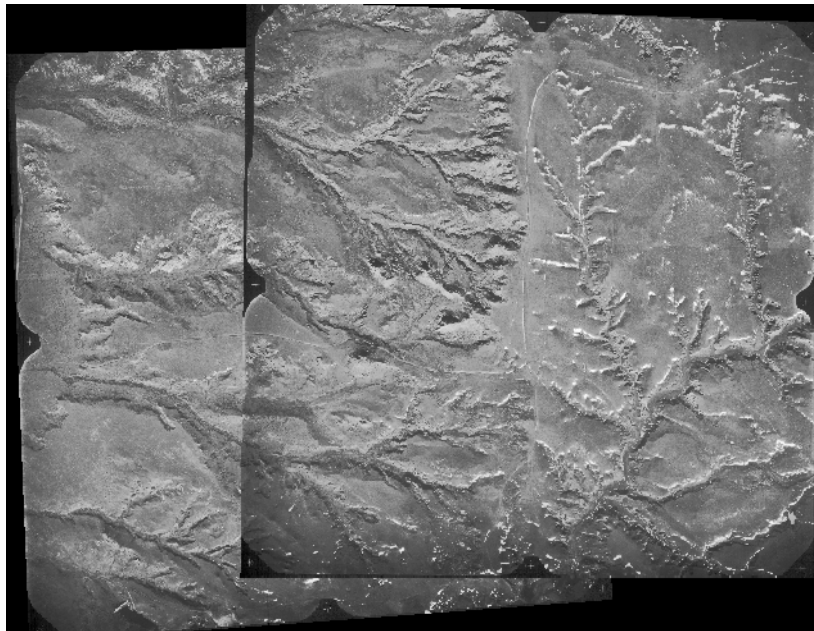
Fig. 55. Displacement in aerial photos caused by yaw.

4. Datum and Projections

The Earth is not a perfect sphere nor a perfect ellipsoid. Therefore there are mathematical models that attempt to describe the Earth. A key word is Datum, which is the name of the model being used. North America topographic maps have traditionally used the North American Datum - 1927 (NAD27) that uses the Clark Ellipsoid of 1866. An update is a 1983 version, NAD83, that uses the GRS 1980 ellipsoid. This is similar to the World Geodetic System 1984, WGS 1984, for acronym and ellipsoid, that is the default system for GPS use worldwide. There are hundreds of local and regional datums in existence. Differences between them can be significant, especially when using location measurements at centimeter scales.

The Earth is has a generally curved ellipsoidal surface. Maps are usually flat planar surfaces. Therefore projections are used to convert Earth positions onto planar maps. The USGS offers a paper poster about map projections. Numerous projections are described and illustrated. The latitude/longitude coordinate system is not a projection. Those coordinates can be converted into a true projection by appropriate mathematical formulas. One of the projections typically used for Reclamation work is Universal Transverse Mercator (UTM), which divides the earth into 60 narrow zones that are 6 degrees of longitude wide; knowing the appropriate zone is important. The Space Oblique Mercator can be used for Landsat satellite images. Conic projections are common, such as the Lambert Conformal Conic and the Albers Equal Area Conic. The State Plane, which can divide a state into 1 to 6 (10 for Alaska) zones, is a variation of the Lambert Conformal Conic. Map products should always indicate the projection being used, especially if the area extent is large enough that Earth curvature is significant.

For a random example of the importance of Datum and Projections, consider a GPS measurement (WGS 1984) location at N 40°, W 105°, elevation 5000 feet (1524 meters), which is northwest of Denver, Colorado, but not necessarily at the ground surface. Using the NAD83 Datum gives the same values. Converting to the NAD27 Datum gives the same elevation, but a position of N 40° 00' 00.055", W 104° 59' 58.073". The UTM position needs Zone 13; using WGS 1984 gives coordinates of northing 4,427,757.219 meters, easting 500,000.000 meters and the same elevation. Switching to NAD27 gives coordinates of northing 4,427,548.876 meters, easting 500,045.692 meters and the same elevation. The northing difference is 208.343 meters and the easting difference is 45.692 meters, for a total (diagonal) difference of 213.295 meters. That is a large difference compared to typical GPS precision. State Plane for Colorado North (NAD83) has coordinates of northing 378,940.842 meters, easting 957,097.095 meters and the same elevation. Switching to Colorado Central (NAD83) results in northing 545,448.335 meters, easting 957,101.063 meters. There are some Datum changes (I was comparing values in Ecuador) which change the elevation values because of ellipsoid differences.

5. Global Positioning Systems

The Defense Department operates a constellation of at least 24 satellites as part of a Global Positioning System (GPS). The satellites have orbital periods of about 12 hours and are distributed in 6 orbital planes so that at least 4 satellites are usually visible in the sky at any given point on the Earth. Receiver stations (many brands - such as Garmin and Magellan - and various qualities, mostly portable) measure the distances to the satellites and triangulate the geographic position of the receiver antenna. Vertical accuracy is less than horizontal accuracy.

In addition, the Russians operate their own network of satellites (GLONASS) and the Europeans are planning a system (Galileo). The systems have two or three levels of accuracy. As originally configured, the American system had a condition known as selective availability. The GPS signals were intentionally degraded to about 100 m accuracy. That option is not presently activated, giving typical hand-held GPS receivers about 5 m accuracy. Military grade receivers, known as PLGR, are available on a restricted basis. They are not subject to the selective availability, even if that degradation option is being applied.

A more accurate mode of operation is known as Differential GPS (DGPS). It depends on a GPS receiver at a fixed location (base station) that determines the error in the signal. That error can be applied to GPS data recorded by a roving receiver within about 300 km of the base station and sub-meter accuracy can be achieved. The corrections can be made in post-processing mode with the recorded data. Some base stations broadcast the error correction in real time. Suitably equipped receivers can use the WAAS correction signal to achieve the greater accuracy.

A survey grade GPS uses a different signal type to achieve centimeter accuracy, but such units cost tens of thousands of dollars and need to be at a fixed location for hours of integration.

The GPS signal is not receivable within most buildings. Tree canopies and cliffs can block the signal, limiting the number of satellites in view. Tall buildings can deflect the signal, causing inaccuracies. It is best to operate with an open sky. That may mean placing a receiving antenna on the roof of a vehicle to get an unobstructed view of the GPS satellites while traveling. GPS receivers can be carried by hand around places of interest, erected on fixed tripods, and attached to vehicles roving an area. They can be attached to aircraft to record the positions at which imagery was gathered. Fig. 56 illustrates a GPS track (red) from a PLGR with roof antenna while traveling on roads shown in an IKONOS image near the intersection of Dodson Road and Frenchman's Creek Road, southwest of Moses Lake, Washington. Only slight deviations from the road are present because of the clear view of the GPS satellites.

Fig. 56. GPS Track in central Washington state.

In contrast is the track shown in Fig. 57 of a Garmin GPS-12 unit carried in a side pack through the Forbidden City of Beijing, China, shown on a QuickBird satellite image (0.6 m resolution). The image has been split so that the upper left matches the lower right. North is at the right. The red line is the GPS track and the cyan line closely approximates the actual route walked. There was loss of signal when passing through buildings. There may have been distortion of signal from reflections from buildings and absorptions by the human body beside the GPS unit. Significant positional errors were therefore caused by having blockages of at least parts of the sky and by reflections of signal. Similar effects should happen with a GPS unit used within a canyon with steep walls.
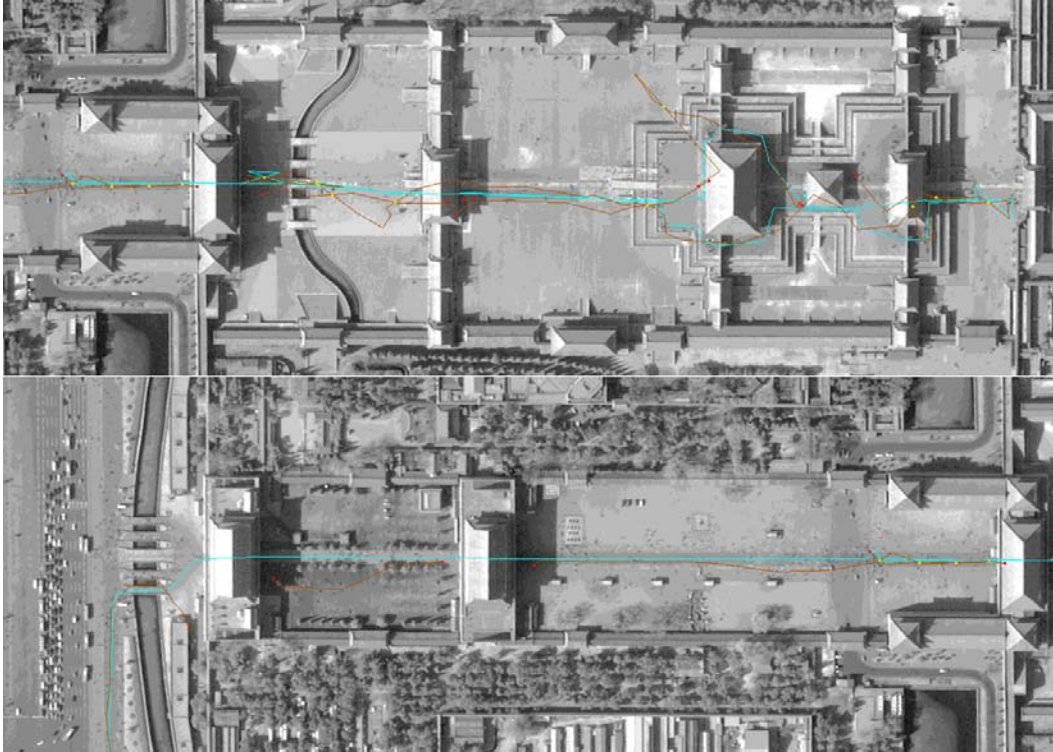
Fig. 57. Distortions and dropouts in GPS track caused by buildings.

6. Image Processing

Adjusting Contrast

Imagery on the computer display (or sent to a printer) can be adjusted for better visibility or for special effects. For illustration the sample scene will be a close-up image of embryo ice crystals formed in a super cooled cloud by a cloud seeding technique of chilling some air colder than -40°. The event took place in a chest freezer in the late 1940s with a black velvet background. Some contrast adjustments may have already taken place as a B&W photo was scanned to form this image. A variety of adjustments will be shown, using graphics captured from TNTmips software displays.

The figures are in pairs, with graphics first and then the resulting output image. The graphics has three parts. The large square in the center to lower right is a graph showing the relation between input pixel numerical values (vertical axis) and output pixel numerical values (horizontal axis). To the left is a histogram, showing the distribution (horizontal axis) of input numerical values (vertical axis). At the top is a similar histogram, showing the distribution (vertical axis) of output numerical values (horizontal axis).

First will be a version "as is" as it comes from the 8-bit grayscale file image using a linear contrast scale from 0 to 255. The left side of Fig. 58 (and similar graphical figures) shows the histogram of the digital numbers in the image. Most pixels have small values, as shown by the bimodal distribution at the left, but there are a few pixels that are bright, as shown by the trailing tail at the upper part of the distribution. Scanned photography will often have such a distribution. The output histogram, displayed across the top of the graphics, has the same shape as the input histogram. The relationship between the input and output images is shown by the diagonal line across the large square. The type of contrast relationship (Linear) is displayed near the bottom, as are the ranges for the input and output numbers. Fig. 59 shows the scene with this linear contrast.
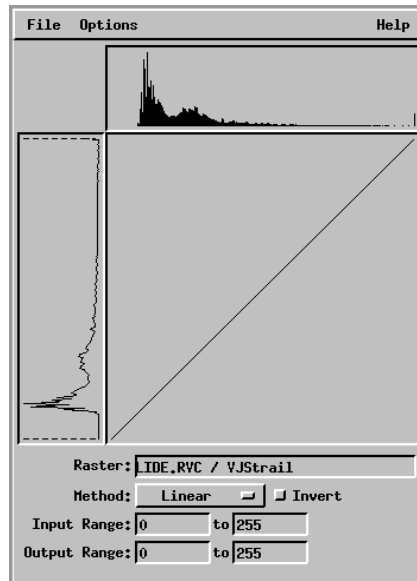
Fig. 58. Graphical representation of full linear contrast.
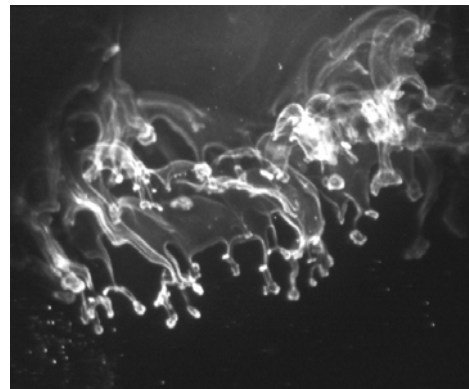
Fig. 59. Snow crystal embryos with full linear contrast.

This software lets the input range be adjusted by sliding the dashed lines in Fig. 60 to different positions. I have selected a lower limit of 17 and an upper limit of 90 in order to isolate the black velvet background and the cloudy air, ignoring the brighter snow particles. Alternatively, I could have simply typed those values in the Input Range boxes. The resulting display in Fig. 61 shows saturated snow but the cloud is more visible. The graph in the large square shows a diagonal line stretching between the limits indicated in the range boxes at the bottom. When adjusting for atmospheric haze, it is useful to place the lower limit at the darkest feature in the scene, such as a lake.
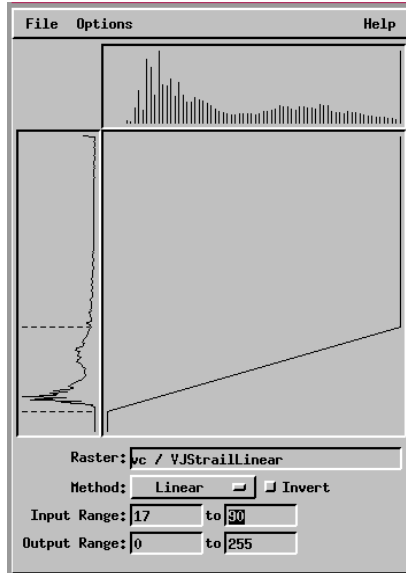
Fig. 60. Graphical representation of partial linear contrast.

Fig. 61. Snow crystal embryos with partial linear contrast.

Then displaying an image with an initially unknown histogram, the "Normalize" contrast method . The histogram of the input image is resampled, so that its output distribution somewhat resembles a normal curve (as defined in probability and statistics). In this case the bimodal distribution prevents a near-perfect fit to the normal curve (Fig. 62), but the result (Fig. 63) is a pleasing rendition that shows all image features: black velvet, cloud, and ice crystals. The normalize process also found that the darkest pixel had a value of 17 and therefore started its distribution at that number. Notice the wavy line in the large square box. The logarithmic contrast method will greatly brighten the dark values while keeping the bright pixels from saturating. The curve in the large square box of Fig. 64 has a shallow slope initially but then a smooth transition to a steep slope. The image in Fig. 65 has a gray background as a result.
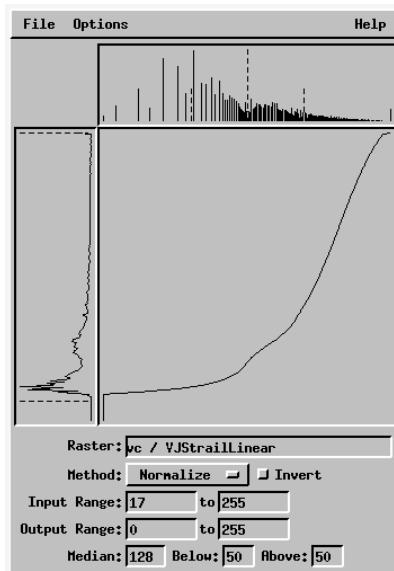
Fig. 62. Normalized contrast
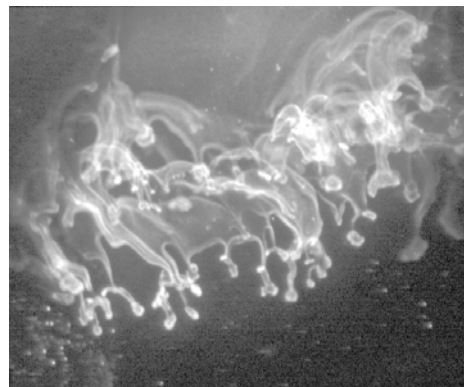
Fig. 63. Snow crystal embryos with normalized contrast.

44
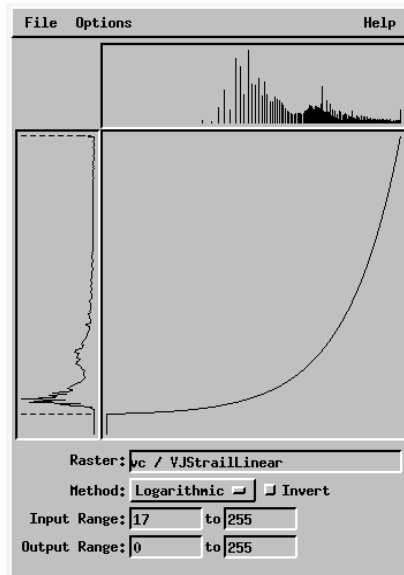
Fig. 64. Logarithmic contrast.
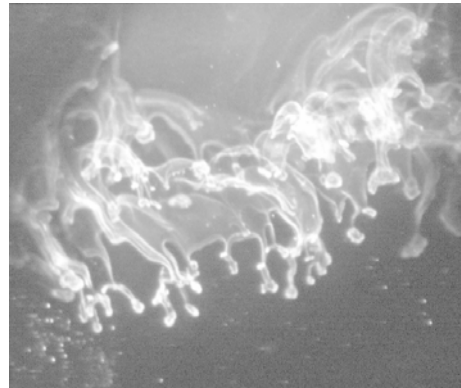
Fig. 65. Snow crystal embryos with logarithmic contrast.

The exponential contrast method gives the analyst much control over the appearance of the output. An exponent of 1.00 (default) is the same as a linear contrast method. An exponent of 0.50, shown in Fig. 66, lies between a linear and a logarithmic relationship. The exponent number may be typed into the box at the bottom or the cursor can drag the curve to its new position (in this software, if not in the others), yielding exponents ranging in hundredths from 0.01 to 100.00. The result in Fig. 67 is a generally pleasing view without saturations.
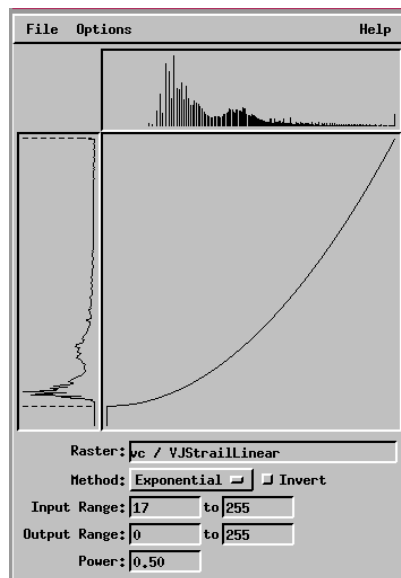
Fig. 66. Exponential contrast with power 0.5.
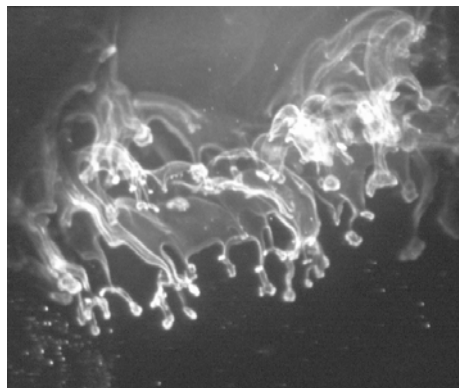
Fig. 67. Snow crystal embryos with exponential contrast with power 0.5.

45

If the exponent is greater than 1.00, the bright values are enhanced and the darks are made darker. In Figs. 68 and 69 a value of 2.00 effectively eliminates the black velvet and the cloud, leaving only the higher concentrations of ice crystals.
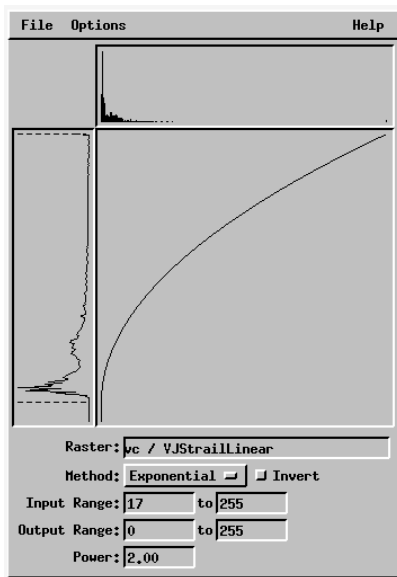
Fig. 68. Exponential contrast with power 2.0.

Fig. 69. Snow crystal embryos with exponential contrast with power 2.0.

Sometimes the input image may be a negative and the contrast needs to be inverted, as shown in Fig. 70. This produces in Fig. 71 black ice crystals on a bright background, much like astronomers often display pictures of stars.
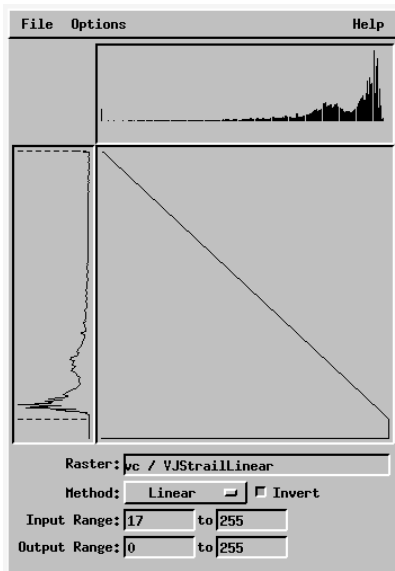
Fig. 70. Inverse linear contrast.
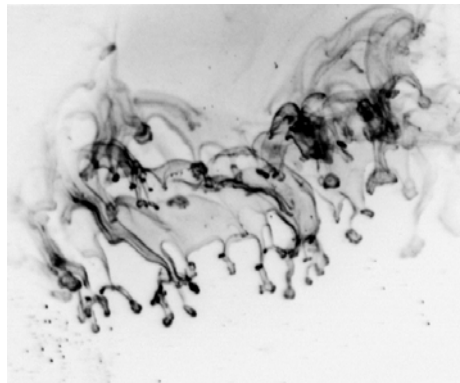
Fig. 71. Snow crystal embryos with inverse linear contrast.

These illustrations have been with single band monochrome images. When a color image is displayed as Red-Green-Blue, each band may be individually enhanced with possibly a

different contrast method. However, it is usually good to keep the contrast method the same but possibly vary the Range limits. Similarly to the last illustration, color negatives can be inverted to get positive images.

Gray scale imagery that is 8-bit can be artificially colorized. In the color look-up table of Fig. 72 the values of 96 to 254 have been given a spread from Blue through Red to purple, enhancing the ice crystals. The values saturated at 255 have been left as white and all dark values remain the same. Random colors could also be assigned. The colors highlight regions of the scene in Fig. 73.
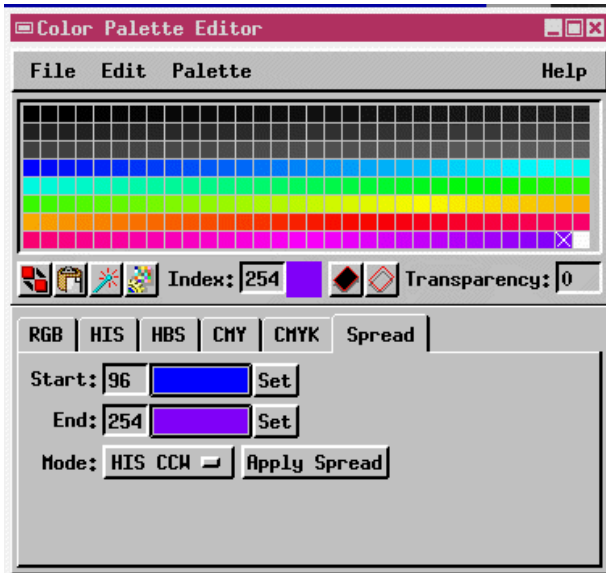
Fig. 72. Color table used to colorize snow crystal embryos.
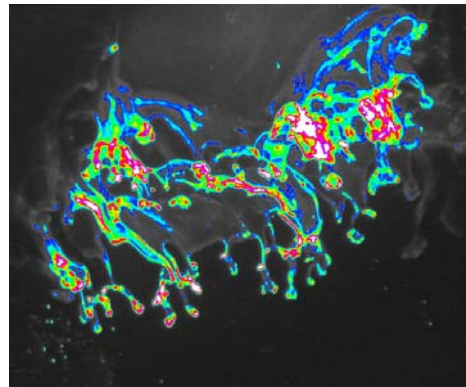
Fig. 73. Colorized snow crystal embryos.

Displaying Color

In Fig. 74 I have selected a portion (300x300 pixels at 15 meter resolution) of a scene from the North Rim of the Grand Canyon, as seen by the ASTER camera on the Terra satellite. The actual color bands are green, red, and NIR, which display to the standard false-color infrared rendition (healthy vegetation is red). At the bottom of the view are the headwaters of Bright Angel Creek. The image was converted from R,G,B separate bands to 24-bit, 16-bit, and 8-bit composite color images. Within the scene, slightly lower than center, a region of individual pixels was selected about the pixel at line 215 and column (row) 169, as shown in the image extract with the cross-hair symbol in Fig. 75.
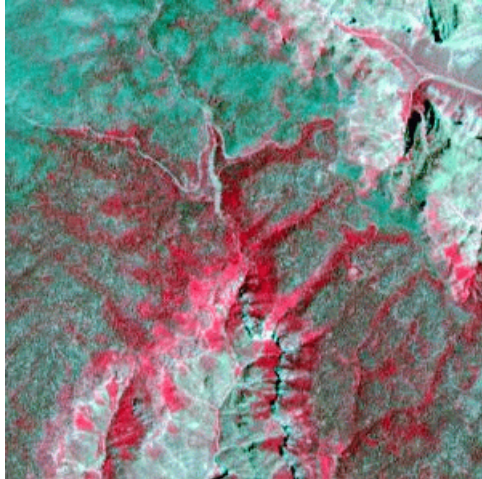
Fig. 74. ASTER view of part of the Grand Canyon
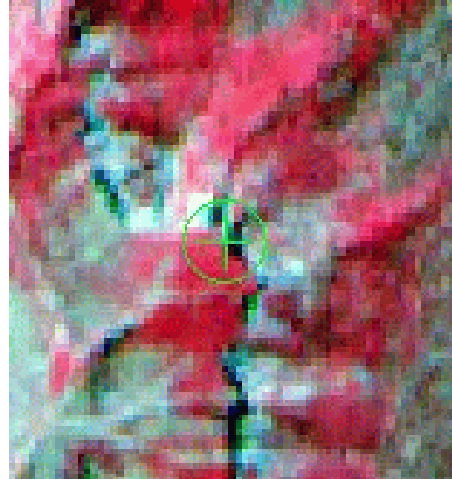
Fig. 75. Subset of the ASTER view, marking a particular pixel.

The pixels in a 24-bit composite image are made of 24-bit integers (3 bytes). Each of the 3 bytes represents an 8-bit Intensity, ranging from 0 to 255. The byte order may be RGB or BGR. The TNTmips software allows the examination (and direct modification) of nominated pixel values. The first illustration, Fig. 76, of the table of pixel values has a box around the pixel at (215,169). Within the brackets are the numbers 109, 84, and 153. Therefore Red has a value of 109 out of 255, Green a value of 84, and Blue a value of 153. To the right is a pixel with values [0 0 0], indicating pure black. To the lower left are many pixels with greater amounts of red. Two and three pixels above the target pixel are values of 255 for both blue and green. This software allows direct editing of individual pixels; any other numbers can be typed into the "Raster Value" boxes to permanently change them in the image.

The 16-bit images have 5 bits per color. Notice in the Fig. 77 table that the color values range from 0 to 31.
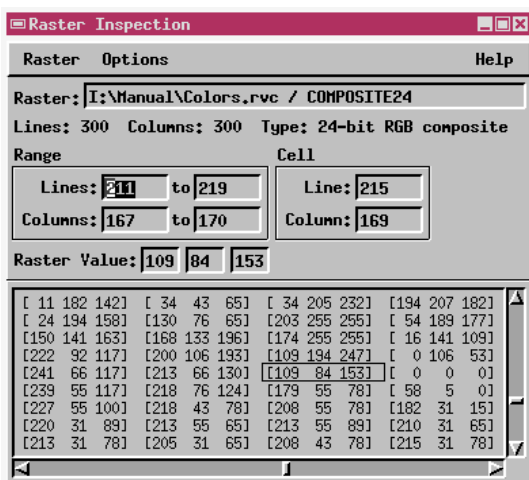
Fig. 76. Pixel values for a 24-bit color composite image.
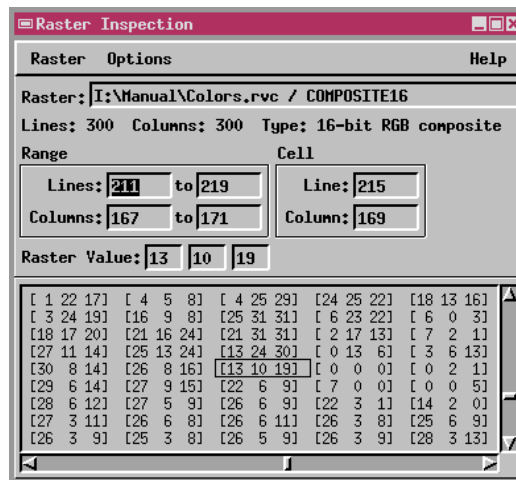
Fig. 77. Pixel values for a 16-bit color composite image.

48

The 8-bit images have a very different structure. The numbers 0 to 255 are assigned randomly to a look-up table of the various colors in the image. (In conversion from 24 or 16-bit color to 8-bit color, the closest of the 255 possible colors is used.) In this software, the most frequent colors are assigned to the smallest integer values and the rare colors to the largest values. Notice in the illustrated Fig. 78 table for the 8-bit image that the numbers seem quite random, unrelated to the scene. The color look-up table is displayed in Fig. 79 for reference.
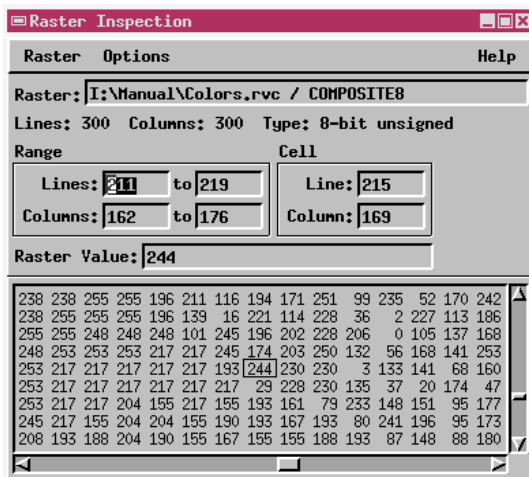
Fig. 78. Pixel values for an 8-bit color composite image.   Fig. 79. The 8-bit map for the ASTER image.
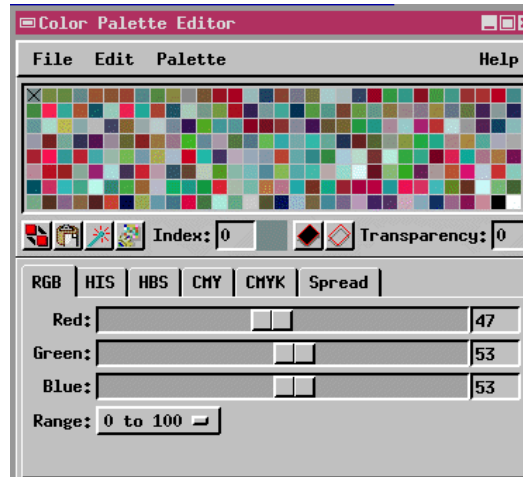
Resampling Styles

Resampling of images to change sizes, orientation, or projection gives the analyst three choices: (1) nearest neighbor (NN), (2) bilinear interpolation (BL), and (3) cubic convolution (CC). NN selects the pixel of the former image that is closest to the target position in the newer image, simply copying its value or color assignment. BL takes the four former-image pixels surrounding the target position and combines the linear interpolation between the opposite pairs of pixels. The resulting value will be somewhere within the range of the values of the 4 pixels. CC uses 16 former-image pixels about the target location for a more precise selection of a new pixel value. Where a linear feature is in the image that is not parallel to the lines or columns of the image, the NN process will usually cause a slight offset in the line in various places. The BL and CC processes will have smoother transitions.

It is very important to understand the color style when selecting a resampling style. There is a trap! If a 24-bit or 16-bit color image is resampled, there will not be a problem. For example, the ASTER image of the Grand Canyon was edited to make a vertical black line 2 pixels wide. The image was then rotated 5 degrees clockwise using the 3 resampling styles. A 100x100 subset of the result was extracted for each style and shown in Fig. 80. The edited 24-bit image was also converted to an 8-bit image and the 8-bit image was rotated 5 degrees using the 3 resampling styles. The same subset was extracted from the 8-bit rotations and shown in Fig. 81.
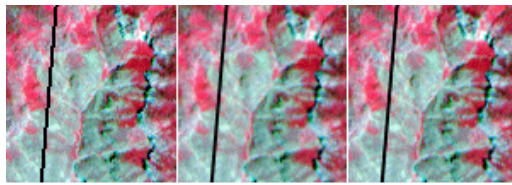
Fig. 80. A 24-bit sample ASTER image   Fig. 81. An 8-bit sample ASTER image
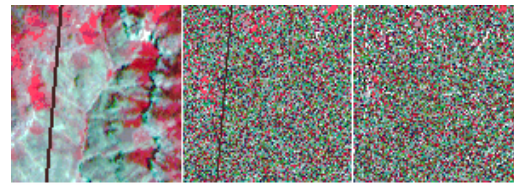
The 24-bit NN style shows a segmented black line. The BL and CC styles have a smoother line, with the CC having a slightly better image. The 8-bit NN style looks like the 24-bit NN rotation. However the BL and CC images do not resemble the scene! That is because the resampling by the BL and CC methods interpolate the digital numbers and assign a new one to the result. But the color table remains the same and the pixel gets a random color assignment. For this reason, 8-bit color images must use the NN resampling method. If the 8-bit image is only a monochrome, gray-scale image, then the other methods may be used. Similarly, when resampling an image in which the numbers represent classifications, NN must be used to avoid having pixels reclassified to something else.

Filters

Imagery can be cleaned up of artifacts and filtered. Many filter types are available and the choice depends upon the particular need. The first example is an image with much dust on it. A 35 mm slide view of the north end of the Dead Sea was copied commercially to a duplicate slide, but unfortunately the original had dust on it that was not removed. The duplicate slide was scanned to produce the initial image (Fig. 82). (The dust may not show at this enlargement scale.)

Fig. 82. The Dead Sea with dust on original slide photo.

An efficient way to clean up the image is to convert to HIS and then work with the Intensity image. A subset of the initial dusty image is shown at the left of the triple series in Fig. 83; all three are shown with Normalized contrast to make the dust more visible. A simple 3x3 Low Pass Filter was applied for the middle view. Unfortunately, it is just a simple average of the nine pixels centered on the output pixel; extreme values affect such an average. The dust is blurred but is still visible. For the right view the initial Intensity image was hand edited at the large dust spots, manually typing in replacement numbers that were similar to the pixels adjacent to the dust; perfection was not attempted. Next a 3x3 Median Filter was applied. It takes the median value of the nine pixels around the output pixel and assigns that median to the output. Extreme values are thereby ignored. The dust and other noise in the image was removed. An exponential

50

contrast, with power 0.50, was applied to the result to make the dark foreground more visible.
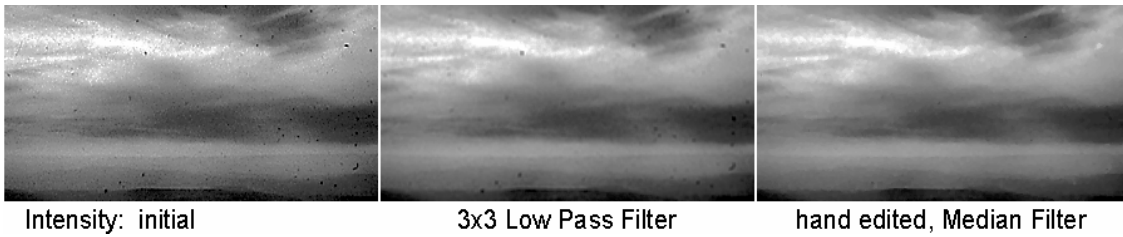
Fig. 83. The raw and filtered intensity portion of the dirty image.

The former Hue and Saturation (which still contained some residual dust signatures) were combined with the median-filtered Intensity to produce a revised color image, which is shown as Fig. 84. However, what if the dusty and other features need to be made more visible? There are other filters available. Three are shown as examples in Fig. 85. The general advice is simply "try it and see."

Fig. 84. The cleaned and brightened version, Dead Sea.
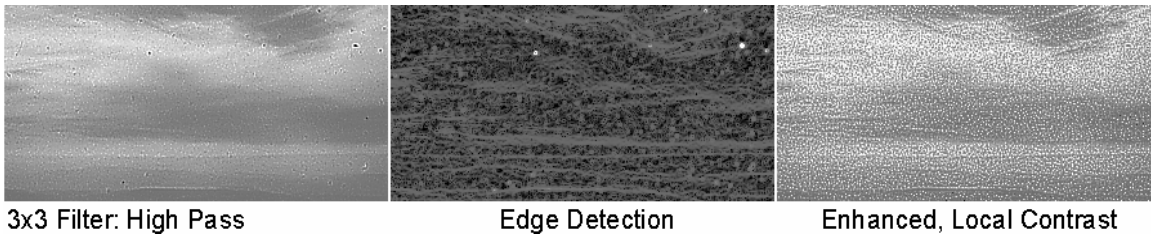
Fig. 85. Three enhancement filtered images.

Fast Fourier Transform Filters

Sometimes instrumental noise creates banded or repetitive patterns in an image. That could be from a 60 Hz hum or other special frequencies. An example here is an image from a FLIR (Forward Looking InfraRed) instrument taken in the early 1990s. The image was written to NTSC television format, scanned in pairs of lines. There are two sensors that may differ in calibration, as is the case here. Their line order alternates: 1,2,2,1,1,2,2,1,... Therefore it is similar to a scanning sensor with 4 detectors per sweep. A full scene (omitting the numerical data below the image) is shown as the example in Fig. 86, with a portion from the middle right enlarged by a factor of 4 in Fig. 87.

51
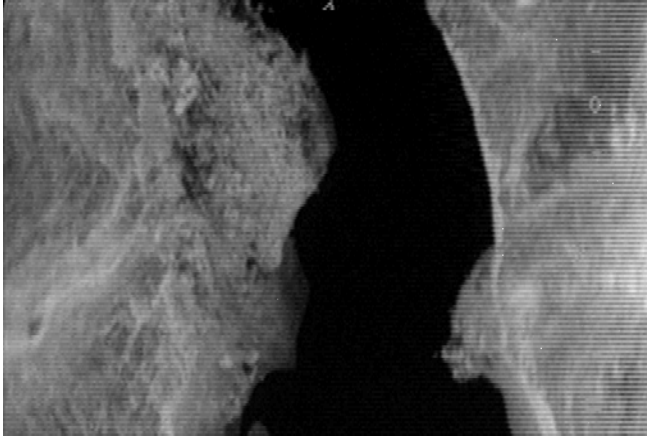
Fig. 86. A raw FLIR image of the Colorado River.
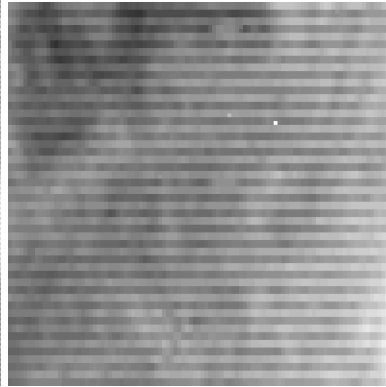
Fig. 87. An Enlargement of the FLIR.

The original image is then transformed by a Forward Fast Fourier Transform (FFT) to a complex raster image, Fig. 88, with magnitude and phase information. It looks like a scatter diagram with some prominent clustering of points along particular lines. This figure pictures the series of sinusoidal waves that can express the data in the original image. It seems to have no relationship to the scene in the original picture. (It is like a hologram which seems to contain meaningless patterns but through which a 3D image can be viewed.)
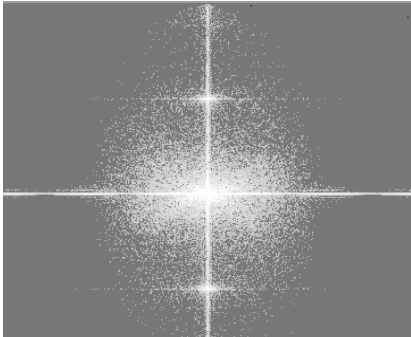
Fig. 88. Fourier transform of the FLIR image.

A special editor is then used to cut out portions of the FFT image, particularly pieces of the preferred lines. In this case, the upper and lower crossbars were removed and the upper and lower 3/4 of the vertical axis. (Trial and error may be the best method for discovering what works best.) The software then used the remainder of the FFT image to do the Reverse FFT process and recreate in Fig. 89 the original image, minus the banding. The same subset of the right side of the image is again enlarged by a factor of 4 in Fig. 90.
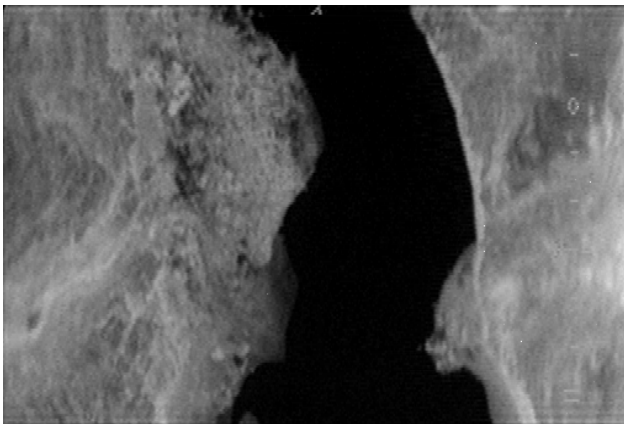
Fig. 89. The FLIR image cleaned by the FFT process.
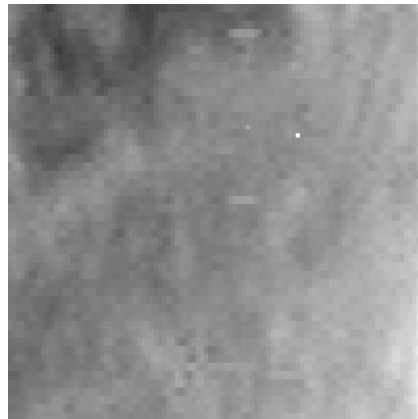
Fig. 90. Enlargement of the FLIR image.

52

During the original analysis of these FLIR images the banding was removed by using a low pass spatial filter of size 4 lines by 1 column. That preserved horizontal resolution and blurred the vertical resolution, but the result got rid of the banding problem. A temperature analysis was then performed on the Colorado River portion of this image from the Grand Canyon.

Band Combinations

Spectral bands can be assigned in any order to the RGB components of a display, often

Fig. 91. Linear contrast for ASTER thermal bands viewing the Grand Canyon.
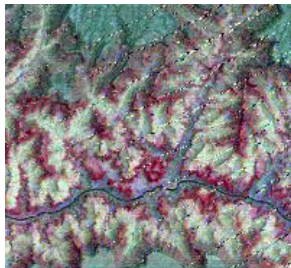
Fig. 92. Band ratios with normalized contrast for ASTER thermal bands, Grand Canyon

producing a false color combination. For example, the ASTER thermal IR view of the Grand Canyon was chosen. There are 5 narrow thermal bands named 10, 11, 12, 13, 14, all at 90 meter resolution as 16-bit integer data. Fig. 91 shows a 13, 12, 10 assignment as RGB with linear contrast. The South Rim is at the bottom of the view and the North Rim at the top. The Bright Angel Fault follows the diagonal valley. The Colorado River is the dark curved line. The sun angle from the lower right creates shadows in this topography. There are subtle color changes with rock types. Band ratios are typically used to reduce shadowing effects. (A special ratio, called the normalized difference, will be presented later.) In this thermal data set, band 14 was brightest. The other bands were divided by band 14 and the result was multiplied by 255. The ratioed bands 13, 12, and 10 were combined with normalized contrast to form Fig. 92. Instrumental noise, shown by the dotted lines running diagonally through the image, become more visible. Notice that the shadowing is indeed reduced. Furthermore, there is a greater contrast among the colors. The light and medium greens are the limestone layers. The reds are shale and sandstones. The inner gorge by the river, predominately of igneous and metamorphic rocks of granite and schist, is bluish.

Fig. 93. Five principal components for ASTER thermal scene, Grand Canyon.

All five thermal IR bands (any number of bands can be used) were converted to principal components (PC), whereby an artificial set of bands is produced that are mathematically orthogonal. That shows the maximum variability in the data but may leave the analyst wondering what the differences really mean. The results are shown in Fig. 93. PC-1 always shows the dominant brightness patterns in the data, in this case the basic brightness from albedo, topographic and shading effects. PC-2 gives rock type information for this data

set. The remaining PC's show decreasing signal and increasing noise, including the instrumental noise.

Similarly, a decorrelation stretch version can be produced from any number of bands. It

uses a principal components routine to remove the correlation between spectral bands and show only the significant differences within the original spectral bands. The decorrelation stretch bands 13, 12, and 10 are shown in RGB order in Fig. 94. The process maximizes the differences between the bands, producing much bolder color patterns. The color interpretation for basic rock types is the same as for the band ratio image.

Fig. 94. Decorrelation stretch of the ASTER thermal scene, Grand Canyon.

Image bands can also be combined by means of arithmetic functions (add, subtract, multiply, divide, ratio, rescale). They can be thresholded, to convert bands to a simple

Fig. 95. Decorrelation stretch inset of visible Landsat bands; Lander, Wyoming.
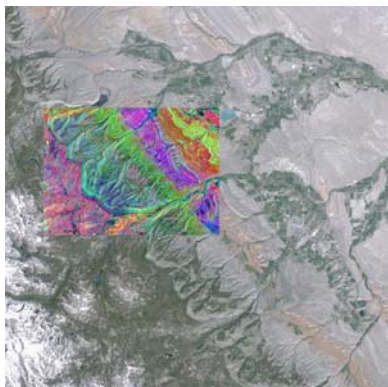
Fig. 96. Principal component inset for Landsat bands; Lander, Wyoming.

binary relationship indicating imagery parts greater than or less than the threshold value. Artificially colorizing a narrow range of digital numbers in a single band can help isolate an appropriate threshold value. As a further illustration of the power of principal components and decorrelation stretch, a Landsat scene of a region near Lander, Wyoming, has been chosen. Fig. 95 shows the Landsat scene in approximate natural color. There are agricultural regions to the upper right and forested regions to the lower left. In the lower left corner snow still covers the tops of the Wind River Mountain Range in this scene from early July. The geology is that of multiple strata dipping towards the northeast. They are eroded to sawtooth forms by the streams draining the highlands. The inset is the decorrelation stretch (a subset from the entire scene) of the same bands, showing stronger colors, particularly of the Triassic Red Beds. Other shales became bluish.

Fig. 96 of the same area has the inset from a principal components analysis. Components 2, 3, and 4 are shown as R,G,B. The area of analysis was restricted to only the area of the inset, avoiding lakes, snow, and the agricultural areas. (Including the entire scene decreased the color contrast.) The Red Beds are now purple. Other strata become more distinct, showing three types to the left and at least two to the right of the purple band. Using components 3, 4, and 5 also separate these strata well. However, they were not as separable when the entire

scene was included in the analysis because more of the computational power was devoted to the snow, lakes, and agricultural areas.

A pair of rasters can be used to create a 2-dimensional histogram (scatter diagram) in which the brightness or color at each pixel (picture element) represents the number of pixels in the original two bands that have the same particular numerical values. The ASTER scene of the North Rim of the Grand Canyon, shown in the Displaying Color section, was chosen as an example. The X-axis in Fig. 97 shows the distribution (histogram) for band 2 (actual red) and the Y-axis shows that for the band 3N (actual near-infrared). The red area of the scatter diagram shows the brightness combinations with the maximum frequency in the scene. In presenting such a 2-D diagram, some software types also put in a scatter of white points (called "dancing pixels" in the ENVI software) that give the pixel values near the cursor when it is placed over the original image. That helps the analyst know what parts of the diagram apply to particular land cover types. The data represented by such diagrams can be partitioned to provide a basis for a classification (such as water, bare land, growing vegetation, fallow land, clouds, etc.). For this band combination, pixels representing water and black parts of the scene are plotted in the lower left. Pixels with healthy vegetation (dark in red, bright in NIR) are plotted in the upper left. Barren soil and rock typically plot along the main diagonal. Sometimes the scatter diagram for this band combination is called the "tasseled cap".

Fig. 97. 2-D histogram for the red (X-axis) and NIR (Y-axis) for ASTER view, Grand Canyon

That classification can be applied to the original imagery to describe a landscape. There are many supervised and unsupervised classification systems that can take data from any number of spectral bands. Classified imagery can be summarized by pixel counts converted to area units, or by converting the data to vector polygons for GIS analysis.
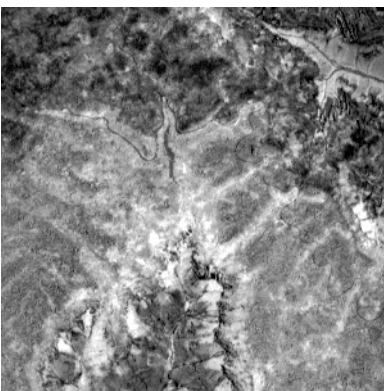
Fig 98. Normalized difference vegetative index version of Bright Angel ASTER scene.

A particularly useful 2-band combination is called the normalized difference (ND). For bands A and B, ND = (B-A) / (B+A). This is like a band ratio, but it gives a stronger signal. Fig. 98 sets A = band 2 and B = band 3 for the ASTER scene of the North Rim of the Grand Canyon. This makes the ND a vegetative index, with the normal acronym NDVI. Notice that the healthy vegetation is bright white. The dark area in the upper left should have been bright, but is part of a fire swath, hence dead vegetation. Barren soil and rock, as well as water, are also dark. NDVI is typically used for the red and NIR

55

bands of several satellites (like AVHRR, MODIS, SPOT, IRS) to measure the health of vegetation globally on a weekly basis. There is also a "greenness" and a "wetness" index.

Any number of spectral bands can be combined in a linear regression analysis, showing the correlation between the bands. Pieces of different habitats in the western U.S.A., as seen by the Landsat satellites, were mosaicked together for a linear regression analysis. The resulting table of numbers showed that band 1 (B) was related to bands 2 (G), 3(R), and 4 (NIR) by a particular formula:

$$B = 14.9358 + 1.0784*G - 0.1443*R - 0.1143*NIR.$$

Though the constants may vary with a different selection of scenes, this equation can be useful for predicting a blue image for satellites that do not record it (SPOT, ASTER) or when the blue image is contaminated with too much haze. A blue band was thereby predicted for the North Rim scene. It was combined with ASTER bands 1 (G) and 2 (R) to give a natural color version of the scene in Fig. 99. Unburned trees are green, burned areas are gray, and there are pink rocks where expected.

Fig. 99. Simulated natural color version of the Bright Angel ASTER scene.

Automatic classifications

Caution needs to be used when working with automatic classifications of scenes. For an example I have chosen an IKONOS satellite view of the intersection of the Winchester Wasteway in Washington and Interstate-90, taken 18 August 2000. The 4-band multispectral imagery was at 4 meter resolution, but was reduced to 8 meters for these examples. Fig. 100 shows the natural color view and Fig. 101 shows the color-infrared (CIR) view, both with normalized contrast stretching. Fig. 102 shows a manual classification done with the original 4 meter imagery. It started with threshold partitioning for water (NIR <171), highways (170<NIR<360 and 214<red<341), and roofs (and some hay stacks and a dried pond) (204<red). Thereafter hand analysis drew boundaries around fields showing a healthy crop, medium crop, freshly sprouting crop, and plowed fields; wetlands; sand dunes; and other; giving 10 classes.
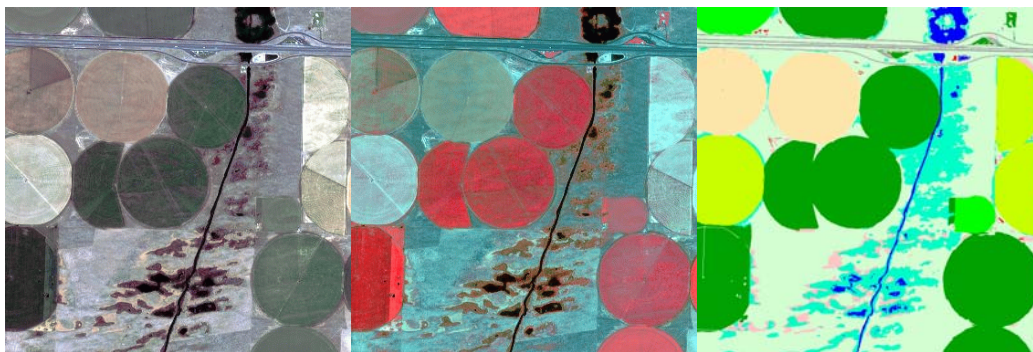
Fig. 100. IKONOS natural color.　　Fig. 101. IKONOS CIR.　　　　Fig. 102. Hand classified.

56

Automatic classification was done using the indicated routines, all 4 spectral bands, partitioning into 10 classes and using the same default values for any other parameters. Fig. 103 for Simple One-Pass Clustering. Fig. 104 is for K-Means. Fig. 105 is for Fuzzy
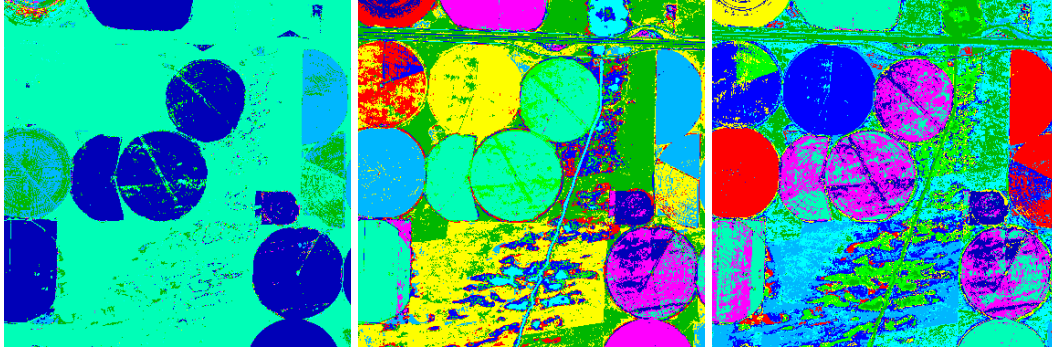
Fig. 103. One-Pass Clustering.   Fig. 104. K-Means.   Fig. 105. Fuzzy C Means.

C Means. Fig. 106 is for Minimum Distribution Angle. Fig. 107 is for ISODATA Classification. Fig. 108 is for Self Organization. Fig. 109 is for Adaptive Resonance. The processes produce a "distance" raster, whereby small values (black) indicate a close match to the spectral center of a class and large values (white) indicate a more doubtful match. Fig. 110 shows the distance raster for the Fuzzy C Means, using normalized contrast spreading. The same colors are used for the automatic classifications, though they are seemingly randomly assigned to the various classes.
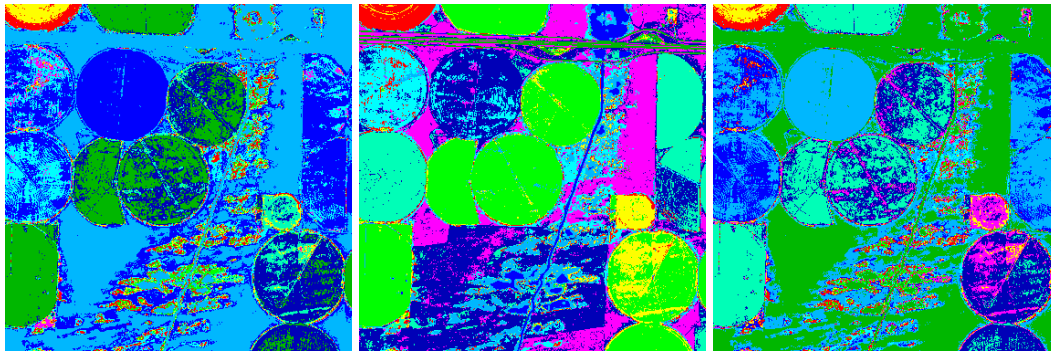
Fig. 106. Minimum distribution angle. Fig. 107. ISODATA classification.   Fig. 108. Self organization.
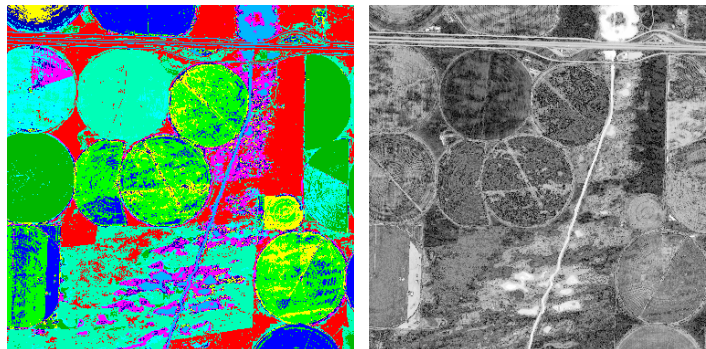
Fig. 109. Adaptive resonance.   Fig. 110. Distance raster for fuzzy C means.

The Simple One-Pass Clustering seems to use up most of its classes doing fine detail in the field of the upper left corner, making the rest of the scene crudely classified. Four of the seven techniques do not discriminate between water and road. Some of the techniques highlight irrigation within a field. Some of the techniques could be useful for precision farming analyses that seek to understand variations in plant health within a field. In general, the automatic classifications may not match a more laborious hand classification that stresses logical and useful classes for specific purposes.
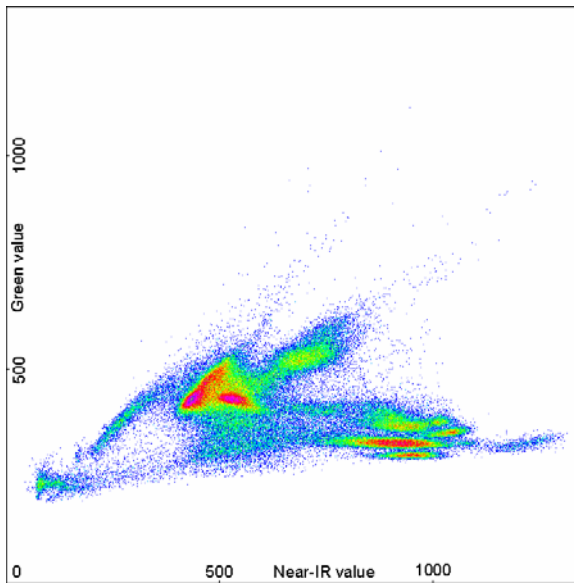
Fig. 111. The NIR-Green histogram of IKONOS scene.

Other classification strategies are possible. A 2D histogram can be created from two of the color bands. For this scene the Near-IR and green bands provide the greatest separation of features, shown in Fig. 111. This was specially prepared using axes of 1350 for the digital range of pixel values rather than a default rescaling to a 0 to 255 range. The colors in the figure indicate frequency of pixels having particular pairs of values.

The lower left cluster is water. The diagonal band on the left is the highway. The main central patch of red and green represents the barren fields and sparse vegetation areas. The upper central green patch is for the very light green fields. The weak patch in the bottom center is for the wetlands. The various patches on the lower right represent the numerous agricultural fields with some form of crop present. It is possible to partition this diagram into rectangular or triangular areas and express various thresholds for the possible classifications. A patch might be represented by a combination of rectangles in a process named parallelepiped classification.

It is also possible to use such a histogram as a guide to make a lookup table made with polygons partitioning the histogram. Fig. 112 shows a possible partition that carefully separates 27 peaks in the distribution. Fig. 113 combines those into ten classes resembling the hand analysis of Fig. 102. Using the 10 partitions the region was classified according to the pattern shown in Fig. 114. It shows more detail than the hand classification, including the location of the central pivot irrigation line in the upper left field. The sand dune areas (tan around wetlands) received the same class as the light green and white fields. The fields with a thick crop have different separations from the hand analysis. Fig. 115 shows the results of using all 27 classes of Fig. 112. Details of the fields and water bodies are evident.
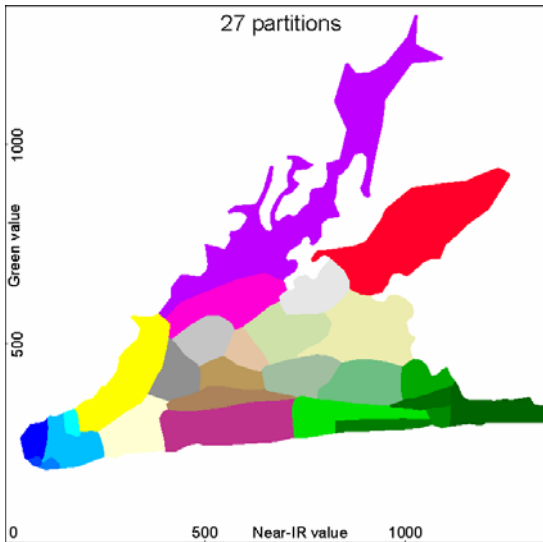
Fig. 112. The histogram in 27 partitions.
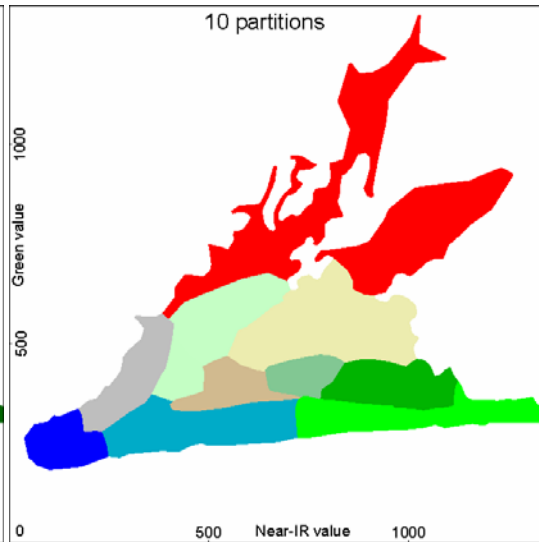
Fig. 113. The histogram in 10 partitions.
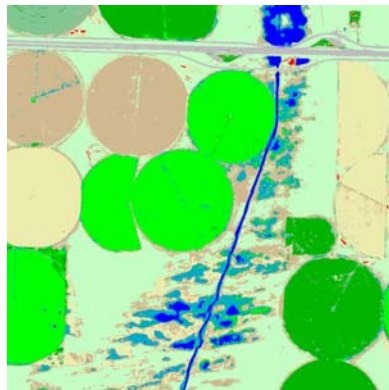
Fig. 114. Classified with 10 partitions.
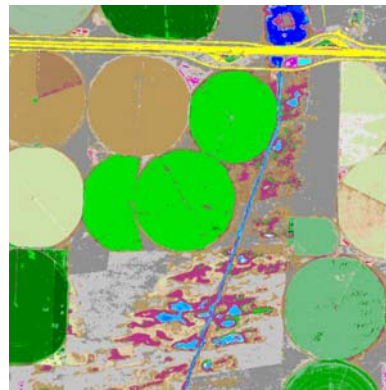
Fig. 115. Classified with 27 partitions.

Water Studies

The Landsat series can and has been used for studies of some of the properties of water bodies. For illustration purposes, portions of a scene from 2 July 1989, near the Wind River Range in Wyoming, is shown. The bands are not surface calibrated but serve as proxies for the properties. There are several lakes on the southwestern side of the range that receive meltwater from the snow-capped mountains. TM band 6 gives the surface temperature of the scene; dark is cold and bright is warm. Fig. 116 has been colorized over the narrow temperature range of the lakes such that each digital number has a different color, with blue being coldest, red being warmer and magenta and then purple
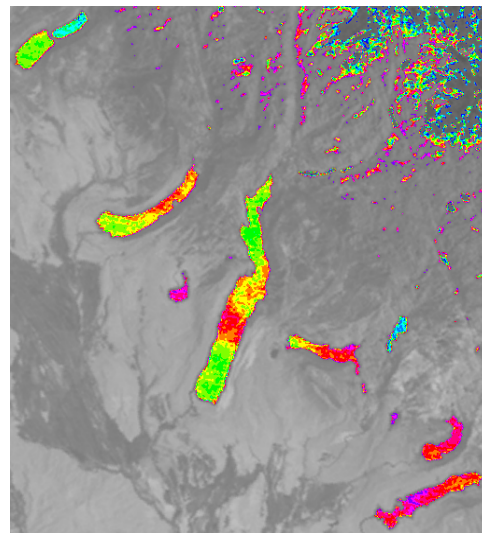
Fig. 116. Colorized according to surface temperature.

59

being warmest. The land areas are warmer than the water. The snow pack is in the upper right and is much darker but with colored edges, indicating that the colored temperatures are close to the melting value. Each lake has a different pattern. The two at higher elevations are cold (light blue). Two have significant temperature patterns within the lake. Notice also that the irrigated agricultural fields in the lower left are cooler (darker) than the barren land.

Another area, to the northeast of the Wind River Range was selected. The main feature is Ocean Lake, surrounded by an agricultural area with water distribution canals. The scene is northwest of Riverton, WY. The natural color version of Fig. 117 shows a lightly blue colored lake, suggesting fine sediments from a glacial source in the mountains. This scene is used as a base map for the next views, in which water bodies are colorized to show other water properties.
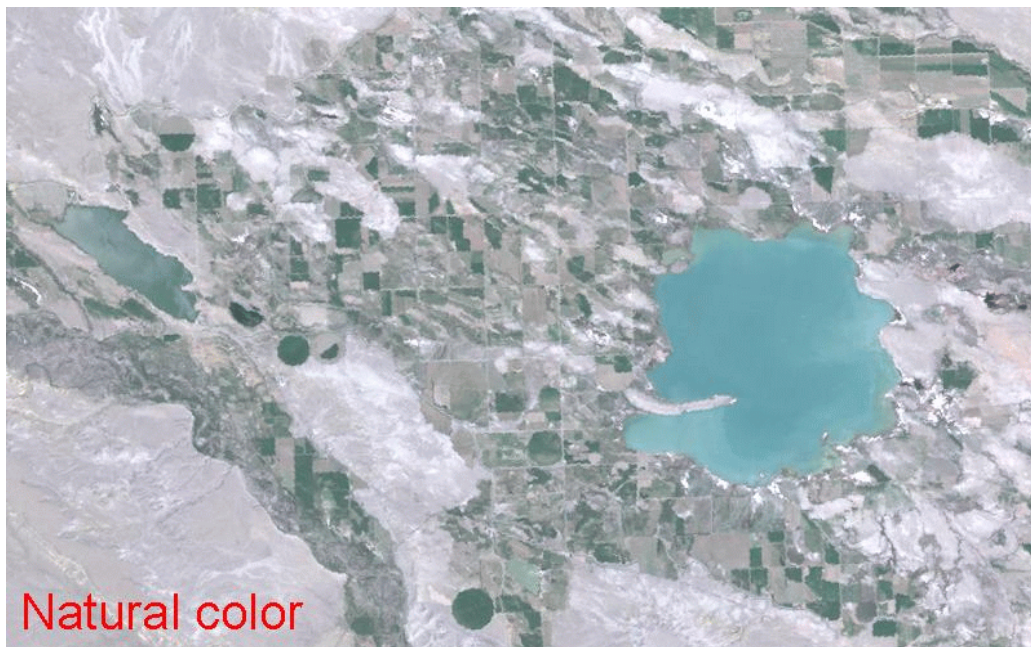
Fig. 117. A natural color version of the Ocean Lake, WY region.

The uncalibrated temperature patterns (TM band 6) show little variation across the lakes in Fig. 118. The western lake is the coldest. The two largest lakes show warmer (greenish) shorelines, probably because the shallow water lets the satellite see to the bottom sediments which are easily warmed by the sun. Along the upper left is a canal with very warm (red) water. The river in the lower left is cooler (green).

60
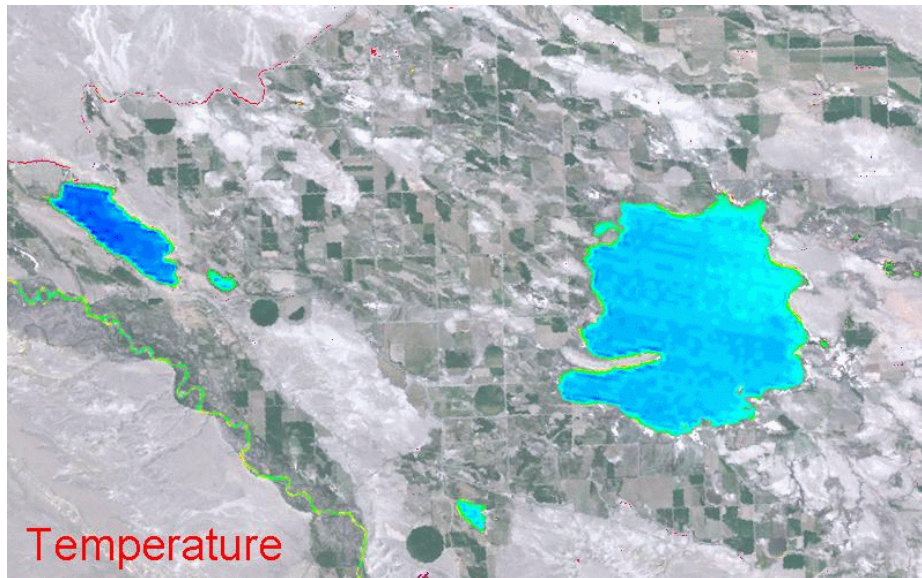
Fig. 118. The Ocean Lake scene with water colorized by temperature.

Band 1 (blue) was chosen as a proxy for turbidity. The large Ocean Lake shows strong patterns in Fig. 119 with red indicating the greatest mud content. There is a small pond at the left that has the cleanest (blue) water. The upper left canal is muddy (reds and oranges) and the lower left river is intermediate (greens). A proper calibration would require field observations of secchi depths - the depth to which a white disc can be seen in the water.
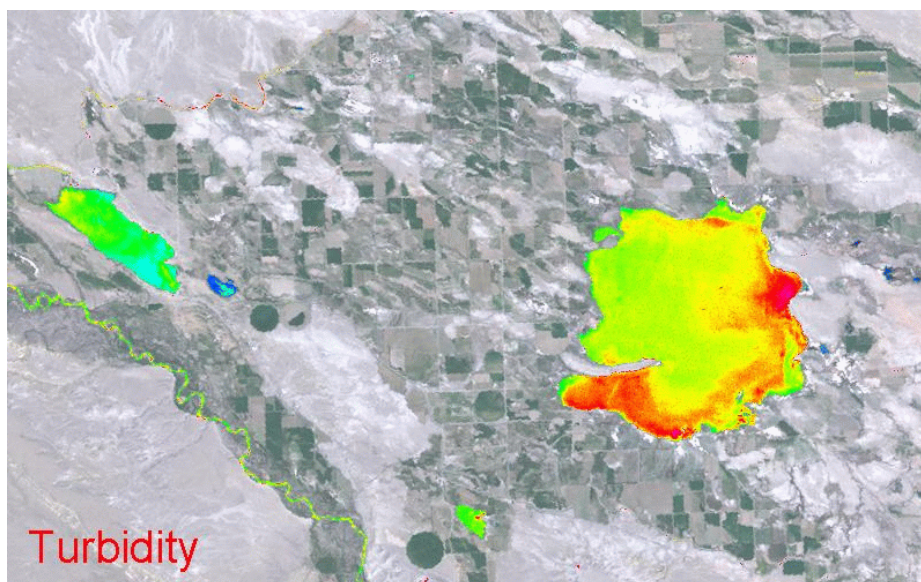
Fig. 119. The Ocean Lake scene with water colorized by turbidity.

Bands 4 (near-IR) and 3 (red) were combined as a normalized difference vegetative index. This index is greatest for growing vegetation. Though darkened by the water, it serves in Fig. 120 as a proxy for chlorophyll content. Reds (small western pond, lower

left river) indicate the greater amounts of growth while greens indicate lesser amounts. A proper calibration for chlorophyll makes a regression analysis among the TM bands.
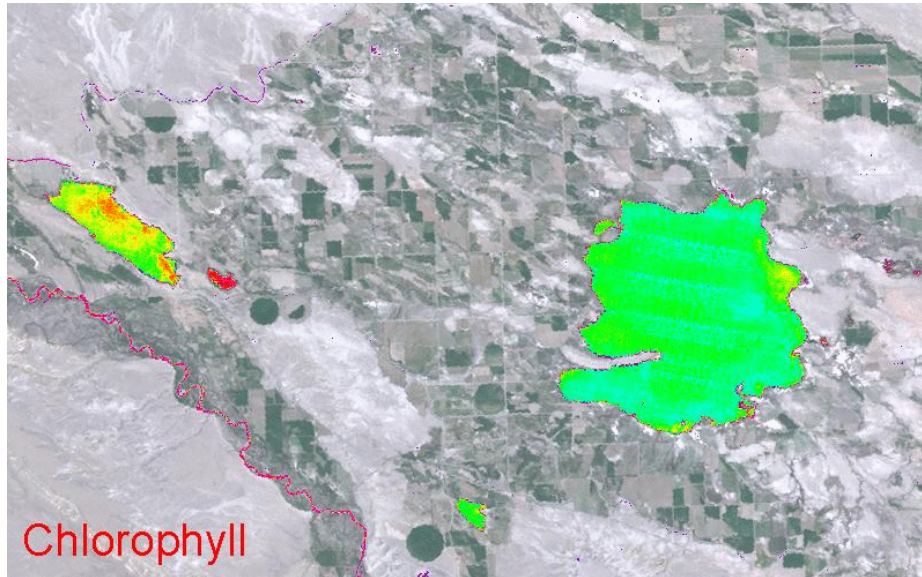
Fig. 120. The Ocean Lake scene with water colorized by chlorophyll content.

All six reflective TM bands (not band 6) can be combined in a "tasseled cap" analysis to create three mathematically orthogonal bands labeled Brightness, Greenness, and Wetness. For this Ocean Lake scene in Fig. 121 these products are displayed as R, G, and B, respectively. Only a few fields showed a wetness signal. Growing vegetation had variable greenness. Barren areas had the strongest brightness.
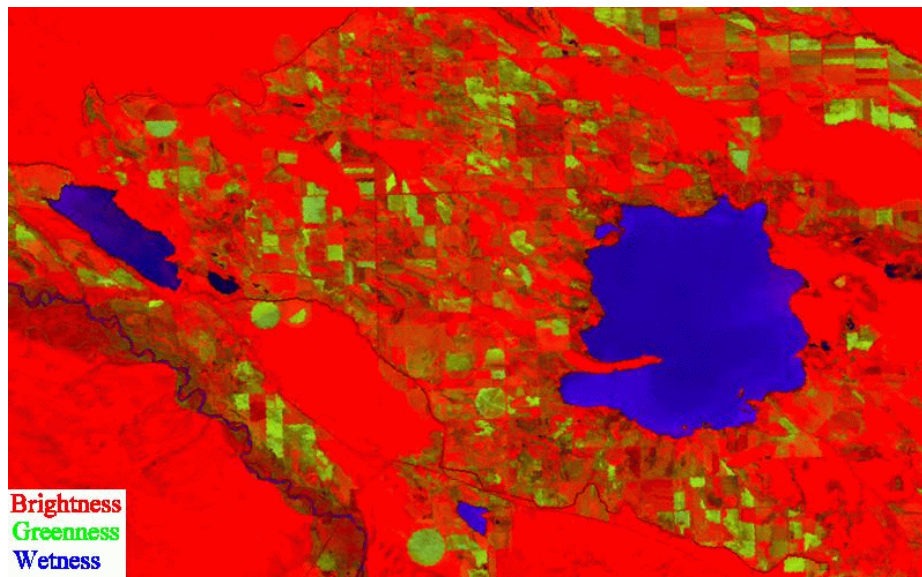
Fig. 121. The Ocean Lake scene with false color rendition of brightness, greenness, and wetness.

Pan-sharpening

Panchromatic systems, rendering a scene as a single band (B&W), can achieve a finer resolution because there are more photons available to the instrument in the broad panchromatic band than in the individual color bands. Satellites like SPOT and Landsat-7 have panchromatic bands with resolution at half the size of the multispectral bands. The IKONOS, QuickBird, and Orbview-3 satellites have panchromatic resolution of 1/4 that of the multispectral bands. For illustration, an IKONOS scene was selected, showing the intersection of Dodson Road and Frenchmans Creek Road, south of the Winchester Wasteway and southwest of Moses Lake, Washington. The individual bands (Fig. 122), natural color (Fig. 123) and CIR (Fig. 124) versions are shown at 4 m resolution, as is the 1 m panchromatic version which has more detail than shown in Fig. 125.

blue   green   red   near-IR

raw IKONOS multispectral, 4 meter resolution
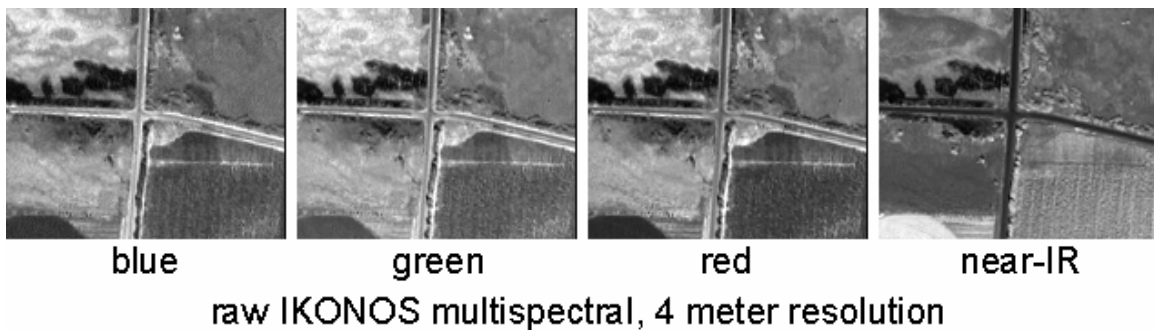
Fig. 122.   The 4 IKONOS multispectral bands of the road intersection.
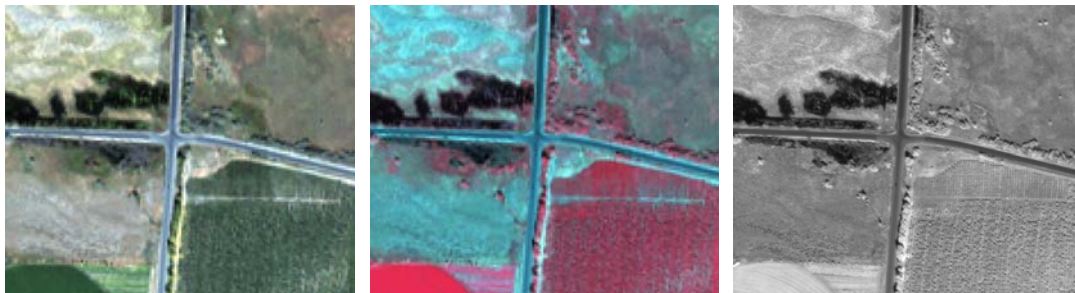
Fig. 123. Natural color.   Fig. 124. CIR version.   Fig. 125. Panchromatic version.

Pan-sharpening (pan-fusion) first involves subsampling the multispectral images to the fine resolution of the panchromatic images. One technique then transforms 3 multispectral bands as RGB into HIS, substituting the panchromatic image for the Intensity image, and transforming back into 3 bands to be displayed as RGB. The other technique transforms any number of bands into principal components, substitutes the panchromatic image for the first principal component, and then reversing the transformation back into the original bands. However, there is a problem of spectral matching that can severely affect the result. The SPOT panchromatic band spectral range overlaps that of the G-R-NIR multispectral bands, avoiding this problem. However, other satellites have the panchromatic spectral range overlapping four multispectral bands (B-G-R-NIR). If one wants a natural color version of pan-sharpening, the NIR
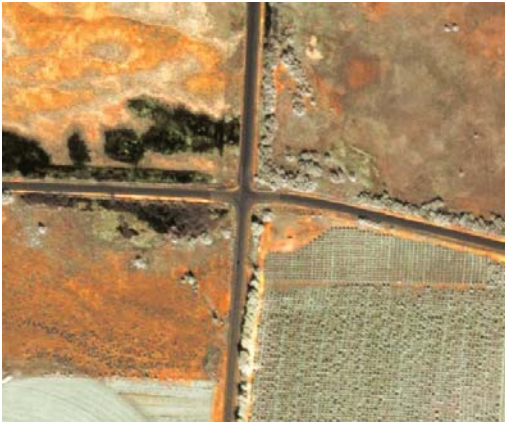
Fig. 126. Pan sharpened version, using a simple HIS substitution routine.

Fig. 127. Visible band panchromatic image from the 4-meter bands

component will greatly brighten the panchromatic image where there is growing vegetation, resulting in abnormally bright vegetation in the resulting pan-sharpened image or distorted colors as shown by the orange tones in Fig. 126.

One way of working around this problem is to create an apparent visible band panchromatic image (Fig. 127) by averaging the subsampled B,G,R components. A regression equation is then created relating the visible band panchromatic to the subsampled NIR and original panchromatic image. That relationship is then used with the subsampled NIR and original panchromatic image to calculate a better (finer resolution) visible band panchromatic image (Fig. 128). It is that calculated image that is used to substitute for the Intensity image in the HIS transformation or the first principal component before reversing the transformation. The resulting pan-sharpened image in Fig. 129 is much closer to natural color and has superb resolution. Texture is now visible in the crop in the lower right, showing the rows more prominently. There are details within the ponds in the upper left that are missed in the 4-meter multispectral bands. Shadowing is now visible beside the trees in the lower right and elsewhere, allowing an interpretation that considers plant height.

Fig. 128. Simulated visible band panchromatic.

Fig. 129. Pan-sharpened version.

Georegistration

In order to be useful in a Geographic Information System, each raster (image) needs to be georegistered. It is best to assume that all physical materials used to generate raster and vector data are not perfectly scaled. Paper (and similar media) products can contain wrinkles and tears. They may change size with temperature and humidity. Scanned products and Xerox copies will usually have subtle scale differences between the x and y coordinates because the optical scales are not perfectly matched to the scanner movement scale. It is therefore imperative that all such products are individually georeferenced to re-establish the correct scale factors. That means that a sufficient number of control points are identified with respect to some geographic coordinate system.

The georegistration of topographic maps and orthophotoquads can be accomplished by telling the software the location of coordinate tic marks (+ signs) on a map. The initial setup for georegistration is important. The proper coordinate system needs to be specified, though it may be possible, for example, to enter coordinates (and view them in a table) in the latitude/longitude system but save them in the UTM system. The proper Datum and Geoid need to be specified. Topographic quadrangles are typically in the NAD1927 Datum with Clark 1866 Geoid. Properly made maps should have such information in the margins. There are display projection choices with various mathematical complexities: affine, plane projective, bilinear, polynomial, and piecewise versions. They dictate how an image is warped. The cursor is typically used to place a cross hair at a tic mark, with fine adjustments being made by keyboard arrow keys until the overlap is nearly perfect. In Fig. 130 the location is marked with a red symbol and labeled with a number. In the accompanying table in Fig. 131 is a list of the 16 coordinates of the tic marks.
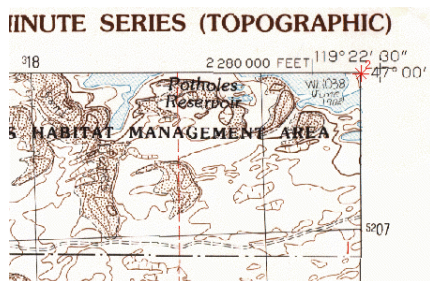
##	Column	Line	Latitude	Longitude	Residual (m)
1	172.12	162.50	N 47 00 00.0	W 119 30 00.0	5.926
2	2508.63	153.58	N 47 00 00.0	W 119 22 30.0	2.802
3	2524.14	3558.49	N 46 52 30.0	W 119 22 30.0	4.064
4	182.40	3568.43	N 46 52 30.0	W 119 30 00.0	3.876
5	1743.38	3562.14	N 46 52 30.0	W 119 25 00.0	1.722
6	963.49	3565.61	N 46 52 30.0	W 119 27 30.0	2.750
7	2518.60	2423.46	N 46 55 00.0	W 119 22 30.0	1.194
8	1738.51	2427.08	N 46 55 00.0	W 119 25 00.0	2.595
9	958.50	2430.55	N 46 55 00.0	W 119 27 30.0	3.242
10	177.52	2433.47	N 46 55 00.0	W 119 30 00.0	4.772
11	2513.54	1288.49	N 46 57 30.0	W 119 22 30.0	1.468
12	1733.61	1292.50	N 46 57 30.0	W 119 25 00.0	4.672
13	954.54	1295.51	N 46 57 30.0	W 119 27 30.0	3.720
14	174.48	1298.57	N 46 57 30.0	W 119 30 00.0	3.431
15	1729.53	156.61	N 47 00 00.0	W 119 25 00.0	2.897
16	951.39	159.96	N 47 00 00.0	W 119 27 30.0	4.027

Fig. 130. Georegistration of a topo at tic marks.   Fig. 131. A table of Georegistration numbers for a full quad.

The right column contains a list of residuals. That shows the calculated error associated with each location. Such errors should be minimized. Sometimes that can be done by choosing a different display projection choice. In this case, switching from the plane projective system to one of the polynomial powers can reduce these residuals to mostly less than 1 meter. Otherwise each point can be checked and adjusted, starting with the one with the largest error. The example used latitude/longitude tic marks. Alternatively

the UTM grid intersections on the topographic map could have been used, such as that in the lower left corner of the Fig. 130 example.

For fine resolution work a topographic map seldom has enough features that can be used as control points for an aerial photo or video image. Sometimes a coarse resolution aerial photo needs to be used as an intermediate georeference standard. Points in common between the aerial photo (left side, Fig. 132) are paired with the same features in the topographic map (right side, Fig. 132). After the residuals are minimized by appropriate adjustments or deletions of bad points, the software creates the proper georeference for the intermediate aerial photo. Ideally, a digital orthophoto quarterquad will be available, with 1 meter pixels, to serve as a reference image. Its georeference will be provided, eliminating the need for the previous two steps and providing a superior resolution. Then common objects like trees, rocks, road intersections, buildings, etc., can serve as georeference points, as illustrated in Fig. 133 (colored aerial photo on left, older B&W digital orthophoto on right). In addition to providing the locations of all positions in an image, the georeference process establishes the scales (meters per pixel) in the x and y (or column and line) directions for the image. Those scales may differ, particularly in rugged terrain.
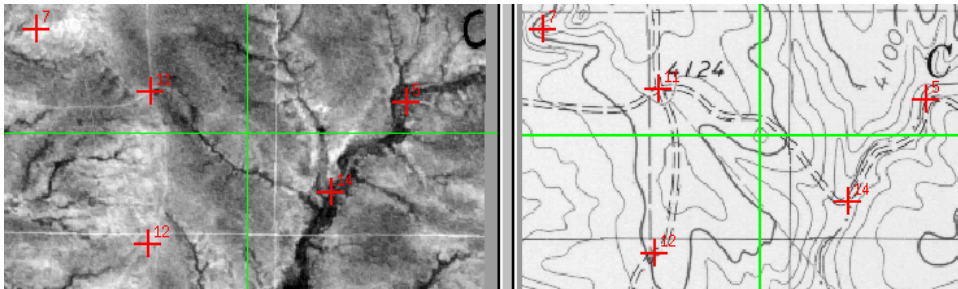
Fig. 132. Tie points used to georeference an aerial image, using a topographic map as reference.
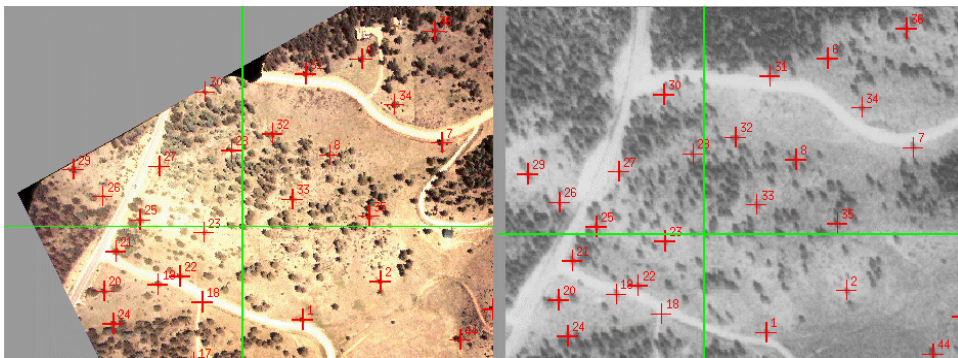
Fig. 133. Tie points used to georeference an aerial image, using an orthophoto as reference.

7. Photogrammetry

Photogrammetry, as defined by the American Society for Photogrammetry and Remote Sensing (ASPRS), is the art, science, and technology of obtaining reliable information about physical objects and the environment through processes of recording, measuring,

and interpreting photographic images and patterns of recorded radiant electromagnetic energy and other phenomena.

Originally the science was applied to analyzing photographs, either ground based or obtained using an airborne platform such as a balloon, blimp or piloted aircraft. In recent years photogrammetric methods and analysis have extended into fields such as Light Detection and Ranging (LIDAR) and digital imagery, and the airborne platforms now include un-manned aerial vehicles (UAV's) and satellites. However, the principal data source for photogrammetric analysis continues to be film based photographs.

Reclamation primarily uses photogrammetric methods, analysis, and products in the forms of aerial photography, orthophotography, digital elevation data (DEM, DTM, TIN, contours, cross-sections, etc.), topographic maps, and photographic interpretation (PI). Aerial photography, taken with a calibrated large-format (9"x9"), metric aerial survey mapping camera is usually of primary data source. In the past couple of years, larger format digital aerial cameras/sensors (Z/I DMC, Leica ADS40) have been developed, purchased, and are in use by several large North American mapping companies. On occasion Reclamation has a need to use ground based terrestrial or close-range photogrammetric methods to meet special project requirements. Close-range photogrammetry, defined as having a 300-meters or less object-to-camera distance, is based on the same scientific principles and similar data needs as the more familiar aerial based photogrammetry.

Aerial photography and photogrammetric methods have many applications within Reclamation, including compilation and production of many types of maps and digital data; crop maps, wetland maps, land use and management, infrastructure, vegetation, irrigation components/networks, riparian vegetation, geologic studies, geomorphology/sediment transport, hydraulic models, wildlife and aquatic habitat, change detection, trespass, and trend analysis.

Photographs are taken from essentially a point location, using a lens that may add some radial distortion (more obviously seen in a fish-eye lens) with respect to the center of the image. Perspective from that point location makes objects that are vertically near the camera appear at a radially greater distance from the center of the photograph than objects farther away. A vertical object, such as a building, tree or pole, as viewed in aerial photography, will appear to lean back radially from the image center. The same applies to topographic differences; hilltops will similarly lean away from the image center. Therefore aerial photographs will not have its viewed objects in exactly the same relative positions as should appear on a map. A computationally intensive process is used to correct for the lens and terrain distortions to produce a special type of image known as an orthophotograph.

In the past stereo analysis of aerial photography required large manual machines and manual operation by the person viewing the imagery. Perhaps fifteen years ago software was written for mainframe computers to semi-automate the process. More recently, some PC and workstation software packages allow the semi-automated analysis of a pair of

stereo images. Sometimes the phrase "soft copy photogrammetry" is used. After some initial definitions for scale, orientation, geographic registrations, elevation ranges, and an assortment of tie points (same physical object in both images), the software generates a pair of "epipolar" images in which all elevation displacements are along an axis parallel to the line between the photo centers. Additional tie points are then added, especially along ridges, depressions, and slope changes. The software then uses an autocorrelation
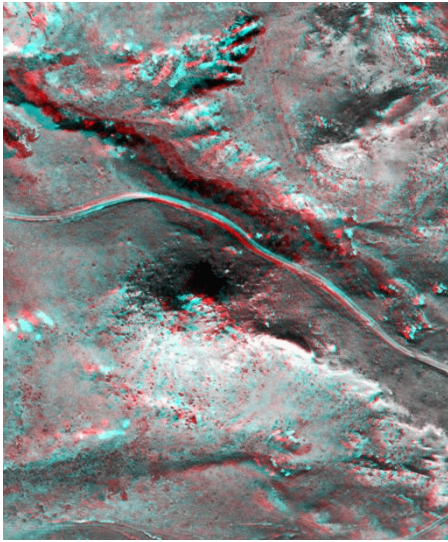
Fig. 135. A hill and valley stereo pair as left = red, right = cyan.

technique to identify other points that are the same object in both images, then convert their positional differences (parallax), parallel to the line between the centers of the two images, into elevation values. The result is a digital elevation model (DEM), expressing the elevation everywhere across a scene within the overlap of the two stereo images. The elevation data can be contoured to provide a map representation. In a related process, if the digital elevation data are known, the picture can be warped to remove distortions caused by elevational differences. The resulting product is known as a digital orthophoto. Quadrangle versions are known as DOQ and DOQQ. They are excellent products for georeferencing aerial and satellite imagery. As an example, Fig. 134 shows a small stereo pair of a badland hilltop and adjacent stream valley with the left image on the left and right while the right image is in the center. The left and center views can be

used with a stereoscope or viewed directly by people who can see straight-on stereo. The center and right views are for people who can do cross-eyed stereo viewing. Another version in Fig. 135 shows a superimposed, colored version with red for the left image and cyan for the right. When viewed through anaglyph glasses with red over the left eye and cyan over the right, the topography will appear in 3-dimensions. However, if the colored lenses are reversed, hills will appear as pits and valleys as ridges.
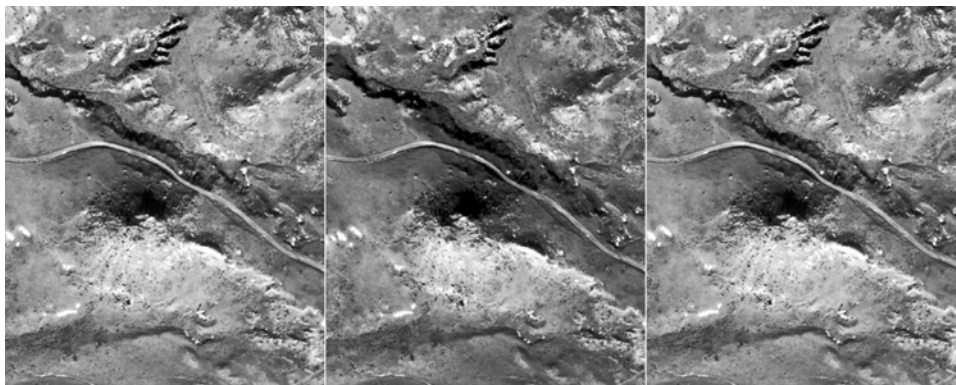
Fig. 134. A hill and valley stereo pair as left-right-left.

After the DEM has been generated by the software, it is usually good to run a median filter over the result to remove some of the noise and small blemishes. For comparison, the topographic map, with 20 foot contours was resampled as Fig. 136 to the extents of the stereo view. The DEM derived from the stereo pair is colorized in Fig. 137 at 1 meter vertical resolution, with the dark bands at 5 meter intervals. There is much more detail in the stereo-derived DEM, much from rocks and grass tufts, but there are also some blemishes caused by shadows and other things that confused the autocorrelation process.
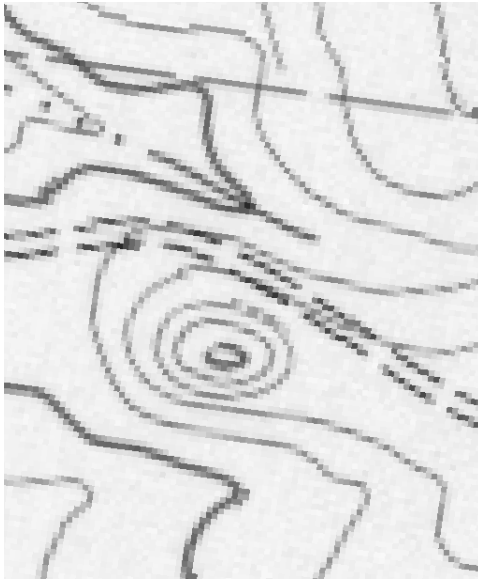
Fig. 136. Topographic map with 20' contours.
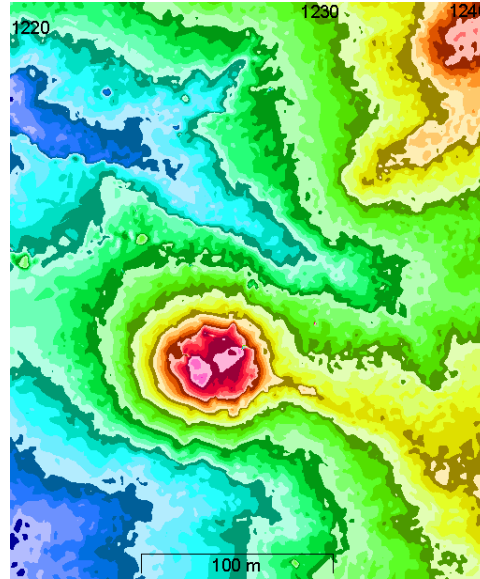
Fig. 137. Colorized DEM derived from stereo pair.

An example of the value of orthophotographic rectification is shown by a view of the Interstate-70 cut through the hogback west of Denver. The aerial photograph was taken at a relatively low altitude and therefore experienced strong radial displacements of high topography. The scene was georeferenced to an orthophoto produced by a combination of IFSAR (interference synthetic aperture radar) derived topography and an IKONOS satellite image. The aerial photo was then warped by software designed to produce an orthophoto from an aerial photograph and a DEM (digital elevation model). The result was superimposed on top of the IKONOS image. It is useful to watch for mis-matches along the edges of the warped photograph. They indicate the quality of the software adjustments. It is seen in Fig. 138 that the picture edges are

Fig. 138. Aerial photo of I-70 warped to an orthophoto.

greatly distorted by a reversal of the radial stretching in the original view. The amount of change in this image of rugged topography shows the need for orthophotographic corrections of an aerial image.

A scanner uses the forward motion of the aerial or satellite platform to assemble a series of cross-track image lines into a 2-dimensional picture. The instantaneous view is only along a narrow slit perpendicular to the flight direction. All elevation distortions are perpendicular to the flight line. Higher things lean back away from the flight line. Elevations can be derived only from parallel passes, not imagery from a single pass, and then from a more specialized software algorithm.

Some satellites are able to take off-nadir views intentionally. Such images can be used as stereo pairs to derive elevations of the landscape. The early SPOT satellites took their off-nadir views perpendicular to the orbital path, requiring that the pairs were taken on different orbits and days. The ASTER camera on the Terra satellite routinely takes a nadir view and a backwards view (along orbital path) in the NIR band 3, designated 3N (nadir) and 3B (backwards). The newest generation of high-resolution satellites, IKONOS (Space Imaging), Orbview-3 (OrbImage), and QuickBird (Digital Globe) have the capability to obtain 1-meter or better spatial resolution images in the panchromatic wavelength band. These images, properly manipulated, are suitable for many applications including orthophotgraphy and digital elevation data extraction. They can acquire imagery at any angle with respect to the vertical and orbital path. Off-nadir and scanner geometries require special software algorithms for deriving elevation models.

Reclamation currently has three aerial photography and mapping services IDIQ contracts in place; UC-Salt Lake City (Bureau wide), GP-Billings, and MP-Sacramento. You must be able to effectively communicate your data requirements to the Reclamation Contracting Officers Representative (COR/COTR) and in turn the photogrammetric mapping contractor to ensure success for your mapping project. Reclamation offices in Denver, Phoenix, and Sacramento also have persons knowledgeable in photogrammetry and photogrammetric workstations. Depending on the size and needs of your project you may want to consult with Reclamation people and tap into their experience.

Proper planning is essential to the success of any photogrammetric mapping project. One of the first things that needs to be determined are your data requirements, including the accuracy needed. Data requirements include being able to accurately describe or delineate on a map where you want your photogrammetric data collected and when. Higher accuracy or resolution data does cost more than lower accuracy/resolution data.

A typical scope of work (SOW) for photogrammetric data acquisition would include things such as; project area map, scale of aerial photography needed, film type (panchromatic/BW, color, color infrared), timing of aerial photo acquisition, targeted map/data accuracy, ground control and/or airborne GPS control needed (accuracy driven), contact prints-diapositives-enlargements needed, digital orthophotographs needed (w/pixel size stated), elevation data needs (DEM/DTM, mass points/breaklines, spot elevations, contours, cross-sections, hydro-corrected DEM, etc..), planimetric

features to collect (scale driven) such as roads, curbs, hydrology, buildings, infrastructure, vegetation, etc., file formats and sizes, flight line maps (digital & hardcopy), are any hardcopy map plots needed or just the digital data, delivery dates, etc.

A photogrammetric workflow process should include:
1. Define area to be mapped, data and mapping products needed.
2. Prepare a detailed scope of work.
3. Plan aerial photography and control (ground and/or airborne GPS) acquisition.
4. Aerotriangulation
5. Digital elevation (terrain) model (DEM, DTM) data collection.
6. Digital orthophotographs; radiometric correction, editing, mosaic, format, image compression (if needed).
7. Triangular irregular networks (TIN) and contours.
8. Planimetric feature collection.
9. Edit contours and planimetric features.
10. Map graphics and data file tiling (if needed).
11. Data file formatting; image files, AutoCAD files for engineering, ArcInfo for GIS, etc.
12. Map plots on paper or film; edit, legends, size/scale, index map, etc.
13. Production of FGDC compliant metadata.

The primary pieces of information needed for a photogrammetric mapping project are an image source (aerial photographic film or digital imagery), ground control and/or airborne GPS coordinate data, and a camera calibration report. If these pieces have been properly collected for your project area you can then use photogrammetric equipment and techniques to extract and produce various types of data.

Map accuracy standards

The primary accuracy standards in use today are the National Map Accuracy Standard (NMAS) initially developed in 1947 and expanded upon during the last decade by subcommittees of the Federal Geographic Data Committee (FGDC), and the ASPRS Accuracy Standards for Large-Scale Maps (1990) class1, class 2, and class 3. The ASPRS Class 1 standards are more rigorous (costly) and contain more definitive statistical map testing criteria, lower classifications will be more economical, with decreased accuracy.

NMAS Horizontal accuracy: NMAS states that for maps of publication scales larger than 1:20,000, not more than 10-percent of points tested shall be in error more than 1/30th of an inch, measured on the publication scale; for maps of publication scales of 1:20,000 or smaller, 1/50th of an inch. These limits of accuracy apply only to well-defined points (easily visible or recoverable on the ground). For example; a 1:24,000 scale map should have a horizontal accuracy of 40-feet (1/50th inch), and a 1:12,000 scale map should have a horizontal accuracy of 33.3 feet (1/30th inch).

NMAS vertical accuracy: As applied to contour maps at all publication scales, shall be such that not more than 10-percent of the elevations tested shall be in error more than one-half the contour interval; i.e. a 10-foot contour interval map should be within 5-feet vertically.

Table 1. ASPRS Class 1: Planimetric Feature Accuracy (X or Y coordinate in feet, for well defined points. (From ASPRS and COE)

Map Scale 1"= x feet	Ratio feet/feet	Limiting RMSE in X or Y (feet)
40	1:480	0.4
50	1:600	0.5
100	1:1200	1.0
200	1:2400	2.0
300	1:3600	3.0
400	1:4800	4.0
500	1:6000	5.0
600	1:7200	6.0
800	1:9600	8.0
1000	1:12,000	10.0
1667	1:20,000	16.7

Target contour Interval (feet)	Topographic Feature Points	Spot Elevation Points
1	0.33	0.17
2	0.67	.33
3	1.0	.50
4	1.33	0.67
5	1.67	0.83
10	3.33	1.67

Table 2. ASPRS Class 1: Elevation Accuracy for Well-Defined Points. (From ASPRS and COE). ASPRS Limiting RMSE in feet

Keep in mind that Reclamation IDIQ mapping contractors have been selected in part due to their rigorous quality control (QC) program. The testing of map accuracy can be costly and time consuming, Reclamation, as with most government entities, relies heavily on the contractors QC program and procedures to check for and catch mistakes. A photogrammetric mapping project should not be an adversarial process, if planned, carried out, and checked properly you will end up with a good project. The vast majority of contractors want to produce good and accurate products, and depend on customers to return with new work. If their reputation suffers due to sloppy or careless work their workload usually suffers too.

Final Map Scale	Pixel Size (ground units) in feet
1"= 50 feet (1:600)	0.25
1"= 100 feet (1:1200)	0.50
1"= 200 feet (1:2400)	1.0
1"= 400 feet (1:4800)	2.0

Table 3. Recommended Pixel Size for Selected Orthophotograph Map Scales:

8. Digital Elevation Models

Digital elevation models of various resolutions and qualities are available for free or purchase from the USGS. The oldest series were derived from 1:250,000 scale topographic maps by the Defense Mapping Agency (DMA) decades ago. They are available in 30 arc-second and 3 arc-second resolution, meaning that data points are every 30 or 3 seconds of arc in latitude/longitude coordinates. This set is continued in the global GTOPO30 DEM for the 30 arc-second series. The user should be aware of flaws in these data. The data do not always match the real topography. Sometimes the georegistration of the data is offset. Some elevations seem quantized at elevations like 200 ft, which is the contour interval on many of the maps used in deriving the DEM. A newer series is the 30 meter DEMs derived from 7.5 minute topographic map contours. More recently, DEMs have been developed as byproducts of digital orthophotos.

In 2000 the Space Shuttle used C and X band SAR radar technology to create a DEM of the entire U.S.A. at 1 arc-second resolution. Since 2003, it can be ordered in Arc-GRID format at http://srtm.usgs.gov/data/obtainingdata.html. The Shuttle Radar Topography Mission (SRTM) is a joint project between the National Imagery and Mapping Agency (NIMA) and the National Aeronautics and Space Administration (NASA). For the rest of the world the project produced digital topographic data for 80% of the Earth's land surface (all land areas between 60 north and 56 south latitude), with data points located every 3-arc second (approximately 90 meters) on a latitude/longitude grid. The absolute vertical accuracy of the elevation data is 16 meters (at 90% confidence). Perhaps a more convenient source in GeoTIFF format is from the University of Maryland site, http://glcfapp.umiacs.umd.edu:8080/esdi/index.jsp, which also has free Landsat and some ASTER data.

Fig. 139. The DMA DEM for the Ohio region showing flaws.

73

To illustrate some of the problems in the older data set, a subset of the 30 arc-second data in the Ohio River valley, N 37° to 41° 20', W 80° to 85° is displayed in Fig. 139. Dark tones are lowlands and bright tones are highlands in this normalized contrast rendition. The Ohio River extends from the upper right to the center left. Across this scene the amount of detail varies significantly. The southern portions have much fine detail. The northwest is greatly smoothed, mostly by the continental Ice Age glaciers. To the right of the center there is a 1-degree square within which are large flat areas, looking very artificial.

For the northwest portion of that DEM data set the software was used to create a solar shading, as if the sun were in the northeast (45° azimuth) at 50° above the horizon (an impossible location). The shaded diagram in Fig. 140, with normalized contrast, is annotated with red marks at the 1° latitude/longitude positions. Notice that there are some edges visible between the 1° squares, indicating a mismatch of elevations. The flat, plateau-like data area is in the lower right portion of this view. Such flaws create severe problems for spatial analysts.
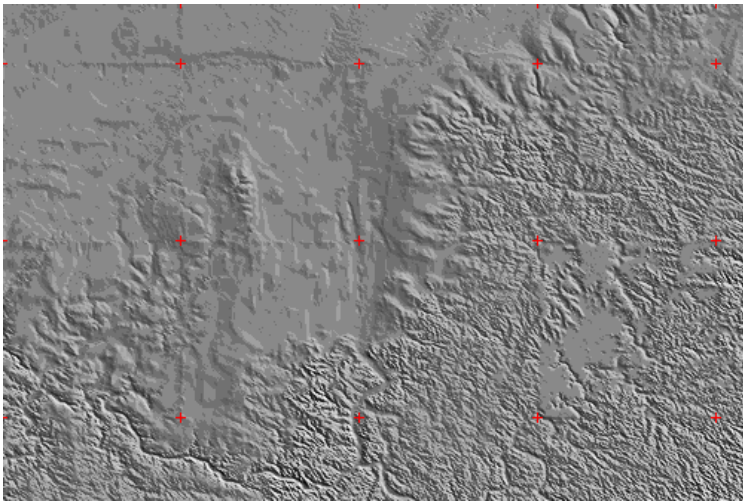
Fig. 140. A shaded relief of the Ohio DEM.

For comparison, the second shaded view in Fig. 141 uses data from the Shuttle mission, subsampled to the same resolution. The flaws are missing and the detail is better. The smooth areas in the northwest now clearly show a set of terminal moraines from the Ice Age glaciers.

When a solar shading image is created, the software must also derive slope and aspect images. Areas in the slope diagram in Fig. 142 with a value of zero are colored red. This highlights the DEM problem areas. Apart from such flaws, slope images are
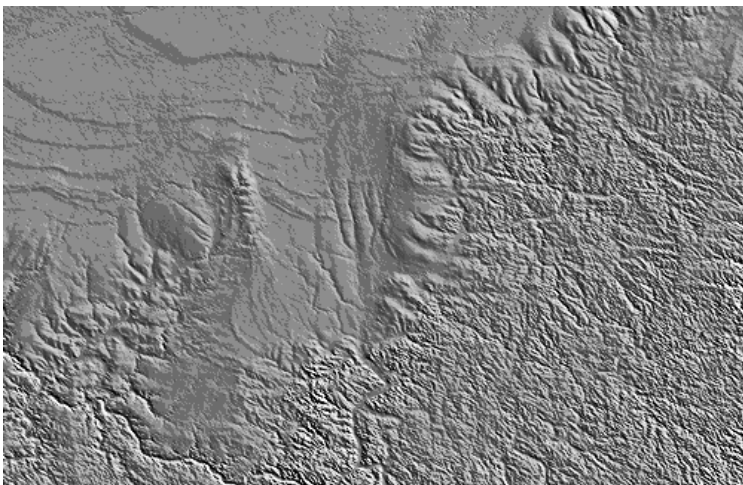
Fig. 141. A shaded relief of the Ohio DEM using Shuttle radar data.

best shown with logarithmic contrast. Steep slopes will be bright. The general texture of slope images is one of a pile of spaghetti. Some lines, as in the upper left, seem artificial where there is a jump in the elevation because of analytical resolution in creating the DEM.
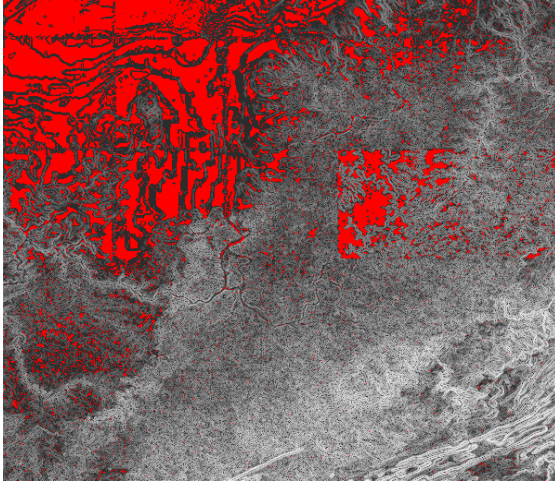
Fig. 142. Slope version of DEM, white are steep slopes
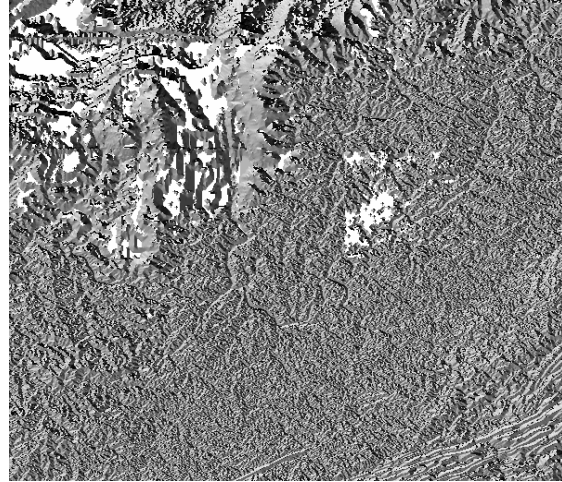
Fig. 143. Aspect version of the DEM.

Aspect images have a different visual texture, that of a metallic surface, shown in Fig. 143. Values of 0 and 240 represent a slope to the north. 60 is eastern, 120 is southern, and 180 is western. Intermediate aspects are proportionally distributed. The white areas in this image are where no aspect could be determined because of zero slope over distances greater than the size of the window within which the aspect is calculated.

Viewshed

DEM data can be used for calculating viewsheds from a particular location. A DEM data set from the southeastern U.S.A. (without serious flaws) has been selected for illustration. (N 32° 40' to 37°, W 80° to 85°). In this solar-shaded view of Fig. 144 the southern
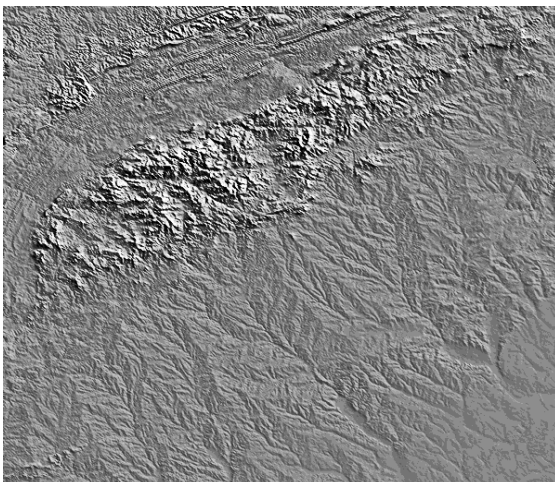
Fig. 144. Shaded relief in southern Appalachians and Piedmont.
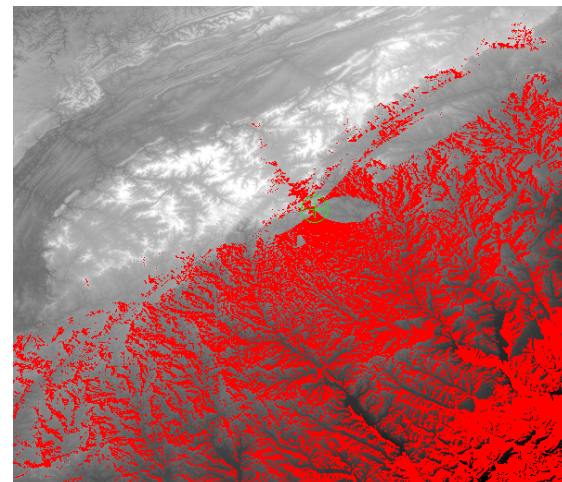
Fig. 145. Viewshed (red) from a mountain peak, sees the Piedmont but not into the mountains.

75

Appalachian Mountains are prominent, as well as the Piedmont. A particular high point was selected on the southeast side of the range. The viewshed program was instructed to show the terrain as viewed from 3 meters above the peak. The flat-earth solution was computed rather than one simulating earth curvature. The viewpoint is at the green crosshair and circle. In Fig. 145 the terrain in view is colored red on the DEM. The view of the lowlands is excellent, being affected only by local topography. The view does not penetrate into the mountains to any significant extent.

The viewshed program is also useful for crudely predicting FM radio propagation, where a signal might reach the ground. In practice, the computation really needs to use an Earth radius of 4/3 the actual Earth radius to simulate the refraction of radio waves in the atmosphere. It is only appropriate for FM transmissions, which are generally line-of-sight, not for AM or short-wave radio which interact with the ionosphere.

Watershed

The same Piedmont DEM was used in the watershed routine, originally written about 1990 at the USGS EROS Data Center, Sioux Falls, SD, and later adapted to numerous
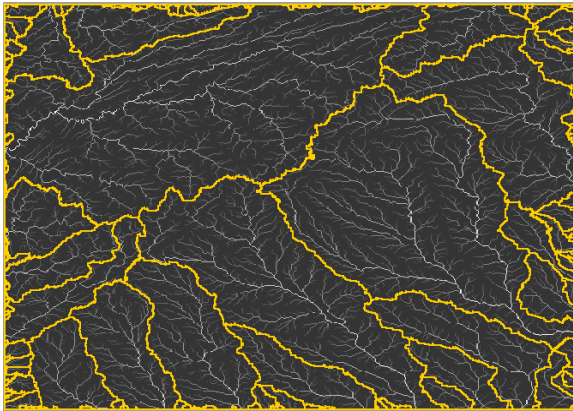
Fig. 146. Water flow accumulation result from a watershed program, with basin boundaries.

software packages. The routine fills in any closed depressions in the DEM, then computes aspects for flow directions. For each pixel it determines the number of pixels upslope, thereby computing an accumulation image. Natural watershed boundaries and flow channels are determined. The routine allows the analyst to nominate one or more "pour points" for the determination of the upstream watershed from that location. This illustration in Fig. 146 is of the flow accumulations (logarithmic contrast) as white lines on a black background, with gold lines being the default watershed boundaries determined from which large channels intersect the edge of the view. Many other products could also be displayed.

Vegetation Gradients
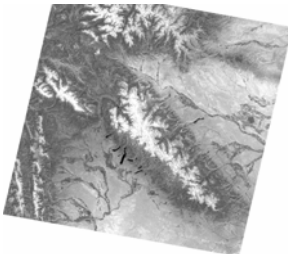
Fig. 147. Landsat view of Wind River Range, Wyoming.

DEMs can also be used as a component in 2-D histograms. A nearly entire Landsat TM scene (red band 3) of the Wind River Range in Wyoming was selected. The elevations of the same area, from the Shuttle SRTM data, were rescaled to an 8-bit range by subtracting an offset and dividing by 12. The scene in Fig. 147 shows bright lowlands with dark irrigated fields. The

highlands are snow covered in this early July scene. In between the slopes are covered with dark conifer trees.
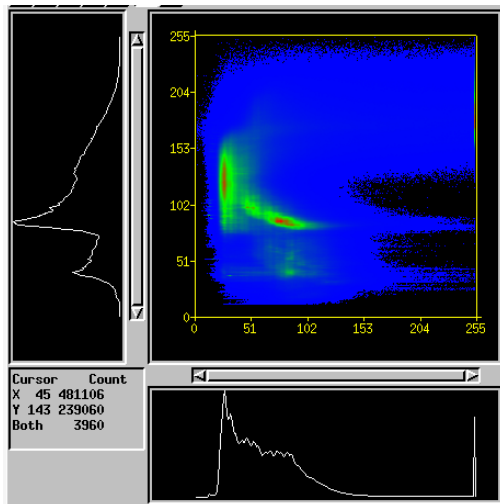
Fig. 148. A 2-D histogram of scene brightness (X-axis) and elevation (Y-axis).

A 2-D histogram of the scene was calculated for Fig. 148. The bottom graph shows the distribution of digital numbers for the red raster, with dark to the left and bright to the right. The left graph shows the distributions of rescaled elevations. The lowest elevations are from the upper right corner, the lower peak from the eastern lowlands, and the main peak is from the southern lowlands. In the colored portion the central green patch with red core represents the southern lowlands, the lower small green dot the eastern lowlands, and the left vertical green patch with red core the conifer covered mountain areas. The snow patches are at the upper right edge, showing saturated brightness. Elevation control of band 3 brightness is strong in this scene.

9. Geographic Information Systems

A Geographic Information System (GIS) is a computer program that organizes data according to their geographic relationships. Originally the term tended to be restricted to a particular software brand and to its descriptions of the boundaries of regions with common properties (fields, roads, rivers, land cover types, etc.). The latest software versions have greatly expanded their capabilities, making the GIS term cover many more techniques.

Rasters

A GIS will usually contain an image processing system that manipulates rasters (2-dimensional imagery). Such imagery can be used as background upon which GIS analyses are overlaid. Rasters are often the source upon which vector (points, lines, areas) interpretations are generated through the process of digitization or direct raster-to-vector conversion.
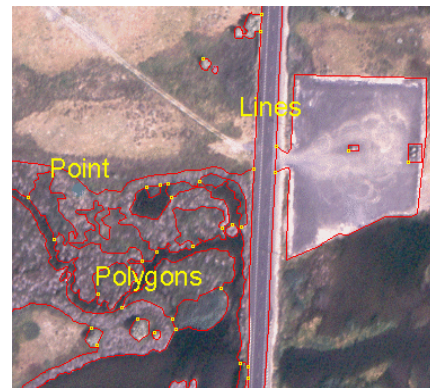
Fig. 149. A view of Winchester Wasteway, illustrating sketched vector features.

Vectors

A vector object is a collection of points, line segments, polygons, and nodes and annotation, illustrated in Fig. 149. Line segments (red) connect points, though some points (cyan) can be left as isolated points to identify locations of particular objects. A set of line segments that encloses an area is called a polygon, which is normally very irregular in shape. Line segments intersect (T, X, or other shape intersection) at a node (yellow). Line segments can end at a dangling node (green). Polygons can be islands within other polygons. Annotation, or Labels, help interpretation. These vector objects can be assigned any desired color and drawing style. Polygons can be filled with solid colors or patterns and be shown with or without border lines.

Vectors can be generated directly from paper (or other physical medium) maps and imagery by the process of digitization. The paper is fastened to a digitizing tablet. The coordinates (x,y pairs) are read electronically as a cross-hair device is moved over the features of interest. The same can be accomplished on a computer screen by "heads-up" digitizing. The map or imagery is scanned and displayed on the computer screen as a raster; the cursor is moved over the features of interest to get the coordinate pairs. Software techniques exist to convert lines in raster imagery into vector lines, as shown later for contour following.
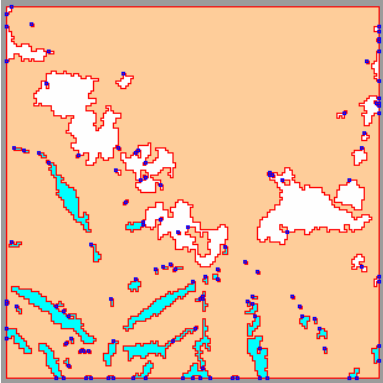
Fig. 150. Vector generated from automated classification.

Similarly, boundaries of solid colors in a raster (created by a classification process) can be converted to polygons. In Fig. 150 a raster was created from Landsat data by a partition process. The white areas are clouds and the cyan are snow on the ground (tan). Nodes are dark. The vector polygons were generated at the pixel edges, as shown by the square-stepped borders. The polygons were automatically assigned a numerical classification code identical to the code represented by the colors.

Fig. 151. Vector polygon classification of plant types.

Lines can be used to represent roads, railroads, trails, streams, political boundaries, field boundaries, etc. Polygons can be labeled according to the contents of their interiors. Such can be soil types, land cover, water rights, and many other categories. The Fig. 151 example is a plant classification created by visually examining a scene in stereo aerial imagery, hand-drawing boundaries on a basemap image and assigning the classifications to the resulting polygons. Each plant class is assigned its own color code. Here blue is unclassified land and water, yellow is the reed Phragmites, green is cattails and bulrushes, magenta is flowering purple loosestrife, brown is unhealthy purple loosestrife, and tan is dead purple

78

loosestrife, all along the Winchester Wasteway in Washington.

Polygons from different data layers (like elevation zones, soil types, land cover, population density, endangered species locations) can be overlapped to show relationships between the different data layers, possibly generating additional categories for classification. Buffer zones at fixed distances from other objects (points, lines) can be created by the software.

Vector sets generally take less storage space than rasters and are faster to analyze. However, they cannot contain the fine image detail of rasters. They are best for generalizing properties under consideration. Vector objects can have data base and text objects assigned to them, whereby the data associated with some vector object can be viewed at will.

The process of generating vector data, either by hand entries (digitizing) or by conversion from raster data, will usually generate errors. Hand vibrations and pixel edges cause wavy line segments which may need smoothing. Line intersections may have overshoots to be removed, or the lines may not connect at all, requiring "snapping" to form a connection at a "node". A merger of vector data from two sources may have lines that should be the same. However, irregularities in the line data during a merger process cause an artificial creation of tiny polygons along what should be a single line. Such artifacts need to be removed. Vector cleanup is mandatory before analysis can properly begin. For illustration, some vector data were automatically generated from a contour map.

In Fig. 152 the numbers generated junk lines that need to be removed. These are examples of dangling lines. They can be marked for deletion (shown in red) or possibly removed by specifying a short length threshold. Other lines that are not contours also need to be removed. In Fig. 153 there is a small triangular polygon that should not be there. Such artifacts could be removed. In Fig. 154 the errors were generated by contours that were close together. Fig. 155 shows some additional lines (green) were edited manually , while the red lines were marked for deletion. The excess nodes (blue) were then removed.
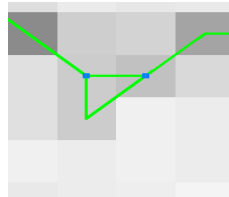

Fig. 152. Dangling line.   Fig. 153. Bubble artifact.   Fig. 154. Multiple bubbles.   Fig. 155. Hand Scketching
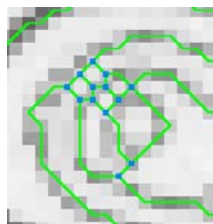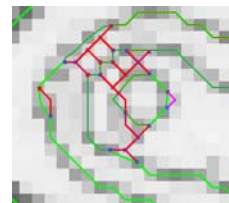
Databases can be attached to vector elements. By touching an element with the cursor the data base information for that element is brought into view. Sometimes values in the database can be used to affect the size of vector symbols.

Though vector sets are normally 2-dimensional, 3-dimensional vectors can be created by assigning elevations to all components. A 3-D representation of a topographic map has the contours with assigned elevations (no contours can cross if their elevations differ) and possibly some individual points (bench markers). Such 3-D contours can be used to generate a surface raster which is a digital elevation model (DEM). The three major steps are shown in Fig. 156
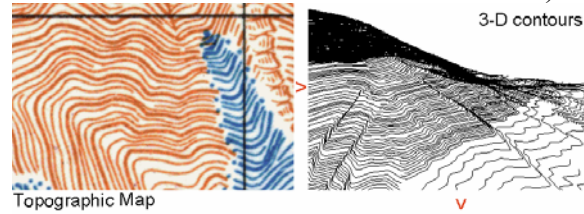
CAD

Vector sets without precise topological rules can be expressed as CAD (computer aided design) objects. Otherwise they are similar.
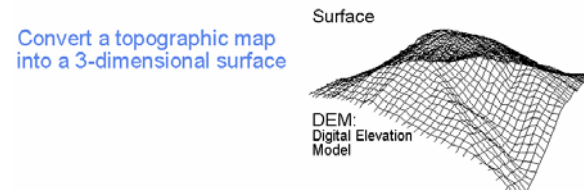
Fig. 156. Steps in making a DEM from a topographic map.

TIN

A triangular irregular network (TIN) is a series of triangles, the nodes of which express some data quantity, such as elevation of a surface. Within each triangle the data are assumed to vary linearly with direction. Where changes are more rapid and non-linear, the triangles are smaller and closely packed. In regions that are generally flat or with a constant magnitude and direction of slope, the triangles are large and sparse. A TIN representation of a variable surface usually takes less data storage space than a DEM and provides computational advantages when generating 3-dimensional perspective surfaces.

Data Bases

Data Bases (DB) allow an organization of data of various types. Software can form an attachment of DB elements to vector objects so that properties associated with the vector objects can be read or interrogated. Sometimes the data base values can be used to control the plotted appearance of the vector objects, such as symbol size or orientation. Queries can be made to quantify and map particular DB values. Data Bases, such as Dbase, Oracle, and Informix, could be easily linked to a GIS. This creates more value for storing, archiving, and analyzing data sets.

Conversions

Rasters can be converted to vectors and CAD. Vectors and CAD can be converted to rasters. DEMs and TINs expressing elevation can be converted to the other type.

Changes

There are many applications in which documentation of changes is of greatest value. This can be a time series of remote sensing and/or GIS data layers. It can be a comparison of conditions before and after some significant event. Remote sensing

products from satellites showed themselves particularly valuable in documenting the extents of damage following the Asian tsunami of late December 2004 and of Hurricane Katrina in southern U.S.A in late August 2005. A small segment of damage in Biloxi, Mississippi, is shown in Fig. 157. The upper half shows a "before" view from the IKONOS satellite operated by SpaceImaging. The lower half is the same view after passage of the hurricane when cloud-free skies allowed viewing from the satellite. At the right side, notice the destruction of the road causeways. At the left side, notice the movements of the casinos to onshore positions. Trees and houses were destroyed in most locations and their debris piled and scattered. Large buildings, with stronger construction standards, remained intact. In other cities all buildings and vegetation within several city blocks of the shoreline were scoured totally, leaving only remnants of the foundations. The same change detection techniques are applicable to other, lesser disasters.

Fig. 157. Before and after IKONOS views of hurricane Katrina damage at Biloxi, Mississippi.

10. Applications

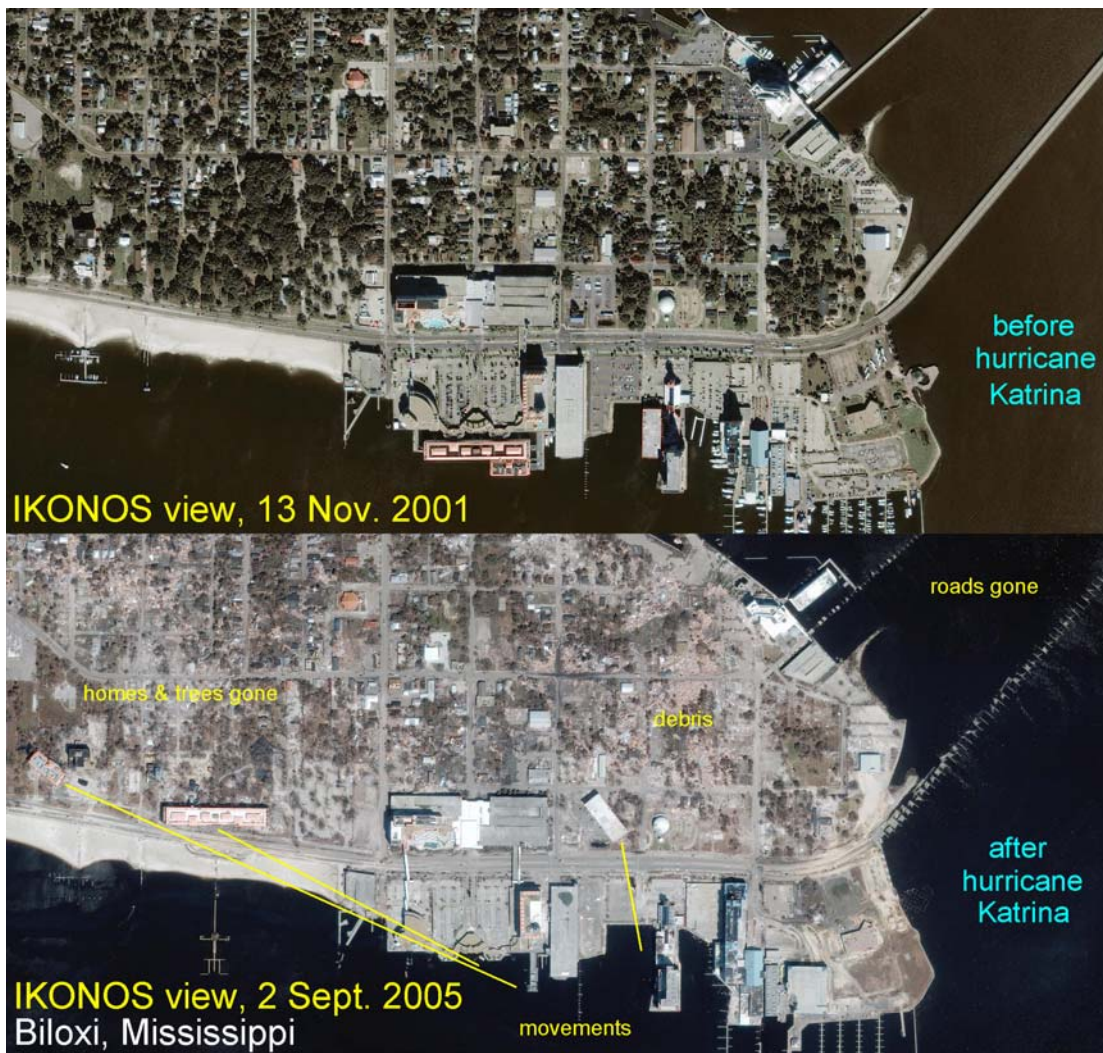Remote sensing data analyses can be valuable in themselves or as components for a geographic information system. Data in use by GIS software can be used to model relationships between variables and create new variables. The model might show the relationship of backwater areas for various river flow intensities. It might show the progress of a flood along a river corridor. It might show the discharge of a watershed in response to radar-detected precipitation within the watershed. A model might predict locations and extents of habitats required by an endangered species. A list of applications could be lengthy, as shown by Part II of projects already completed.

GIS analyses involve many more topics that are beyond the scope of this report. Here are some of them: Geographic analysis: a. Queries; b. Cartographic analysis; c. Buffering; d. Map algebra; e. Spatial analysis; f. 3-D analysis; g. Modeling techniques; h. Network analysis; i. Charts and reports. Geostatistics and Spatial Analysis: a. Software packages strengths and weaknesses; b. Sampling techniques; c. Descriptive statistics; d. Hypothesis testing - parametric and nonparametric tests; e. Analysis of variance: one way, two way, n-way; f. Bi-variate and multi-variate correlation and regression; g. Principal components analysis; h. Factor analysis; i. Cluster analysis; j. Discriminant analysis; k. Surface modeling techniques: kriging, inverse distance, triangular irregular networks, trend surface analysis; l. Network analytics. Accuracy Assessment: thematic, positional. Metadata: formal descriptions of data. Project Planning: a. Collaboration; b. Scoping; c. Interim and final reports; d. System deployment.

Contact the Remote Sensing and Geographic Information Group (D-8260; phone (303) 445-2267) to see if there are technologies available and appropriate for projects of special interest to your own group.

II. Overview of Usage Within the Bureau of Reclamation

The Remote Sensing and Geographic Information Group (D-8260) of the Bureau of Reclamation has several decades (since 1975) of experience in both research and applications. An appropriate technology is selected for each project to accomplish particular goals within the restraints of available time and budgets. We have encouraged the use of RS and GIS within the regional offices, so that local analysts can address local topics.

There are numerous commercial software products available. The Denver Office uses ESRI (ArcGIS, ArcView, etc.), ERDAS (Imagine), MicroImages (TNTmips), and Research Systems (ENVI) software to accomplish the project and research work. Each system has its own characteristics and specialties, but most capabilities overlap. Our workers tend to specialize in one particular brand of software. Data from each software

can usually be imported and exported in formats of the other brands, enabling the outputs to be in whatever format a client desires.

Supporting tools in our analyses include digitizing tablets, stereoscopes, light tables, printers, flat-bed scanners, and video capture equipment. Computer terminals are networked, allowing easy transfers between computers and servers. Internet access allows rapid download of data available from public sources.

Reclamation Project Examples

The following listing is for projects conducted by the team at the Denver Office since 1975. Regional offices have conducted studies of similar nature. These are listed to give inspiration about the range of possible projects and appropriate technologies. (Many of these could be classified into finer groups and lumped, naming the geographic regions in which a technique was applied.)

CIR photography for vegetative analysis along Rio Grande.
- Aerial imagery analysis for vegetative associations of Spring Canyon and Rifle Range Pumped Storage Survey sites, Lower Colorado region.
- Mapping of vegetative associations at Whipple Wash Pumped Storage site, Lower Colorado.
- Aerial photographic study of Ochoco Dam and Reservoir area, Oregon.
- Land cover analysis for the Republican/Solomon Rivers Water Management Study, Kansas/Nebraska.
- Photointerpretation for wildlife mitigation, New Rockford Canal right of way, Garrison Diversion Unit, Dakotas.
- Aerial photo studies of Clark Canyon Dam and Reservoir area, Montana; Hagmmaier Pond Dam South, Calif.; Tufa Stone Dam, Arizona.
- Land cover analysis and inventory of Tularosa Basin, NM.
- Mapping of Garrison area (Sand Lake, Dakota Lake, Hyatt Slough, Arrowhead Lake), National Wildlife Refuge Monitoring Program.
- Evaluation of riparian vegetation trends in the Grand Canyon using multitemporal remote sensing techniques.
- Post construction analysis at Calamus Dam, North Loup, Upper Missouri Basin.
- Determining impacted wildlife resources in the Grand Valley, CO, by remote sensing.
- Land cover mapping and analysis for Lower Gunnison Basin Unit, North Fork area, CO.
- Aerial photographic documentation of perennial vegetation changes near Granite Reef and Salt Gila Aqueducts, AZ.
- Vegetation identification and mapping for Gila River Indian Reservation, AZ.
- Photo interpretation along Snake River, Minidoka Project, Jackson Lake Dam.
- Vegetation mapping for All American Canal, Calif.

- Use of RS and GIS for estimation of irrigation water use in the Upper Gunnison River Basin of Colorado.
- Use of satellite RS and GIS for estimation of irrigated land acreage in the Newlands Project Area, NV.
- Baker Valley Irrigation District GIS data base and mapping.
- Use of aerial photography for vegetation monitoring along Heyden-Rhodes Aqueduct.
- Use of oblique slides with PC image processing system for Big Horn Sheep habitat analysis, Waterton Canyon, CO.
- Land use and land cover mapping at American Falls Reservoir, PN region.
- Evaluation of wetland changes on Klamath Lake with multitemporal remote sensing.
- Black Sands Area study for land cover trend analysis.
- Pecos River habitat quantification using aerial photography and videography.
- Wetland and riparian mapping along La Plata River, CO.
- Blunt Reservoir, Pierre Canal wetland and wildlife habitat mapping.
- Rio Grande land use inventory.
- Vegetative assemblage mapping of the Nueces River Delta, Texas.
- Using aerial photography (1:5000 scale, natural color positive transparencies in stereo), hyperspectral scanner, and IKONOS satellite imagery to map invasive noxious weed infestations (purple loosestrife, leafy spurge) and biocontrol effectiveness at the Winchester Wasteway, Washington and in the areas near Denver. The latter includes the Spring Creek and Buffalo Creek fire swath areas infested with leafy spurge, for the Forest Service.
- Inventory of wetlands and riparian communities for Animas/Laplata, CO.
- Mapping of riparian vegetation of the Lower Colorado River from Davis Dam to the international border, CA/AZ.
- Seedskadee NWR vegetation inventory.
- USGS - NPS vegetation mapping - Jewel Cave National Monument, SD.
- USGS - NPS vegetation mapping - Devils Tower National Monument, SD.
- USGS - NPS vegetation mapping - Mount Rushmore National Memorial, SD.
- USGS - NPS vegetation mapping - Wind Cave National Park, SD.
- USGS - NPS vegetation mapping - Badlands National Park, SD.
- USGS - NPS vegetation mapping - Theodore Roosevelt National Park, ND.
- Banks Lake and Conconully land use land covering maps.
- USFS Nebraska National Forest, Buffalo Gap National Grassland prairie dog colony mapping.
- Wetlands inventory and drained wetlands water storage capacity estimation for the St. Joe - Calio Coulee subbasin of the Greater Devils Lake Basin, ND.
- Cheyenne Bottoms Wildlife Management area, KS.
- Potholes Reservoir vegetated exposed bed.
- Vegetation mapping using vertical aerial videography along the San Luis Valley Project - Conveyance Channel Closed Basin Division - CO.
- Central Platte River land cover land use mapping, Nebraska.
- Ridgway State Park, CO, vegetation survey and mapping.

- Trinidad State Park, CO, vegetation survey and mapping.
- Rifle Falls and Rifle Gap State Parks vegetation survey and mapping.
- Yampa River Legacy State Park - Elkhead Reservoir vegetation mapping.
- Jemex Mountain, NM - habitat mapping project.
- Sunset Crater Volcano National Monument, AZ, vegetation mapping project.
- Lacreek National Wildlife Refuge, SD, vegetation mapping project.
- Ouray National Wildlife Refuge, UT, vegetation mapping project.
- Jasper Fire area vegetation mapping.
- Mapping of Route 285 for Colorado Dept. of Transportation.
- Knife River Indian Villages National Historic Site vegetation mapping project.
- Fort Union Trading Post National Historic Site vegetation mapping project.
- Zion National Park vegetation mapping.

Agricultural studies
- RS study of land use and irrigated crops in the Lower Sevier River Basin, Delta, Utah.
- Basin-wide remote sensing of irrigated lands in the Bear River Basin of Wyoming.
- Inventory of irrigated lands and reservoir surface areas in the Upper Green River Basin, Wyoming.
- Detailed sprinkler and land classification analysis, Lincoln Valley, Upper Missouri.
- Using Landsat TM imagery for cultivated lands identifications, James River/Oaks, ND.
- Land use, habitat mapping in Imperial Irrigation District, Calif.
- Using Landsat, SPOT and Indian IRS satellite data to map irrigated lands in Upper and Lower Colorado River basins.
- Mapping irrigated lands in the Yakima River Basin, WA, using digital satellite data.
- Mapping irrigated lands in the Clark Fork / Flathead River Basin of western Montana using digital satellite data.

Land Suitability studies
- Vegetation, salt, and soil inventory for McElmo Creek Salinity Control Unit, Upper Colorado.

Geologic mappings
- Lineament analysis at Brantley Dam, NM, using 1:24,000 scale imagery
- Using Landsat imagery of the Strawberry Reservoir area, Utah, for seismic hazard evaluation.
- Using Landsat imagery for lineament analysis of Stillwater Tunnel area, Utah.
- Photogeologic studies of landslide deposits at Lake Sherburne Dam, Montana; of Lake Darling Dam and Reservoir, North Dakota; of Ganado Dam area, Arizona; of Assayi Dam area, New Mexico; of Glendo Dam and Reservoir area, Wyoming; of El Vado Dam and Reservoir area, New Mexico.

- Using Landsat imagery for lineament analysis of Shell Creek Drainage, Wyoming.
- Demonstrated a technique for combining watershed analysis (using DEMs) with a map of Grand Canyon geologic formations, to be used by USGS to evaluate potential for each side canyon to produce debris flows.

Water studies (see also thermal and hyperspectral)
- A study of seepage along the Dry Gulch Canal, Uinta Basin Project.
- Using Landsat imagery to measure the area of Eagle Lakes, Columbia Basin.
- River bank recession analysis, Oroville-Tonasket Pumping Plant, Okanogan River, Pacific northwest region.
- An inventory of playa lakes, Llano Estacado.
- Water quality mapping of Flaming Gorge Reservoir, Wyoming.
- Multispectral Landsat imagery of chlorophyll-a in Flaming Gorge Reservoir, Wyoming.
- Water quality imagery of Bear Lake, Idaho/Utah.
- Using Landsat multi-date imagery of October, 1983, flood extents near Phoenix, AZ.
- Using airborne scanner imagery of Blue Mesa Reservoir, CO, for water quality patterns.
- Using Landsat data to quantify turbidity and chlorophyll content and measure surface temperature patterns in Lakes Havasu, Mead, Powell, Klamath; Flaming Gorge Reservoir.
- Remote sensing study for East Highline Canal seepage, Imperial Irrigation District, Calif.
- Using MAMS 12-channel scanner data for surface water quality patterns on Lake Pleasant, Arizona.
- Using remote sensing (aerial photography, videography) and GIS for backwater studies, sediment transport, channel characteristics along Green River, Utah, below Flaming Gorge Dam.
- Backwater habitat mapping for Colorado River in Grand Canyon.
- Use of SPOT satellite data for mapping chlorophyll on Lahontan Reservoir.
- Aerial photography documentation of changes and vegetation along Coachella Canal, Calif.
- Fontenelle Dam tailwater mapping.
- Remote sensing of San Juan River for habitat mapping for endangered fish.
- Routine monitoring of Green, Colorado, San Juan Rivers by aerial videography.
- Erosion mapping of Audubon Lake Island.
- Water quality studies on Hanks Marsh, Klamath Falls, OR.
- Using aerial video from helicopter flying about 100 ft above canal of Central Arizona Project to quantify and locate patches of aquatic weeds that hinder water transport, for measuring the effectiveness of biocontrol of weeds by grass carp.
- Using aerial video to map rapids and riffles along Yakima River.
- Limnological applications of multispectral remote sensing.
- High/Low flow studies of wetted area and river channels in the Rio Grande River.

- Using aerial photography (1:12,000) to map all man-made structures (dams, canals, channels, pumps, diversions, fish screens) related to water usage in the John Day River Basin, Oregon.
- Utility of GIS for the National Irrigation Water Quality Program in the Grand Valley.
- Green River waterline mapping at 10,900 cfs using airborne videography.

Dam Safety studies
- Clark Canyon Dam, MT, dam failure inundation study.
- Use of geospatial technology to automate dam breach inundation mapping and emergency management within Reclamation.
- Green River flooded bottomlands mapping for two flows.

Thermal studies
- Studies of geothermal sites at Susanville, Holtville.
- Thermal IR imagery at Meeker Dome for salinity control.
- Thermal IR imagery downstream of Theodore Roosevelt Dam.
- From pre-sunrise aircraft flight over the Platte River, Nebraska, to count the number of Sandhill Cranes on each island and sandbar before they moved into the fields to feed..
- Thermal IR imagery of Fontenelle Dam, Wyoming.
- Thermal IR imagery of the New Waddell Dam site, Arizona.
- Using FLIR system (thermal scanner and visible video) from helicopter below the canyon rims in the eastern Grand Canyon and the canyon of the Little Colorado River, to measure the temperatures of the rivers and backwaters and to identify warm springs, to locate favored habitats for endangered fish.
- Using a Daedalus scanner in the Grand Canyon and Little Colorado River to measure river and backwater temperatures.
- Using a Daedalus scanner along the lower Yakima River, Washington, to measure water temperatures in the Columbia and Yakima Rivers, backwaters, isolated ponds, and canals, especially comparing the temperatures of water entering the rivers with the river temperatures there.
- Using Landsat band 6 to measure surface temperature patterns in Lakes Mead, Powell, Klamath.

Hyperspectral studies
- Using ASDI Field Spectrometer to measure fine details of spectra of various rocks, minerals, soils, plants, flowers, Autumn colored leaves, sky, clouds, snow, and man-made substances, with a stress on invasive noxious weeds at various seasonal stages. The more than 4600 measurements are available on a CD or a web site for use by others as reference spectra.
- Using the Probe-1 (128 channels) scanner at the Winchester Wasteway, central Washington, to view a habitat of mixed sand dunes, wetlands and irrigated fields, examining in particular the effects of biocontrol beetles on purple loosestrife infestations, plus distributions of Phragmites (cane), bulrush, and cattails.

- Using the AVIRIS (224 channels) scanner for water quality studies at Klamath Lake, Oregon.

Social, Economical, and Demographic studies
- Numerous population at risk and economic impact studies for modeled dam breach flood zones for many of Reclamation's high and significant hazard dams.

EIS studies
- Garrison Diversion: Photointerpretation for Wildlife Mitigation on New Rockford Canal. 1982
- Remote Sensing for Sandhill Crane Roosting Habitat on the Platte River 1983
- Glen Canyon Environmental Studies, for the Biological Assessment : Evaluation of Riparian Trends in Grand Canyon 1986
- Biological Assessment for the operation of Flaming Gorge Dam, Mapping backwaters in the Green River 1987
- 1988- Platte River Studies mapping Channel Changes
- Environmental Assessment for Coachella Canals Wetland Mapping study 1989
- Refuge Monitoring for environmental Assesment on the James River in North and South Dakota 1990
- Sediment Transport for channel mapping below flaming Gorge in support of the Biological Assesment 1992
- Animas / LaPlata wetland inventory for the EIS 1995

Infrastructure studies
- Closed Basin Infrastructure Mapping.

Environmental Justice studies
- Keechelus Reservoir

Archaeological studies
- A review of available technologies appropriate to archaeological surveys.

Weather remote sensing
- Satellite estimates of incident solar radiation in the western states.
- Using AVHRR imagery from polar orbiting satellites to exclude clouds and measure snow-covered area on the ground, for operational use by the National Weather Service.
- Using NEXRAD radar data to estimate the accumulation of snow in terms of water equivalent and depth, for operational use by the National Weather Service as well as by Reclamation. The results are continuously available on the Internet for numerous areas, such as northern plains, Pacific northwest, lower Colorado River.

Specific-regional GIS and models
- Development of a GIS for Garrison Diversion Unit, Dakotas.
- Creation of a GIS with numerous data layers for monitoring the status and changes within the Grand Canyon.
- The Middle Rio Grande GIS Data Base.
- US Forest Service R2RIS GIS Data Base.
- Development of GIS Data Base for American Falls Reservoir management.
- GIS data bases for Potholes and Scooteney Reservoirs.
- Browns Park NWR GIS data base, vegetation inventory.
- Cheyenne Bottoms Wildlife area GIS, KS.
- Comparing 1990 and 2000 census data for Reclamation dam failure population at risk analysis.
- Walker and Truckee River Basin Lahonton cutthroat trout recovery plan GIS.

Foreign studies
- Remote sensing of cropping patterns along the Lower Nile River System.
- Satellite observations of snow covered area in the High Atlas Mountains of Morocco.
- guidance for projects in Brazil and Spain.